LATERAL LOADING OF SMALL-SCALE SHEAR WALL BUILDINGS WITH FLOOR SLABS

LATERAL LOADING OF SMALL-SCALE SHEAR WALL BUILDINGS WITH FLOOR SLABS

by

JOHN W. SPEIRS, B.ENG (CIVIL)

A Thesis

Submitted to the Faculty of Graduate Studies

in Partial Fulfilment of the Requirements

for the Degree

Master of Engineering

McMaster University

March 1969

MASTER OF ENGINEERING (1969)
(Civil Engineering)

McMASTER UNIVERSITY
Hamilton, Ontario

TITLE: LATERAL LOADING OF SMALL-SCALE SHEAR WALL BUILDINGS WITH FLOOR SLABS

AUTHOR: John W. Speirs, B.Eng. (Civil), McMaster University

SUPERVISOR: Dr. A. C. Heidebrecht

NUMBER OF PAGES: xi, 113

SCOPE AND CONTENTS:

This thesis describes the construction and testing of small-scale shear wall buildings with rigidly connected floor slabs, but without wall openings. A micro-concrete material was used in the casting of both the basic small-scale shear wall buildings and the floor slabs. The vertically cantilevered buildings were tested by applying a transverse static load at the top of the buildings.

The behaviour of buildings with only floor slabs was compared with that of buildings containing only wall openings. The results of static loading of the buildings were compared with those results predicted analytically using Vlasov's thin-walled elastic beam theory.

ACKNOWLEDGEMENTS

I wish to express my deepest gratitude to Dr. Heidebrecht for his advice and patience during the course of this thesis work. Also, I would like to thank Dr. Tso and A. Ghobarah for their time spent in discussions concerning Vlasov's theory.

This investigation was made possible through the financial assistance of the CANADA EMERGENCY MEASURES ORGANIZATION, to whom I extend my sincere thanks.

TABLE OF CONTENTS

LIST OF FIGURES

LIST OF TABLES

LIST OF PLATES

NOTATION

δ	wall thickness of the building
A	cross-sectional area
O	centroid of section
S	shear centre of section
a_X, a_Y	co-ordinates of shear centre
E	modulus of elasticity of concrete material
G	modulus of elasticity in shear
μ	Poisson's ratio
u	longitudinal displacement in Z direction
v	transverse displacement directed along the tangent of the profile line of the cross-section
w	transverse normal displacement
ε	longitudinal strain
ℓ	length of the building
ω	principal sectorial area
I_X, I_Y	moments of inertia of plane area with respect to X and Y axes
ξ, η	displacements of the shear centre in the X and Y directions respectively
θ	rotation of the section about the shear centre
P	external static loading
e	eccentricity with respect to the shear centre
I_ω	sectorial moment of inertia
I_d	torsional rigidity
B	bimoment, a generalized balanced force system statically equivalent to zero

H	torsional moment, the generalized force factor in the transverse direction
α_X	distance of the shear centre from middle surface of the back wall, along the OX axis
h	thickness of the floor slabs
Ω	twice the area of the floor slab
X,Y,Z	principal axes of the cross-section

CHAPTER 1

INTRODUCTION

1.1 DESCRIPTION OF SHEAR WALL STRUCTURES

In recent years, there has been a rapid increase in the number of tall buildings built for commerical and residential purposes. This increase has necessitated the need for a greater understanding of the behaviour of such structures under service conditions.

As a building increases in height, it is most important that sufficient lateral stiffness exists in the building to resist the effects of wind loading, seismic action and blasts. Sufficient stiffness in tall buildings can be effected in the case of framed structures by bracing members, by increasing the joint rigidity or by infilling the frame with shear resisting panels. This leads to the use of a shear wall element to assist in providing additional stiffness in a tall building.

A shear wall is used as a structural element in a tall building to provide stability against wind, earth tremors and blasts. Deriving its stiffness from its structural form, the shear wall is extremely stiff and shear resistant in its own plane. The shear wall element can consist of a plane wall, a curved wall, a closed loop, or of a rectangular box of a system of concentric or eccentric cores.

Parallel shear walls are connected by floor slabs to form one type of shear wall building. The box-core is another type of shear wall building in which two channel shaped shear walls are aligned so that they form a box-like system connected by floor slabs.

Architecturally, the shear wall building with floor slabs permits

maximum flexibility of internal layouts and eliminates the obstructions associated with internal beams and columns. This type of building provides inherent accoustic insulation and also is extremely fire resistant. From the viewpoint of construction, the building can be erected quickly and economically following a logical sequence of operations using a repetitive form of construction.

The floor slabs act as diaphragms which distribute the horizontal loads to the stiff shear walls. The shear walls transmit the loads to the foundation which in turn distributes them over a sufficient area to prevent a soil failure. Further, the floor slabs which are extremely stiff in their own planes, increase the lateral stiffness of the building by their complex interaction with the walls.

The shear walls can contain openings for doors, windows and corridors at regular intervals throughout the height of the building. When the stiffness of the shear wall element is determined, account must be taken of the locations and sizes of the wall openings.

It can be readily seen that the three dimensional behaviour of a tall building comprised of perforated shear walls, floor slabs and service cores is extremely complex. Approximate design methods can be used to proportion the elements, but these analyses do not take account of this three-dimensional interaction. Clearly, more sophisticated analysis techniques are required.

The general purpose of research on shear wall structures is to first provide more information on their behaviour and secondly, to develop more realistic design criteria.

1.2 SHEAR WALL PROJECT

The Canada Emergency Measures Organization is currently sponsoring an extensive program of experimental investigations into the behaviour of shear wall buildings. The project is being conducted in the Department of Civil Engineering and Engineering Mechanics at McMaster University, Hamilton, Ontario. It consists of building small-scale shear wall buildings and studying their responses to static and dynamic lateral loadings.

Experimental investigations are being conducted on monolithic assemblies of shear walls which take the form of small-scale shear wall buildings. The basic small-scale shear wall building was designed so that it was geometrically similar to actual tall buildings. It would also allow floor slabs and wall openings to be introduced. This procedure would permit a basic continuity of test structures during the various phases of the project.

The basic structure as shown in Figure 1 was E shape in cross-section and stood eight feet in height. A non-reinforced micro-concrete was designed and used as the structural material of the buildings.

In the first phase of the project, Afsar (1) studied the behaviour of the basic building without transverse slabs or wall openings, subject to a transverse static loading. The second phase of the experimental program was the investigation by Qureshi (2) into the behaviour of the building with two vertical rows of circular openings in the back wall. Modifications to the design of the concrete material, the construction procedure and the testing of the buildings

were initiated in this phase of the program.

The present study, phase three, is an investigation into the behaviour of the building with rigid floor slabs, but without wall openings. The modifications introduced by Qureshi were incorporated into this study.

The next phases of the shear wall project will include the application of dynamic loads to the basic building which has neither wall openings nor floor slabs. Future investigations will also include the dynamic response of the small scale shear wall building with floor slabs.

1.3 ANALYSIS OF SHEAR WALL BUILDINGS

Coull and Smith (3) have compiled a comprehensive summary of the published literature concerning the analysis of shear wall buildings.

In general, a shear wall building can be comprised of interconnected shear walls and floor slabs. The walls do not act as independent cantilevers due to the coupling action of the floor slabs. Further complications in the behaviour of the building are introduced when the walls have openings.

Afsar (1) has outlined various analytical and experimental approaches used in the study of shear wall structures.

Qureshi (2) has compiled a detailed survey of the literature dealing with the behaviour of shear wall structures comprised of shear walls with rows of openings. A popular method of analysis of this type of structure is the frame analogy method. The shear walls with rows of openings are idealized as interconnections of columns and beams. Extensions of this method were used by Beck (4) Eriksson (5) and Rosman (6) who treated the rows of beams connecting shear walls as a continuous medium in pure shear.

Another popular approach is the method of panel elements. The shear wall is considered to be a system of elements whose behaviour when assembled is similar to that of the continuous structure. This approach is characterized by the finite element method used by McLeod (7).

Vlasov (8) in his book, "Thin-Walled Elastic Beams" proposes an analysis which can be applied to the small-scale shear wall building. Analyses based on Vlasov's theory can be used to predict the

behaviour of various thin-walled beams subjected to a variety of boundary and loading conditions. The important feature of this method is the consideration given to the longitudinal extension of the beams resulting from torsional loads.

Qureshi (2) conducted an experimental investigation into the behaviour of a micro-concrete shear wall building with two symmetrical rows of openings in the back wall. He found that Rosman's theory can be used to predict the behaviour and maximum deflection of such small scale shear wall buildings. The area of the rectangular openings in the theoretical model should be set equal to the area of the circular openings in the experimental building. The strain distributions predicted using Rosman's theory agreed with the experimental distributions.

Qureshi (2) concluded that Vlasov's theory could not be used to predict the behaviour of the small scale shear wall building with circular wall openings.

Afsar (1) studied the behaviour of the basic small-scale shear wall building without wall openings or floor slabs. A comparison of the experimental results of a lateral loading of the building was made with results predicted by Vlasov's theory and qualitative agreement was reported. It was suggested that Vlasov's theory could be applicable to the description of the behaviour of the building with floor slabs.

1.4 INVESTIGATIONS INTO THE BEHAVIOUR OF SHEAR WALL BUILDINGS COMPRISED OF SHEAR WALLS AND FLOOR SLABS

An investigation into the behaviour of one and two storey reinforced concrete shear wall assemblies was conducted by Benjamin and Williams (9). The one-quarter scale buildings studied had parallel shear walls connected by a reinforced concrete diaphragm. The buildings were loaded in torsion at the diaphragm level. The authors concluded that if shearing distortion predominated in the walls of a tall building, the structure could be analyzed using single-storey theory. This recommendation was not verified.

Taranath and Morice (10) used the virtual work method to determine the elastic deformations of an open-box beam system. The authors reported agreement between the stress patterns found theoretically and experimentally using perspex models.

The stiffness method approach was used by several investigators. Tezcan (11) analyzed a shear wall structure comprised of interconnected shear walls and frames. Using a method suggested by Khan and Sbarounis (12), the floor slabs were considered as beams between adjacent columns. In Tezcan's analysis, the shear walls were considered as uni-dimensional members. Greater accuracy could have been achieved by idealizing the shear wall as a grid framework of two-dimensional plate units. Clough (13) and Tezcan (14) have given the stiffness matrices of two-dimensional plate elements. The assembly of columns, shear walls and frames of a tall building was then analyzed following a standard stiffness analysis. The shear distribution obtained

compared well with that distribution found using the method outlined by Khan and Sbarounis (12).

Jenkins and Harrison (15) used the stiffness matrix method to analyse tall buildings with shear walls. Two types of shear wall structures were examined and the results were compared with the results of experiments performed on perspex models. The use of the stiffness matrix method permitted the introduction of the finite element technique to determine the stiffness of the floor slabs. It was found that the stiffness matrix approach provided a suitable method for the analysis of tall structures containing shear walls.

Rosman (6) and Beck (4) each offered an analysis of shear walls interconnected by beams of rectangular cross-section. Barnard and Schwaighefer (16) determined the width of the strip of slab which acted as the coupling media between the walls. Then, the analysis of Rosman (16) and Beck (4) was applied to a slab-shear wall building. Tests were conducted on models constructed from 1/4 inch epoxy sheets. It was concluded first that the entire slab width was to be considered as the connecting medium between adjacent shear walls and secondly; that Rosman's theory predicted the stress distribution in the walls. A simplification of Rosman's theory was also proposed.

Coull (17) investigated the effective width of floor slabs acting in conjunction with a pair of in-line shear walls. Tests were conducted on a perspex model of a twenty-five storey shear wall building consisting entirely of walls and floor slabs. The author modified the analysis of Chitty (18) which replaced the discrete set of connections by an equivalent continuous medium. The modifications

took into account the finite depth and shear deflections of the walls. The behaviour of the building was somewhere between the two limiting cases of independent wall action and cantilever action of the building.

Coull (17) concluded that the building behaved as a set of coupled shear walls in which the coupling action of the floor slabs induced considerable axial force in the walls. On the basis of his investigations, the author suggested that the continuum technique was not capable of describing accurately the behaviour of such complex, three-dimensional structures. It was also suggested that further research in this field was necessary.

From the literature reviewed, it can be seen that there is an abundance of analytical approaches focused on the problem of the behaviour of planar shear wall buildings. However, the majority of the experimental investigations have been conducted on perspex models, using a wide variety of building and testing procedures. The problem of the three-dimensional shear wall building has been simplified to essentially a plane stress problem in these investigations.

It is evident that both analytical and experimental investigations into the behaviour of tall, three-dimensional shear wall buildings are necessary. The experimental investigation reported in this study deals with the behaviour of such a structure.

1.5 PRESENT INVESTIGATION

The purpose of this experimental investigation is to study the overall effect of the rigidly connected floor slabs on the behaviour of the basic small-scale shear wall building subject to a transverse static loading. For purposes of providing continuity between the various phases of the shear wall project, the shape and dimensions of the basic structure developed by Afsar (1) were used in this investigation. Qureshi (2) also maintained this policy of continuity between various phases of the program although certain modifications to the micro-concrete mix, the loading system and casting technique were initiated. These modifications were incorporated in this investigation so that the only difference between phases II and III of the project was the introduction of the circular wall openings in the second phase and floor slabs in the third. In this way, a direct comparison of the individual effects of circular wall openings and floor slabs on the behaviour of the small-scale shear wall building is possible.

CHAPTER 2

CONSTRUCTION OF BUILDINGS

2.1 CONSTRUCTION TECHNIQUE AND MATERIAL

In the first phase of the shear wall project, Afsar (1) developed a technique of casting small-scale shear wall buildings. The buildings were cast in a 3/4" plywood formwork using a micro-concrete material. The basic small-scale shear wall building is shown schematically in Figure 1.

Qureshi (2) made minor alterations to a second set of plywood forms and cast small-scale buildings with two vertical rows of circular openings in the back wall. Prior to the actual construction of the buildings in phase two of the project, the following major modifications were made in the construction procedure:

(a) The design mix of the micro-concrete material was changed to effect a lower shrinkage strain. The redesigned mix used was the following:

Portland Cement	28.6% *
Fine Ottawa Silica Sand	35.7%
1/8" Dolomitic Limestone	35.7%
Water (% by weight of Portland cement)	47.5%

(*percentage by weight)

(b) The buildings were cast without the attached aluminum base plate in order to eliminate a possible cause of hairline cracks which appeared in the buildings before testing.

(c) The buildings were not attached to the test-bed until shortly before the static loading was applied. This was done in an attempt to further reduce the possibility of the appearance of hairline cracks before testing.

The present experimental investigation deals with the study of the behaviour of the small-scale shear wall building with floor slabs, as shown in Figure 2. The major modifications mentioned above were incorporated into this third phase of the shear wall project. Phases two and three were concurrent investigations.

Using the casting procedures documented by Qureshi (2), two basic buildings were cast without wall openings. The precast floor slabs were installed in each building at a later date.

A senior undergraduate student studied the material properties of the micro-concrete used in each building. Static tests were conducted on 2" cubes and standard 6" diameter cylinders. Dynamic modulus tests were conducted on 4" x 3" x 16" prisimatic beams. The buildings and the test specimens were cured under similar conditions. The specimens were tested after various durations of curing.

The modulus of elasticity of the concrete materials determined by compression tests on standard 6" diameter cylinders ranged from 3.5×10^6 psi for Building I to 4.0×10^6 psi for Building II.

Table 1 illustrates the variations of compressive strengths as determined by tests on 2" cubes of the concrete material of Buildings I and II.

TABLE 1

COMPARISON OF COMPRESSIVE STRENGTHS OF 2" CUBES

CURING TIME	COMPRESSIVE STRENGTHS (psi)	
	BUILDING I	BUILDING II
24 hours	1800	2230
7 days	3930	4310
14 days	5330	5250
28 days	6850	5930

2.2 BUILDINGS WITH FLOOR SLABS

As can be seen in Figure 2, there are seven floor slabs at one foot centres in each bay of the two bay building. While the basic buildings were cast as previously described, the floor slabs were cast in a separate operation., A 3/4" plywood formwork was designed which would permit the casting of seven floor slabs at a time. Two such casting operations produced the required fourteen floor slabs. The slabs were 19 1/4" x 15 1/2" by 1/2" thick. They were made of the same micro-concrete material used in the casting of the buildings.

The method of installation of the floor slabs is seen in Plate 1. In this photograph, it can be seen that one slab in each bay is supported by a plywood falsework while the bonding compound, Colma Dur Gel, (manufactured by Sika Chemicals Co., New Jersey, U.S.A.) effected the bond between three edges of the floor slab and the building. After the bonding agent had cured sufficiently, the falsework was removed from under the installed floor slabs. The framework was then placed on top of the installed floor slab to support the installation at the next floor level. This procedure was continued from floor level to floor level until the last slabs were installed at a level 7' from the bottom of the building. The photograph shows the installation at this level.

2.3 QUALITY OF THE BUILDINGS

The technique of casting the basic buildings produces structures which are free of hairline cracks. These shrinkage cracks which plagued Afsar (1) were eliminated through several modifications introduced by Qureshi (2).

However, mention must be made of the non-uniform wall thicknesses which occurred in both buildings. The walls constituting the buildings were designed to be 0.5" thick. Table 2 shows the variations in wall thickness at various levels of the two buildings. There is no pattern to the recorded variations in wall thicknesses.

Qureshi (2) encountered similar difficulties and recorded higher variations in the wall thicknesses. In his recommendations, he has suggested various possible causes for these thickness variations and suggestions for minimizing their effects. However, the modifications required could not be implemented in this investigation.

Since there is no pattern to the thickness variations along the buildings, the effect of these variations on the behaviour of the buildings cannot be assessed.

TABLE 2

VARIATIONS IN WALL THICKNESS

(1/1000 of an inch)

HEIGHT (inches)	BUILDING I			BUILDING II		
	a	b	c	a	b	c
18	652	500	594	662	576	653
30	703	582	649	658	581	712
42	669	532	593	643	582	702
54	705	620	617	661	590	662
66	632	557	567	608	574	659
78	620	654	626	651	694	650
90	614	626	601	575	619	649

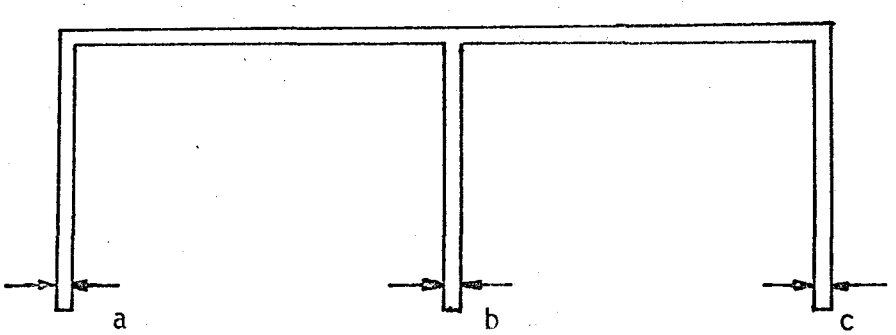

LOCATIONS OF THICKNESS MEASUREMENTS

CHAPTER 3

EXPERIMENTAL SET-UP

3.1 DESCRIPTION OF THE LOADING SYSTEM

In the first phase of the shear wall project, the aluminum loading cap described by Afsar (1) did not give a well-defined line of action of the applied load. This system was redesigned by Qureshi (2) to provide a well-defined line of loading along the back wall of the building. Further, the redesigned system maintained the E-shaped cross-section at the top of the building.

The aluminum plate capping system used in this investigation was similar to that used in the second phase of the project. As seen in Plate 2, it consisted of two parts. The narrow plate provided the line of loading and the wider plate maintained the shape of cross-section at the top of the building. Both parts of the system were comprised of two-inch aluminum angles bolted through slotted holes to a 1/4" thick aluminum plate.

In attaching the capping system to the top of the building, the angles were first loosely attached to the plates. This permitted adjustments to be made while aligning the angles with the walls of the building. After the two plates had been positioned on the top of the building, the angles were bonded to the walls using "Colma Dur Gel". (section 2.2) The nuts and bolts holding the angles to the plates were then tightened down and the bonding agent was allowed to cure.

The application of the transverse static loading along the top edge of the back wall was facilitated by using a manual screw-type jack. A gear

system was installed which permitted the load to be applied in very small increments. The load was transmitted to the capping system on the building through a calibrated load cell (1,2) and connecting devices. Plate 3 shows the loading system and the aluminum plate capping system in position for the testing of a building.

3.2 FIXING THE BASE OF THE BUILDING

Difficulty was encountered by Afsar (1) in his investigation, when several of the buildings cracked before testing. The problem of the cracked buildings was partially attributed to the method of fixing the base of the building. The technique used to fix the base of the building in the first phase of the project was to encase the bottom six inches of the building in a concrete pad. The concrete pad, poured in place around the base of the building, was anchored to the aluminum base plate. The plate was bolted to the floor.

To avoid the problems associated with the concrete base pad, a method of achieving a fixed base using slotted, two inch steel angles was developed. The building was not fixed to the base until after the building had been fully instrumented with dial and strain gauges.

Shortly before testing was to begin, the angles were loosely bolted to the base plate and adjusted so that close alignment was made between the angles and the walls of the building. The angles were bonded to the building and bolted to the base plate in a procedure similar to that described in Section 3.1.

3.3 INSTRUMENTATION

The positions and numbering sequence of the dial gauges used to measure the experimental deflections of the building are shown in Figures 3 and 4. These instruments were mounted on a steel tube framework. In the testing of Building I, thirty-nine dial gauges were used. Forty-eight gauges were used in the testing of the second building. In tests on the second building, three gauges were introduced at the tip of each flange at levels z = 28"; z = 52" and z = 88". The purpose of these gauges was to measure deflections perpendicular to the line of loading.

Figure 5 shows the locations and numbering sequence of the strain gauges used to measure the longitudinal strains developed in the buildings. In addition to the strain gauges shown, there was a total of six gauges mounted on various floor slabs. At the floor levels chosen, one gauge was mounted parallel to the line of the loading at the middle of the floor slab. Slabs at the first, fourth and seventh floor levels were instrumented with a strain gauge. A total of 36 strain gauges was used in both Building I and II.

It was recommended by Qureshi (2) that the installation of the strain gauges at the level z = 88" was unnecessary due to the extremely small values of the strain readings. Since this investigation, and that reported by Qureshi (2) were conducted concurrently, this modification to the instrumentation of the buildings could not be implemented. The recommendation was found to be valid.

Building II, shown in Plate 4, is fully instrumented and ready for testing.

CHAPTER 4

ANALYSIS

4.1 VLASOV'S THEORY

The theory used in the analysis aspect of this investigation is taken from a book by Vlasov entitled, "Thin-Walled Elastic Beams"(3). It is assumed that the theory documented in papers by Afsar (1) and Qureshi (2) is sufficient to describe the basic ideas and terminology of Vlasov's theory. Therefore, the description of theory in this study will concentrate on the application of that basic theory to the small-scale shear wall building with floor slabs.

Long prismatic shells, characterized by the fact that their three dimensions are all of different orders of magnitude, are called thin-walled beams.

The salient feature of thin-walled beams, according to Vlasov, is that they can undergo longitudinal extensions as a result of torsion. Consequently, longitudinal normal stresses, proportional to these strains are created. The longitudinal normal stresses arising as the result of the relative warping of the section are not examined in the theory of pure torsion. They can attain very large values in thin-walled beams with open (rigid or flexible) cross-sections and also in beams with closed flexible cross-sections.

Vlasov's theory is based on two geometrical hypotheses:

(a) a thin-walled beam of open section can be considered as a shell of rigid (undeformable) cross-section.

(b) the shearing deformations of the middle surface (characterizing

the changes in the angle between the co-ordinate lines) can be assumed to vanish.

Based on the first hypothesis, the deformation of a section of a thin-walled beam will consist of a rigid body rotation about the shear centre of the section and translations with respect to the shear centre. The deformation of a section is illustrated in Appendix 1.

If v and w represent the displacements in the OX and OY directions respectively of a point lying on an arbitrary cross-section of the beam, the following relations are obtained:

$$v(z,y) = \xi(z) - (y - a_Y)\,\theta(z) \qquad (4.1.1)$$

$$w(z,x) = \eta(z) - (x - a_X)\,\theta(z) \qquad (4.1.2)$$

In these expressions, x, y and z are co-ordinates of a point on the X, Y and Z axes. Z is the longitudinal axis of the beam. The X and Y axes are the principal axes, forming with Z a left-handed orthogonal co-ordinate system with its origin at the centroid of the section, point O.

ξ and η are the displacements of the shear centre in the direction of the co-ordinate axes OX and OY respectively. θ is the angle through which the section rotates as a rigid body about the shear centre.

From the second assumption concerning the absence of shearing strain in the middle surface, the longitudinal displacement at a section z = constant can be written as:

$$u(z,s) = \zeta(z) - \xi'(z)x(s) - \eta'(z)y(s) - \theta'(z)\omega(s) \qquad (4.1.3)$$

In this expression, $s(x,y)$ is the co-ordinate along the contour line S of the section with respect to a conveniently chosen origin on the contour.

The longitudinal displacements given by the sum of the first three terms of equation (4.1.3) are the results of combined extension and bending in the OXZ and OYZ planes. $\zeta(z)$ is the axial deformation. The bending deformation is represented by the functions $\xi(z)$ and $\eta(z)$ which describe the flexure of an arbitrary axis of the beam in the longitudinal planes OXZ and OYZ. The fourth term represents that part of the total displacement which arises as the result of torsion. Vlasov defines this as the sectorial warping of the section and it is described by the generalized co-ordinate $\omega(s)$, called the sectorial area. The sectorial area concept is described in Appendix A.

Knowing the longitudinal displacements $u(z,s)$ of the points of the middle surface, the longitudinal strain ε can be determined by taking the derivative of $u(z,s)$ with respect to z.

$$\varepsilon = \frac{\partial u}{\partial z} = \zeta'(z) - \xi''(z)x(s) - \eta''(z)y(s) - \theta''(z)\omega(s) \qquad (4.1.4)$$

Equation (4.1.4) shows that the relative longitudinal extensions $\varepsilon(z,s)$, at the section z = constant, are made up of extensions linear in the co-ordinates $x(s)$ and $y(s)$ of the point on the section, and extensions proportional to the sectorial area which arise as the result of the warping of the section.

The displacements and longitudinal strains at any point of the middle surface of a thin-walled beam can be determined using equations (4.1.1), (4.1.2) and (4.1.4) if the functions $\zeta(z)$, $\xi(z)$, $\eta(z)$ and

$\theta(z)$ are known.

These functions are determined using the linearly uncoupled differential equations derived from equilibrium conditions and given by Vlasov (8). By introducing the conditions of an eccentric, transverse load at the top edge of the building, these equations can be simplified to the following:

$$\begin{aligned} EA\zeta'' &= 0 \\ EI_Y\xi^{IV} &= 0 \\ EI_X\eta^{IV} &= 0 \\ EI_\omega\theta^{IV} - GI_d\,\theta'' &= 0 \end{aligned} \qquad (4.1.5)$$

In these expressions, A is the cross-sectional area. I_Y and I_X are the moments of inertia with respect to the Y and X axes respectively.

$$I_\omega = \int_A \omega^2 dA \qquad (4.1.6)$$

is the sectorial moment of inertia and is determined by the shape of the cross-section.

$$I_d = \frac{\alpha}{3} \Sigma\, d\delta^3 \qquad \text{where } \alpha = 1 \qquad (4.1.7)$$

is called the torsional rigidity of the section. E and G are the modulii of elasticity and shear respectively.

With a line of action along the back wall of the building in the negative Y direction, the loading creates an eccentricity e with respect to the shear centre. The effect of this load with respect to the line of shear centres is bending due to the flexural load P and torsion due to a counter-clockwise torsional moment,

$$M = Pe \qquad (4.1.8)$$

It is assumed that the compressive stresses due to self-weight are small enough to be neglected.

4.2 SOLUTION OF DIFFERENTIAL EQUATIONS

In the loading system used in the experimental investigation, there were no externally applied loads in the OZ and OX directions. Consequently, the functions ζ and ξ are both equal to zero. It is then necessary to solve the following differential equations:

$$EI_\chi \eta^{IV} = 0 \tag{4.2.1}$$

$$EI_\omega \theta^{IV} - GI_d \theta'' = 0 \tag{4.2.2}$$

Afsar (1) gave a detailed solution to equation (4.2.1) which is used in this investigation as an approximation to the bending component of the total deformation. The solution to equation (4.2.1) is given by:

$$\eta(z) = \frac{P}{6EI_\chi} \{3\ell z^2 - z^3\} \tag{4.2.3}$$

Consequently, differentiating twice,

$$\eta''(z) = \frac{P}{6EI_\chi} \{\ell - z\} \tag{4.2.4}$$

Equation (4.2.2.) can be rewritten in the form

$$\theta^{IV} - \frac{k^2}{\ell^2} \theta'' = 0 \tag{4.2.5}$$

where $k = \left\{\sqrt{\frac{GI_d}{EI_\omega}}\right\} \ell$

and ℓ is the span length of the beam along the generator making k a dimensionless quantity.

The general solution to equation (4.2.5) as derived in detail by

Afsar (1) is given by

$$\theta(z) = C_1 + C_2 z + C_3 \sinh \frac{k}{\ell} z + C_4 \cosh \frac{k}{\ell} z \qquad (4.2.6)$$

The general integrals for the warping,

$$\theta' = \frac{d\theta}{dz} \qquad (4.2.7)$$

and the generalized internal force factors B and H can also be determined.

The bimoment B, is one of four generalized, longitudinal forces describing the longitudinal displacement of a section. They are obtained by integrating over the area of the section, each of the products formed by multiplying the elementary longitudinal force σdA with the functions 1, x, y and ω.

The first three quantities determine the longitudinal force and the bending moment about the X and Y axes respectively. The fourth term B, the bimoment, corresponds to the sectorial warping of the section. It has units of pound-inch^2.

The bimoment is a generalized balanced force system statically equivalent to zero. It is determined, as described earlier, by

$$B = \int_A \sigma\omega dA \qquad (4.2.8)$$

where σ, from Hookes law, is given by

$$\sigma = E\{\zeta' - \xi''x - \eta''y - \theta''\omega\} \qquad (4.2.9)$$

Since 1, x, y and ω are the principal, generalized co-ordinates which satisfy the conditions of orthogonality,

$$B = -EI_\omega \theta'' \qquad (4.2.10)$$

Similarly, three generalized transverse forces, describing the transverse displacements of the section z = constant, can be determined. The first two are transverse forces while the third is H_ω, a flexural-torsional moment about the principal pole. It is found by using the shear force $\tau\delta$ which acts along the tangent to the contour of the section.

Further, due to the nonuniform distributions of the tangential stresses over the thickness of the wall, a torsional moment H_k must be taken into account. Therefore, by vector addition, H, the generalized external force factor in the transverse direction, is given by

$$H = -EI_\omega \theta''' + GI_d\theta' \qquad (4.2.11)$$

Now, from equations (4.2.6), (4.2.10) and (4.2.11), the total general solution to the homogeneous differential equation of torsion can be written

$$\begin{aligned}
\theta_z &= C_1 + C_2 z + C_3 \sinh\left(\frac{k}{\ell} z\right) + C_4 \cosh\left(\frac{k}{\ell} z\right) \\
\theta'_z &= C_2 + C_3 \frac{k}{\ell} \cosh\left(\frac{k}{\ell} z\right) + C_4 \frac{k}{\ell} \sinh\left(\frac{k}{\ell} z\right) \\
B_z &= -GI_d\{C_3 \sinh\left(\frac{k}{\ell} z\right) + C_4 \cosh\left(\frac{k}{\ell} z\right)\} \\
H_z &= GI_d C_2
\end{aligned} \qquad (4.2.12)$$

In these equations, 1, z, $\sinh\left(\frac{k}{\ell} z\right)$ and $\cosh\left(\frac{k}{\ell} z\right)$ are particular, linearly independent solutions of equation (4.2.5). C_1, C_2, C_3 and C_4 are arbitrary constants.

This system of equations (4.2.12) applies in general to a thin-walled beam subjected to a transverse load which does not pass through the shear centre.

4.3 METHOD OF INITIAL PARAMETERS

The constants of integration of the system of equations (4.2.12) are determined by using the method of initial parameters as described by Vlasov (3).

In this method, the origin of the co-ordinate Z is placed at some arbitrary section of the beam. The geometrical and statical factors involved in the description of the torsion of the beam by the law of sectorial areas have prescribed values for this section. External forces are not considered in the determination of these factors. That is, the beam is subjected to the action of the initial parameters only.

Setting z = 0 for this section and denoting the parameters as θ_{z_o}, θ'_{z_o}, B_{z_o}/GI_d and H_{z_o}/GI_d, the following expressions are obtained from the set of equations (4.2.12):

$$\begin{aligned} \theta_{z_o} &= C_1 + C_4 \\ \theta'_{z_o} &= C_2 + \frac{k}{\ell} C_3 \\ B_{z_o} &= -C_4 GI_d \\ H_{z_o} &= C_2 GI_d \end{aligned} \qquad (4.3.1)$$

Solving for the constants of integration,

$$\begin{aligned} C_1 &= \theta_{z_o} + \frac{1}{GI_d} B_{z_o} \\ C_2 &= \frac{1}{GI_d} H_{z_o} \\ C_3 &= \left(\frac{\ell}{k}\right) \theta'_{z_o} - \left(\frac{\ell}{k}\right) \frac{1}{GI_d} H_{z_o} \end{aligned} \qquad (4.3.2)$$

$$C_4 = - \frac{1}{GI_d} B_{z_o}$$

Substituting for C_1, C_2, C_3 and C_4 in the system of equations (4.2.12), the general equations for the method of initial parameters become:

$$\theta_z = \theta_{z_o} + \frac{\ell}{k} \theta'_{z_o} \{\sinh (\frac{k}{\ell} z)\} - \frac{1}{GI_d} B_{z_o} \{\cosh (\frac{k}{\ell} z) - 1\}$$

$$+ \frac{1}{GI_d} H_{z_o} \{z - \frac{\ell}{k} \sinh (\frac{k}{\ell} z)\}$$

$$\theta'_z = \theta'_{z_o} \cosh (\frac{k}{\ell} z) - \frac{k}{\ell} \frac{1}{GI_d} B_{z_o} \{\sinh (\frac{k}{\ell} z)\} \qquad (4.3.3)$$

$$+ \frac{1}{GI_d} H_{z_o} \{1 - \cosh (\frac{k}{\ell} z)\}$$

$$B_z = - \frac{\ell}{k} GI_d \theta'_{z_o} \{\sinh (\frac{k}{\ell} z)\}$$

$$+ B_{z_o} \cosh (\frac{k}{\ell} z) + \frac{\ell}{k} H_{z_o} \{\sinh (\frac{k}{\ell} z)\}$$

$$H_z = H_{z_o}$$

The set of equations (4.3.3) defines a set of linear transformations of the known flexural-torsional factors of the initial section; θ_{z_o}, θ'_{z_o}, B_{z_o}/GI_d and H_{z_o}/GI_d at $z = 0$, designated by z_o, into the flexural-torsional factors θ_z, θ'_z, B_z/GI_d and H_z/GI_d at the section $z = z$, where z is the longitudinal co-ordinate of the section. The coefficients of this set

of equations are given in tabular form in Table 3.

The initial parameters θ_{z_o}, θ'_{z_o}, B_{z_o}/GI_d and H_{z_o}/GI_d are determined in general by imposing the particular boundary conditions of the beam being investigated to either the set of equations (4.3.3) or the tabular representation of these equations, Table 3.

The method of initial parameters is now extended to cover the integration of the homogeneous equation resulting from various concentrated force factors arbitrarily placed along the beam.

Consider a beam with initial parameters θ_{z_o}, θ'_{z_o}, B_{z_o}/GI_d and H_{z_o}/GI_d at $z = z_o$, and concentrated factors θ_{z_t}, θ'_{z_t}, B_{z_t}/GI_d and H_{z_t}/GI_d acting on the beam at $z = z_t$. For a section $z_1 \geq z_t$, the total factors θ_{z_T}, θ'_{z_T}, B_{z_T}/GI_d and H_{z_T}/GI_d at that level are determined by the superposition of two contributions.

The first contribution; θ_{z_1}, θ'_{z_1}, B_{z_1}/GI_d and H_{z_1}/GI_d, is determined by using the initial parameters θ_{z_o}, θ'_{z_o}, B_{z_o}/GI_d and H_{z_o}/GI_d and the transformation coefficients of Table 3 with the arguement z_1.

The second contribution is comprised of the factors θ_{z_1-t}, θ'_{z_1-t}, B_{z_1-t}/GI_d and H_{z_1-t}/GI_d, which are the result of the action of the concentrated factors θ_{z_t}, θ'_{z_t}, B_{z_t}/GI_d and H_{z_t}/GI_d, In this second case, the contributing factors are computed by using the concentrated factors: θ_{z_t}, θ'_{z_t}, B_{z_t}/GI_d and H_{z_t}/GI_d and the transformation coefficients of Table 3 with the arguement $(z_1 - t)$.

TABLE 3

BASIC TRANSFORMATION COEFFICIENTS *

	θ_o	θ'_o	B_o/GI_d	H_o/GI_d
θ_z	1	$\frac{\ell}{k} \sinh (\frac{k}{\ell} z)$	$1 - \cosh (\frac{k}{\ell} z)$	$z - \frac{\ell}{k} \sinh (\frac{k}{\ell} z)$
θ'_z	0	$\cosh (\frac{k}{\ell} z)$	$- \frac{k}{\ell} \sinh (\frac{k}{\ell} z)$	$1 - \cosh (\frac{k}{\ell} z)$
B_z/GI_d	0	$- \frac{\ell}{k} \sinh (\frac{k}{\ell} z)$	$\cosh (\frac{k}{\ell} z)$	$\frac{\ell}{k} \sinh (\frac{k}{\ell} z)$
H_z/GI_d	0	0	0	1

* by Vlasov's Theory

For that part of the beam where $z < z_t$; say z_2 where $z_2 < z_t$, the factors θ_z, θ'_z, B_z/GI_d and H_z/GI_d are found by using the initial parameters θ_{z_o}, θ'_{z_o}, B_{z_o}/GI_d and H_{z_o}/GI_d and the coefficients of Table 3 with the arguement z_2.

This superposition of the effects of the concentrated factors at the section $z = z_t$ on the level $z = z_1$ is shown by expanding Table 3 to form Table 4.

Using the law of superposition which follows from the linearity of the transformation illustrated by the coefficients of Table 3, the form of Table 4 can be generalized to more complicated cases of loading applied at various sections of the beam. These applied loads can be in the form of concentrated loads at a point of the section or loads continuously distributed over part of the length of the beam.

TABLE 4

GENERALIZED TRANSFORMATION COEFFICIENTS *

	θ_{z_o}	θ'_{z_o}	B_{z_o}/GI_d	H_{z_o}/GI_d	θ_{z_t}	θ'_{z_t}	B_{z_t}/GI_d	H_{z_t}/GI_d
z_T	1	$\frac{\ell}{k}\sinh(\frac{k}{\ell}z_1)$	$1-\cosh(\frac{k}{\ell}z_1)$	$z-\frac{\ell}{k}\sinh(\frac{k}{\ell}z_1)$	1	$\frac{\ell}{k}\sinh\{\frac{k}{\ell}(z_1-t)\}$	$1-\cosh\{\frac{k}{\ell}(z_1-t)\}$	$z-\frac{\ell}{k}\sinh\{\frac{k}{\ell}(z_1-t)\}$
$'_{z_T}$	0	$\cosh(\frac{k}{\ell}z_1)$	$-\frac{k}{\ell}\sinh(\frac{k}{\ell}z_1)$	$1-\cosh(\frac{k}{\ell}z_1)$	0	$\cosh\{\frac{k}{\ell}(z_1-t)\}$	$-\frac{k}{\ell}\sinh\{\frac{k}{\ell}(z_1-t)\}$	$1-\cosh\{\frac{k}{\ell}(z_1-t)\}$
$\frac{z_T}{I_d}$	0	$-\frac{\ell}{k}\sinh(\frac{k}{\ell}z_1)$	$\cosh(\frac{k}{\ell}z_1)$	$\frac{\ell}{k}\sinh(\frac{k}{\ell}z_1)$	0	$-\frac{\ell}{k}\sinh\{\frac{k}{\ell}(z_1-t)\}$	$\cosh\{\frac{k}{\ell}(z_1-t)\}$	$\frac{\ell}{k}\sinh\{\frac{k}{\ell}(z_1-t)\}$
$\frac{z_T}{I_d}$	0	0	0	1	0	0	0	1

* by Vlasov's theory

4.4 MATHEMATICAL REPRESENTATION OF THE EFFECT OF THE FLOOR SLABS ON THE BUILDING

Vlasov (8) found that the effect of a transverse plate situated at a section $z = z_k$ of a thin-walled beam on the behaviour of that beam was a concentrated, longitudinal bimoment.

This bimoment, given by

$$B = \frac{Eh^3\Omega}{12(1+\mu)} \theta'_{z_k} \qquad (4.4.1)$$

represents the effect of a floor slab on the behaviour of the small-scale shear wall building. In this expression, E is the modulus of elasticity of the floor slab material and μ is Poisson's ratio. The geometrical properties of the floor slabs are given by h, the thickness, and Ω, which is twice the area of the plate. θ'_{z_k} is the warping of the beam at the level of the floor slabs.

Based on the system of analysis established in this study, the superposition of the effect of a floor slab on the building can be given in the tabular form of Table 5. In these expressions, z_k is the level of the floor slab in the building and B_{z_k} is the bimoment at that section, representing the effect of a floor slab on the building.

Using Table 5 and knowing the initial parameters θ_{z_o}, θ'_{z_o}, B_{z_o}/GI_d and H_{z_o}/GI_d at $z = z_o$ and the properties of the floor slabs; the functions θ_{z_1}, θ'_{z_1}, B_{z_1}/GI_d and H_{z_1}/GI_d at a section $z = z_1$ can be determined. A typical floor slab is situated at $z = z_k$, where $z_o < z_k < z_1$. The equations relating the initial section $z = z_o$ and the final section $z = z_1$, including the effect of the floor at $z = z_k$ are

TABLE 5

TRANSFORMATION COEFFICIENTS INCLUDING EFFECT OF FLOOR SLAB *

	θ_{z_o}	θ'_{z_o}	B_{z_o}/GI_d	H_{z_o}/GI_d	B_{z_k}/GI_d
θ_z	1	$\frac{\ell}{k}\sinh\left(\frac{k}{\ell}z\right)$	$1-\cosh\left(\frac{k}{\ell}z\right)$	$z-\frac{\ell}{k}\sinh\left(\frac{k}{\ell}z\right)$	$1-\cosh\left\{\frac{k}{\ell}(z-z_k)\right\}$
θ'_z	0	$\cosh\left(\frac{k}{\ell}z\right)$	$-\frac{k}{\ell}\sinh\left(\frac{k}{\ell}z\right)$	$1-\cosh\left(\frac{k}{\ell}z\right)$	$-\frac{k}{\ell}\sinh\left\{\frac{k}{\ell}(z-z_k)\right\}$
B_z/GI_d	0	$-\frac{\ell}{k}\sinh\left(\frac{k}{\ell}z\right)$	$\cosh\left(\frac{k}{\ell}z\right)$	$\frac{\ell}{k}\sinh\left(\frac{k}{\ell}z\right)$	$\cosh\left\{\frac{k}{\ell}(z-z_k)\right\}$
H_z/GI_d	0	0	0	1	0

* by Vlasov's Theory

the following:

$$\theta_{z_1} = \theta_{z_o} + \frac{\ell}{k}\theta'_{z_o} \sinh\left(\frac{k}{\ell} z_1\right) + \frac{1}{GI_d} B_{z_o} \{1 - \cosh\left(\frac{k}{\ell} z_1\right)\} + \frac{1}{GI_d} H_{z_o} \{z_1 - \frac{\ell}{k} \sinh\left(\frac{k}{\ell} z_1\right)\} + \frac{1}{GI_d} \{\bar{k}\,\theta'_{z_k}\} \{1 - \cosh\left[\frac{k}{\ell}(z_1 - z_k)\right]\}$$

$$\theta'_{z_1} = \theta'_{z_o} \cosh\left(\frac{k}{\ell} z_1\right) - \frac{k}{\ell} \frac{1}{GI_d} B_{z_o} \sinh\left(\frac{k}{\ell} z_1\right) + \frac{1}{GI_d} H_{z_o} \{1 - \cosh\left(\frac{k}{\ell} z_1\right)\} - \frac{k}{\ell} \frac{1}{GI_d} \{\bar{k}\,\theta'_{z_k}\} \{\sinh\left[\frac{k}{\ell}(z_1 - z_k)\right]\} \qquad (4.4.2)$$

$$B_{z_1} = GI_d\,\theta'_{z_o} \{-\frac{\ell}{k} \sinh\left(\frac{k}{\ell} z_1\right)\} + B_{z_o} \cosh\left(\frac{k}{\ell} z_1\right) + H_{z_o} \{\frac{\ell}{k} \sinh\left(\frac{k}{\ell} z_1\right)\} + \{\bar{k}\,\theta'_{z_k}\} \{\cosh\left[\frac{k}{\ell}(z_1 - z_k)\right]\}$$

$$H_{z_1} = H_{z_o} = Pe$$

Note that $\frac{B_{z_k}}{GI_d} = \frac{Eh^3\Omega}{12(1+\mu)} \frac{\theta'_{z_k}}{GI_d}$

and that $\bar{k}$ has been substituted for $\frac{Eh^3}{12(1+\mu)}$

4.5 ANALYSIS OF THE BUILDING WITH FLOOR SLABS

The boundary conditions of the vertical cantilever building with floor slabs are the following:

$$\begin{aligned} &\text{at } z = 0, && \theta = 0 \\ & && \theta' = 0 \\ &\text{at } z = \ell && B = 0 \\ & && H = Pe \end{aligned} \tag{4.5.1}$$

Using Table 5 and the stated boundary conditions, the initial parameters can be determined. At $z = 0$, $\theta(0) = 0$ and $\theta'(0) = 0$. Therefore, from Table 5

$$\theta_{z_o} + 0 + 0 + 0 + 0 = 0 \tag{4.5.2}$$

$$0 + \theta'_{z_o} + 0 + 0 + 0 = 0 \tag{4.5.3}$$

It can be seen that $\theta_{z_o} = \theta'_{z_o} = 0$.

When applying the boundary condition that $B(\ell) = 0$, it is necessary to take into account the effect of the concrete floor slabs on the building. That is, it is not possible to relate the initial parameters θ_{z_o}, θ'_{z_o}, B_{z_o}/GI_d and H_{z_o}/GI_d at $z = z_o$ to the functions at $z = z_\ell$, where $B(\ell) = 0$, without taking into account the fact that each floor of the building has an effect on the relationship.

To illustrate this point, consider a building with a single floor slab which is located at the top of the building. Referring to Table 5, the equations relating the initial parameters at $z = z_o$ to those at $z = z_\ell$ can be written.

Therefore,

$$B_{z_o} \{\cosh (k)\} + \{\frac{\ell}{k} \sinh (k)\} Pe + B_{z_\ell} \{\cosh (k)\} = 0 \qquad (4.5.4)$$

Solving for B_{z_o}

$$B_{z_o} = -\left(\{\frac{\ell}{k} \sinh (k)\} Pe + B_{z_\ell} \{\cosh (k)\}\right) \Big/ \{\cosh (k)\} \qquad (4.5.5)$$

since $B_{z_\ell} = \frac{Eh^3\Omega}{12 (1 + \mu)} \theta'_{z_\ell}$

and substituting for B_{z_ℓ} in equation (4.5.5)

$$B_{z_o} = -\left(\{\frac{\ell}{k} \sinh (k)\} Pe + \theta'_{z_\ell} \frac{Eh^3\Omega}{12(1 + \mu)} \{\cosh (k)\}\right) \Big/ \{\cosh (k)\}$$

For this simplified case, B_{z_o} can be found by solving the three simultaneous equations represented by Table 5, for the three unknowns B_{z_o}, θ_{z_ℓ} and θ'_{z_ℓ}.

This simple solution is not possible in the building with seven floor slabs since the effect of each floor slab must be considered in sequence going from the bottom of the building to the top. The condition that $B = 0$ at $z = z_\ell$ cannot be applied until the last floor at $z = z_\ell$ is encountered in the progression from bottom to top.

It is, therefore, necessary to determine B_{z_o} subject to the influence of each of the seven concrete floor slabs and the aluminum capping plate. The procedure used in determing B_{z_o} will now be outlined.

Using Table 5, the relationship between the initial parameters at $z = z_o$ and the functions θ_{z_1}, θ'_{z_1}, and B_{z_1}/GI_d at the level of the first floor $z = z_1$ can be established. H is a constant value throughout the total height of the building and is equal to Pe, where P is the applied load and e is the eccentricity of the applied load with respect to the shear centre of the section. Then, using the functions θ_{z_1}, θ'_{z_1} and B_{z_1}/GI_d as the initial parameters for the second storey, the functions θ_{z_2}, θ'_{z_2} and B_{z_2}/GI_d, at the second floor level $z = z_2$, can be established as functions of θ_{z_1}, θ'_{z_1} and B_{z_1}/GI_d.

This step-by-step procedure is continued from floor level to floor level until the last floor level, the aluminum capping system at $z = z_8$, is encountered. At this level, the functions θ_{z_8}, θ'_{z_8} and B_{z_8}/GI_d will be written as functions of θ_{z_7}, θ'_{z_7} and B_{z_7}/GI_d.

In general, for the building being considered, there are three unknown functions; θ, θ' and B/GI_d, at each floor level, including the base and the aluminum plates at the top. Also, there are three equations which relate any two successive floor levels of the building. This results in a system of twenty-four equations in twenty-seven unknowns.

Introducing the boundary conditions $\theta_{z_o} = 0$, $\theta'_{z_o} = 0$ and $B_{z_8}/GI_d = 0$, the system of equations reduces to twenty-four equations in twenty-four unknowns. Therefore, the value of the initial parameter, B_{z_o} at $z = z_o$,

can be determined for each increment of the applied transverse load.

The four initial parameters at $z = z_o$ are now established. Incorporating the expressions of Table 5, it is now possible to determine implicit values for the functions θ, θ' and B/GI_d at any level of the building.

In the present analysis, the step-by-step procedure described previously is used to determine the functions at the half-way point between successive floors. The co-ordinates of the points being examined are introduced and using equations (4.1.4), (4.1.1) and (4.1.2), the theoretical strains and displacements can be determined.

CHAPTER 5

EXPERIMENTAL OBSERVATIONS AND COMPARISONS WITH THEORETICAL ANALYSIS

5.1 CRACKING PATTERNS

The two small-scale shear wall buildings studied in this investigation both failed suddenly, without any visible signs of the impending failure.

Building I failed in tension at a load of 660 pounds in corner c of the building. (Figure 24) The cracking patterns for Building I are shown in Plates 5, 6 and 7. The first two of the photographs show the pattern in flange 3. (Figure 24) As can be seen, the failure surface penetrated the wall. Plate 7 shows the extension of the failure surface along the back wall of the building. The crack appeared along the bottom of the building, adjacent to the 2" angle. In this photograph the arrow indicates the end of the visible crack.

Building II failed at 720 pounds. Plate 8 shows the cracking pattern on the inside of corner c . The pattern is visible along the inside of flange 3 and partway along the back wall. Plate 9 shows the cracking pattern along the back wall in corner c . The cracking pattern along flange 3 is seen in Plate 10.

Since both buildings failed suddenly, the progression of the failure surface was not observed.

5.2 LOAD-STRAIN RELATIONSHIPS

Figure 6 shows the relationship between the applied load and the resulting longitudinal strain for a typical strain gauge location. The theoretical curve, found using Vlasov's theory, is also shown.

Typical strain distributions for applied loads of 250 and 500 pounds are given in Figures 5, 6, 7 and 8. The distributions are given at levels z = 4" and z = 52" of Buildings I and II. The experimental values measured during the tests are superimposed on those distributions predicted by Vlasov's theory.

Reasonable agreement can be seen between the experimental strain distributions for similar loads on Buildings I and II. The experimental strain distributions are displaced towards the tension (+) side of the theoretical distributions. However, the shifts observed are not uniform in magnitude over the sections shown.

Comparing the observed distributions at z = 4" shown in Figures 7 and 8, there is no obvious relationship between the tension shifts when the applied load is doubled. Similarly, Figures 9 and 10 illustrate the same fact for the level z = 52". There is a qualitative agreement in the apparent tension shifts of the strain distributions in the two buildings tested. Figures 11 (a) and 11 (b) summarize the apparent tension shifts observed in the figures presented. In these figures, the datum used in each case was the theoretical strain distribution. The tension shift was chosen as the positive quantity.

In summary, the comparison of experimental and theoretical strain distributions show little agreement. There is, however, qualitative

agreement between the strain distributions measured experimentally in the two buildings.

5.3 LOAD-DEFLECTION RELATIONSHIPS

Typical experimental deflection patterns along the height of Buildings I and II are shown in Figures 12 and 13. These figures illustrate the relationship between height and deflection as a function of the applied load.

Figures 14 and 15 compare the measured experimental deflections with those deflections predicted by Vlasov's theory. Comparisons are made at 250 and 500 pounds.

The deflection behaviour of the interior points on each of the three flanges of both buildings is shown in Figures 16 and 17. The theoretical deflection patterns for loads of 250 and 500 pounds, as seen in Figures 16 and 17, show that each flange should behave exactly the same. It can be seen that the flanges do have a very similar deflection pattern.

This same comparison for the exterior points on the flanges is shown in Figure 18.

Figure 19 compares the deflections in the direction perpendicular to the line of loading in corners a and c of each building. At a load of 250 pounds, it can be seen that corner a deflects more than corner c. Figures 20 and 21, showing the rotated positions of the buildings, verify this observation. Vlasov's theory predicts that these deflections in the X-direction should be equal in magnitude and opposite in direction.

In Figures 22 and 23 the theoretical deflections due to bending and torsion are shown. It can be seen that the torsion component is considerably larger than the bending component. Shear deflection is

insignificant.

These height-deflection curves point out that there is little relationship between the deflections measured experimentally and those deflections predicted using Vlasov's theory. In each case, the experimental deflections far exceed the predicted deflections.

5.4 GENERAL BEHAVIOUR OF THE BUILDINGS

The height-deflection curves of the small-scale shear wall building with floor slabs are generally linear in form. The extended curves pass through the origin. This deflection pattern is totally unlike the cantilever-type deflection pattern predicted using Vlasov's theory. The theoretical curves become tangent to the height axis and have zero slope at the origin. When the linear, experimental curves are extended towards the origin, they intersect the axis at finite angles.

It is generally observed that for a given load, Building I deflected more than Building II. Referring to Section 2.2, the modulus of elasticity of Building I was less than that of Building II.

On the basis of Figures 16, 17 and 18, it can be observed that the three flanges of each building deflected in the same manner and to the same degree. The monolithic assembly of shear walls with rigidly installed floor slabs behaves as a unit, with all flanges deflecting uniformly.

Figures 20 and 21, showing the rotated positions of the buildings, verify that the two buildings behaved in a similar manner when loaded identically. Further, considering the fact that the material of Building I had a lower modulus of elasticity than that of Building II, it can be said that the two buildings responded exactly the same to the external loading.

As illustrated by the lack of agreement between the experimental and theoretical curves, the experimental buildings and theoretical model did not respond similarly to the applied loading.

5.5 DISCUSSION OF RESULTS

From the previous discussions regarding the comparisons between the theoretical and experimental curves, it is obvious that there is little agreement.

An apparent tension shift is seen in all experimental strain distributions. Vlasov's theory predicts that there is zero strain in the middle flange. However, the recorded experimental strain distributions shown in Figures 7, 8, 9 and 10 clearly show that a strain distribution does exist in this flange. Further, it follows the same trend as in the outer flanges, namely a tension shift. The tension shift is in each flange of the building at both load levels.

An attempt was made to account for this tension shift on the basis of a vertical component of the applied load. However, the vertical pull necessary to produce a uniform tension shift of the magnitude indicated was much in excess of the total applied load.

The appearance of such a strain distribution in the middle flange could be accounted for by a shift of the shear center from the axis of symmetry. Qureshi (2) suggested that a non-uniform wall thickness caused a shift in the shear center. This shift of the shear center resulted in unequal deflections of the corners of the buildings in the X-direction. (Figure 24) Unequal deflections of the corners in the direction perpendicular to the line of loading were observed in this investigation. (Figure 19)

The theoretical and experimental deflection-height curves show little agreement. (Figures 14 - 19) Shear deformation was considered as a possible addition to the theoretical deflections caused by

bending and torsion. Assuming that the shear is carried primarily by the back wall, the shear deformation was found to be negligible.

Vlasov (8) defines a thin-walled beam by the physical characteristic that their three dimensions are all of different orders of magnitude. Denoting the thickness of the wall by δ ; the width of a beam by d ; and the length of a beam by ℓ , Vlasov requires that:

(1) $\delta/d < 0.1$

(2) $d/\ell < 0.1$

The purpose of these general requirements is to ensure that the beam being investigated is flexible in the longitudinal direction. When the beam is flexible in the longitudinal direction, there is very little deformation of the cross-section. If these requirements are met, the thin-walled elastic beam theory is applicable.

The building studied in this investigation had the following ratios:

(1) $\delta/d \doteq 0.01$

(2) $d/\ell \doteq 0.4$

There are two factors which would influence the longitudinal flexibility of the building with floor slabs. First, the ratio, d/ℓ, of the buildings is approximately equal to 0.4. This fact would indicate that the building did not have the required flexibility in the longitudinal direction. Secondly, the introduction of the rigidly connected floor slabs at one foot centres along the height of the building would tend to make the building stiffer than a building without the floor slabs. It is suggested that the combination of these two stiffening factors definitely affected the behaviour of the

building by reducing the longitudinal flexibility. The reduced, longitudinal flexibility could account for the lack of agreement between theoretical and experimental curves.

The use of the concrete micro-mix material for the buildings tested introduces a number of uncertainties.

The extensive vibrating and working of the material, which is necessary in the casting of the building, induces segregation of the aggregates in the concrete mortar. It has been observed that the flange tips of the building are void of the concrete paste while the outside surface of the back wall is generally flaked from the excess of the hardened paste. Recalling that the walls are only 1/2" thick, it follows that a uniform modulus of elasticity does not exist in the building.

Building I was cycled, loaded and unloaded, four times to a maximum of 250 pounds. Loading to failure was carried out in the fifth cycle. Building II was cycled twice to a maximum of 250 pounds before being failed in the third cycle.

It is suggested that the combination of cyclic loading and the characteristic inelastic behaviour of the concrete material affected the values of the modulus of elasticity during the testing of the buildings. The theoretical analysis of the building is not greatly sensitive to changes in the elastic modulus. However, the effect on the experimental results of such changes is not known.

The dominant feature to be considered in the comparison of experimental and theoretical results is that the buildings studied do not completely satisfy the longitudinal flexibility requirements of

Vlasov's thin-walled elastic beam theory. The rigid floor slabs reduced the already insufficient longitudinal flexibility of the buildings. It is suggested that these factors are the major reason for lack of agreement between the theoretical and experimental results.

The cross-sections of the buildings do retain their E -shape as required by Vlasov's theory.

5.6 COMPARISON OF THE BEHAVIOUR OF BUILDINGS WITH WALL OPENINGS AND BUILDINGS WITH FLOOR SLABS

In phase II of the shear wall project, Qureshi (2) tested two buildings with two vertical rows of circular openings in the back wall. Building I failed at a load of 850 pounds and Building II failed at 900 pounds. Building II had two openings at z = 6".

In the investigation reported here, Buildings I and II failed at 650 and 720 pounds, respectively.

The two types of buildings had similar failure patterns with the failure surface generally along the base in corner c (Figure 24).

The deflection-height patterns recorded by Qureshi (2) had the same linear characteristics as those curves recorded in this investigation.

For illustrative purposes, a quantitative comparison of deflections is made for a dial gauge located one inch from the tip of flange 3 at level z = 38". At a load of 250 pounds the first Building investigated by Qureshi recorded a deflection 43% greater than his second Building. The deflection of the second Building was approximately equal to the deflection of the first Building of this investigation and was 31% greater than the second Building.

At 500 pounds, Qureshi's first Building deflected 55% more than the second. His second Building recorded deflections which were 9% and 41% greater than deflection of Buildings I and II, respectively, of this investigation.

The two types of buildings tested in phases II and III of the project had qualitative agreement in the shapes of the strain distributions.

The first Building investigated by Qureshi had strain distributions which agreed with those distributions predicted by Vlasov's theory. Building II produced only qualitative agreement with the theoretical distribution.

In this phase of the project, little agreement between theoretical and experimental strain distributions was apparent.

A general numerical comparison between the strain distributions recorded in these two phases of the project is difficult because of experimental scatter and non-uniform strain patterns. However, an indication of the differences in strain distribution can be seen by comparing strains at a strain gauge located 2" from corner c , (Figure 24), along flange 3 at level z = 4".

The second of Qureshi's Buildings had a strain level 33% greater than his first Building. His second Building also recorded strain levels 7% greater than the first Building tested in this investigation. Building II of this investigation recorded a strain level 50% greater than the second Building investigated by Qureshi.

CHAPTER 6

CONCLUSIONS AND RECOMMENDATIONS

6.1 CONCLUSIONS

It can be concluded, based on the experimental investigation reported here, that the cross-section of the building with floor slabs does not change shape during loading. A basic assumption of Vlasov's theory, which was used as the theoretical model in this investigation, was that the cross-section of the thin-walled elastic beam retain its shape during loading. The experimental building and theoretical model behaved similarly in this respect.

The height-deflection curves, which represent the response of the experimental building to the static loading, were linear in form. If extended towards the origin, these curves intersected the origin at finite angles.

The shape of these curves would indicate that the cantilever-type deflection patterns, predicted by the mathematical model, do not predict the behaviour of the experimental buildings.

Qualitative agreement was observed between the strain distributions determined experimentally for Buildings I and II. There was, however, little agreement between the experimental strain distributions and those distributions predicted by Vlasov's theory.

It is concluded that the experimental buildings responded similarly to the static loading. It is further concluded that the experimental and theoretical models did not respond in a similar manner to the static loading.

6.2 ASSESSMENT OF CONSTRUCTION AND TESTING TECHNIQUES

The technique of casting and construction of the buildings with floor slabs produces sound structures. However, since wood formwork is used in the casting phase, there are certain unaviodable faults with the basic building. The walls of the building are not uniform in thickness and the flanges suffer a segregation of the aggregates. The recommendations made by Quréshi (2) regarding the overhauling of the formwork were not implemented. It is suggested that they be adopted in an attempt to minimize the faults in the buildings.

Based on the findings of the present investigation, certain modifications in the instrumentation of the buildings can be suggested. The top row of strain gauges at the level z = 88" should be abandoned. More strain gauges should be installed at the levels z = 4" and z =52" in order to obtain a more detailed record of strain distributions.

Since the three walls of the building respond similarly to the static loading, it is not necessary to instrument all three walls with dial gauges. Two vertical lines of gauges on one wall will record the lateral displacements of the building. A vertical row of gauges at each outside corner of the building would give the deflection patterns in a direction perpendicular to the line of loading. Several horizontal rows of dial gauges would indicate the rotated position of the building.

In order to minimize the effects of the inelasticity of the concrete material on the experimental information, it is recommended that only two cycles of load be applied. The first cylce, to a low level of loading, would suffice to verify the instrumentation. Then,

the building would be loaded in increments to failure.

6.3 RECOMMENDATIONS

It is recommended that the finite element method be considered as a method of analyzing the complex, three-dimensional behaviour of the small-scale shear wall building with floor slabs. Six deformations at each corner of each element can be accounted for in the stiffness matrix of the building. Part, or all of these deformations could be used to describe the complex behaviour of the small-scale shear wall buildings with floor slabs.

Some considerations are necessary in selecting the unit element, although the form of the building would suggest the use of rectangular elements.

A concurrent investigation is being conducted in which the finite element approach is being used to predict the dynamic response of a T section. The section being tested consists of two 1/2" thick plates cast monolithically using the micro-concrete material used in the small-scale shear wall buildings. This T section is in effect a basic unit of the small-scale shear wall building. It can be seen that the results of this concurrent investigation could be applied to the present problem.

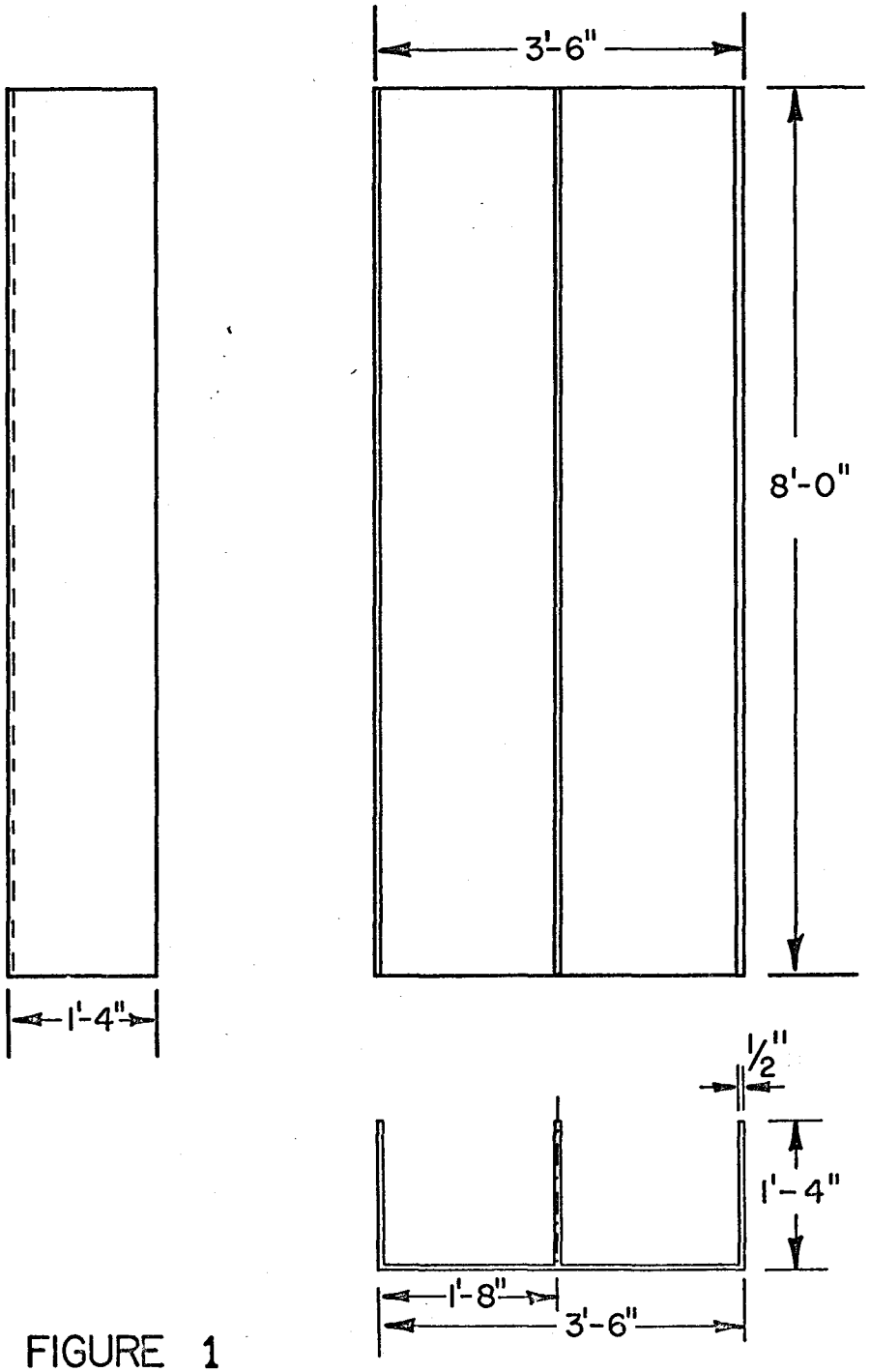

FIGURE 1

BASIC SMALL SCALE SHEAR WALL BUILDING

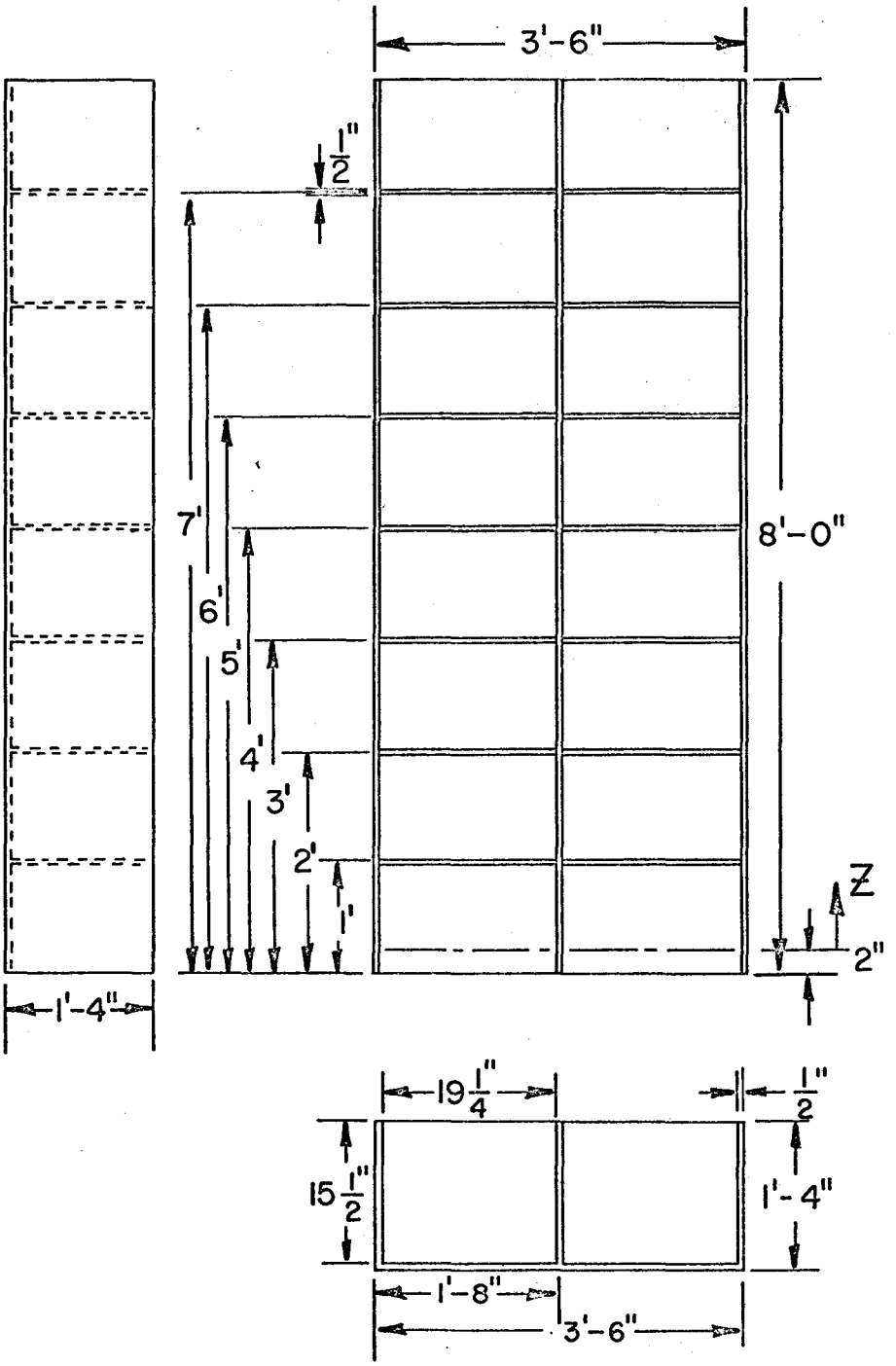

FIGURE 2.

SMALL SCALE SHEAR WALL BUILDINGS WITH FLOOR SLABS.

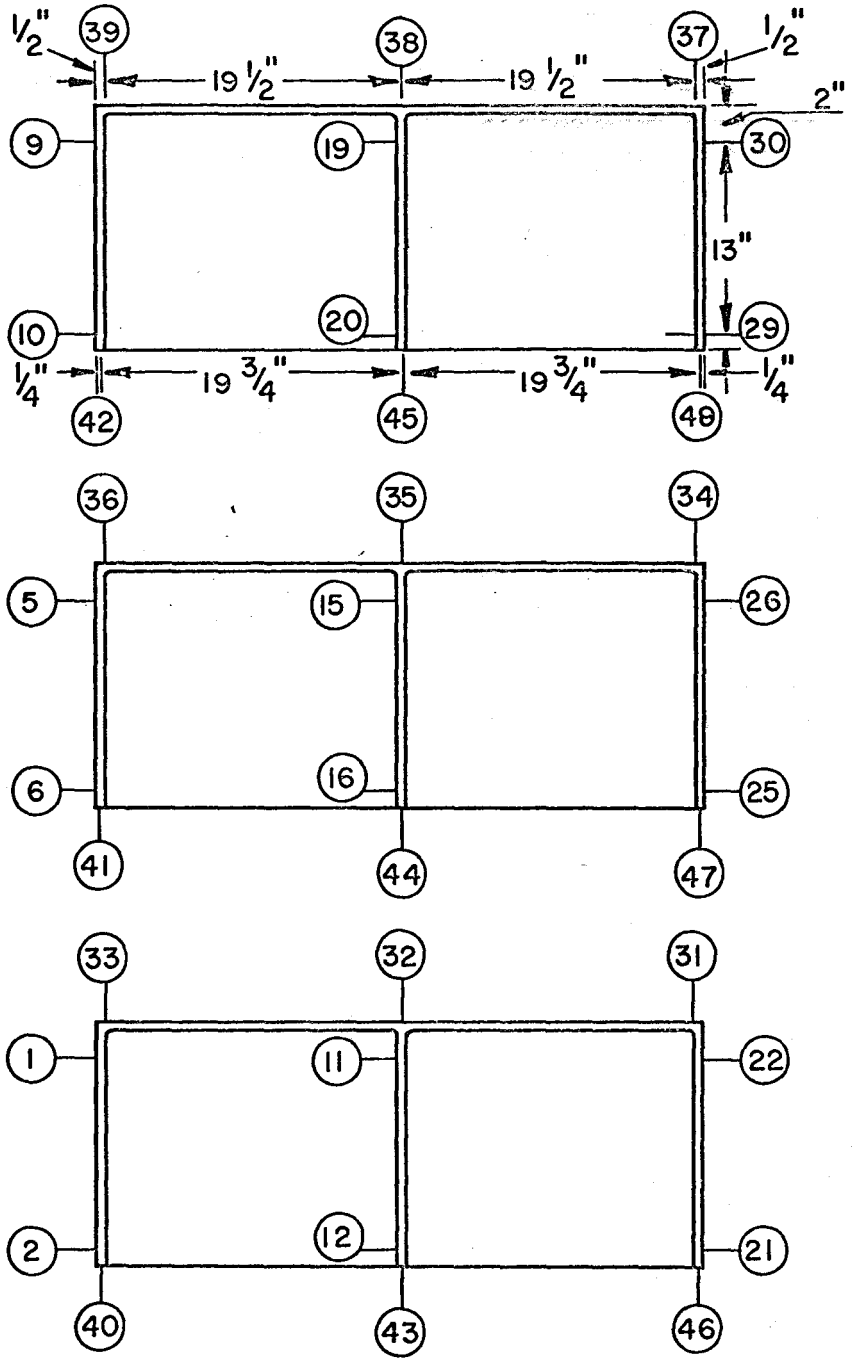

NOTE, EXTRA GAUGES USED ON BUILDING #2 NUMBER FROM 40 TO 48 INCLUSIVE

FIGURE 3.

DIAL GAUGE LOCATIONS AND NUMBERING SYSTEM AT Z = 16"; Z = 52"; Z = 88"

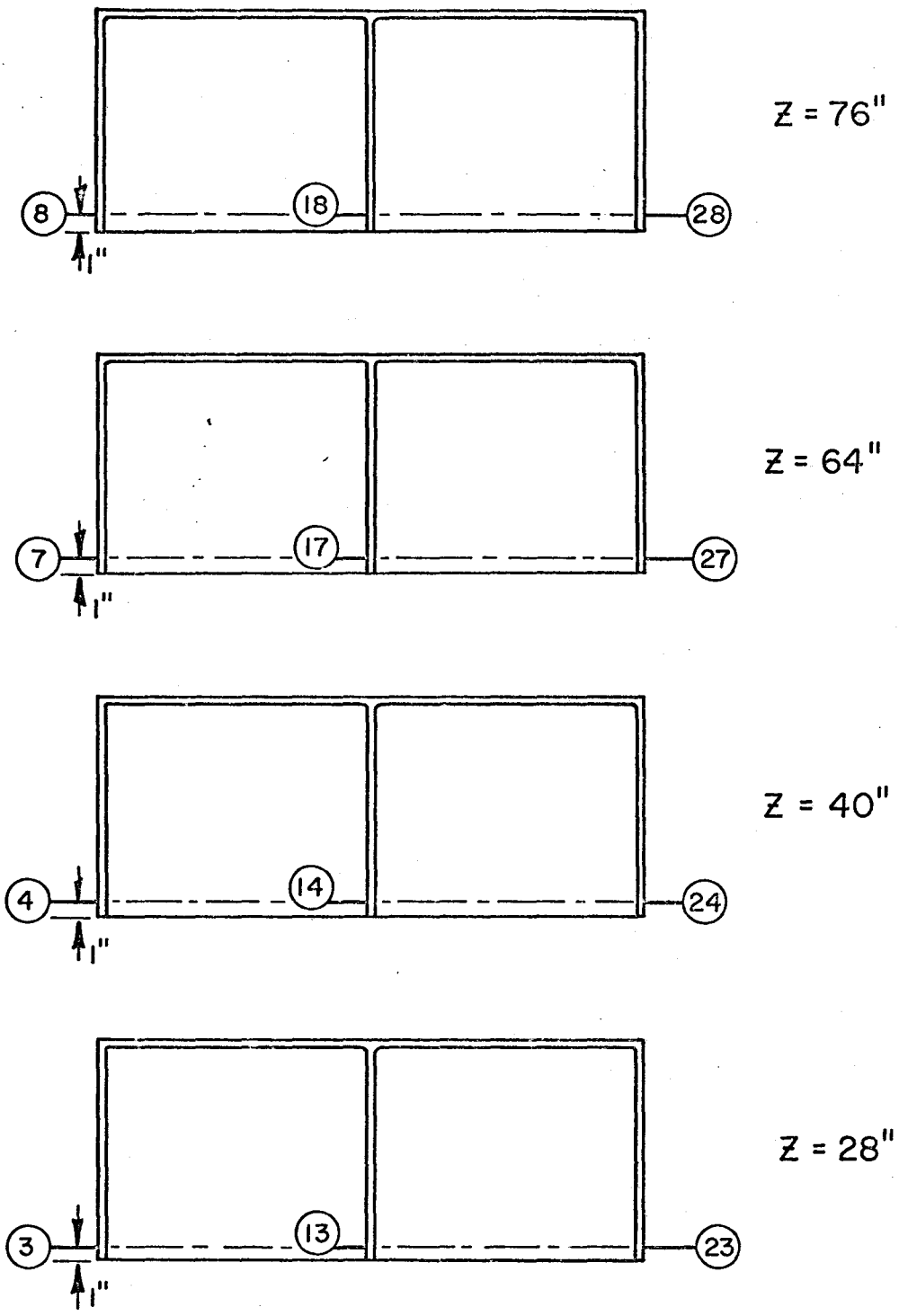

FIGURE 4

DIAL GAUGE LOCATIONS AND NUMBERING SYSTEMS AT Z = 28"; Z = 40"; Z = 64"; Z = 76"

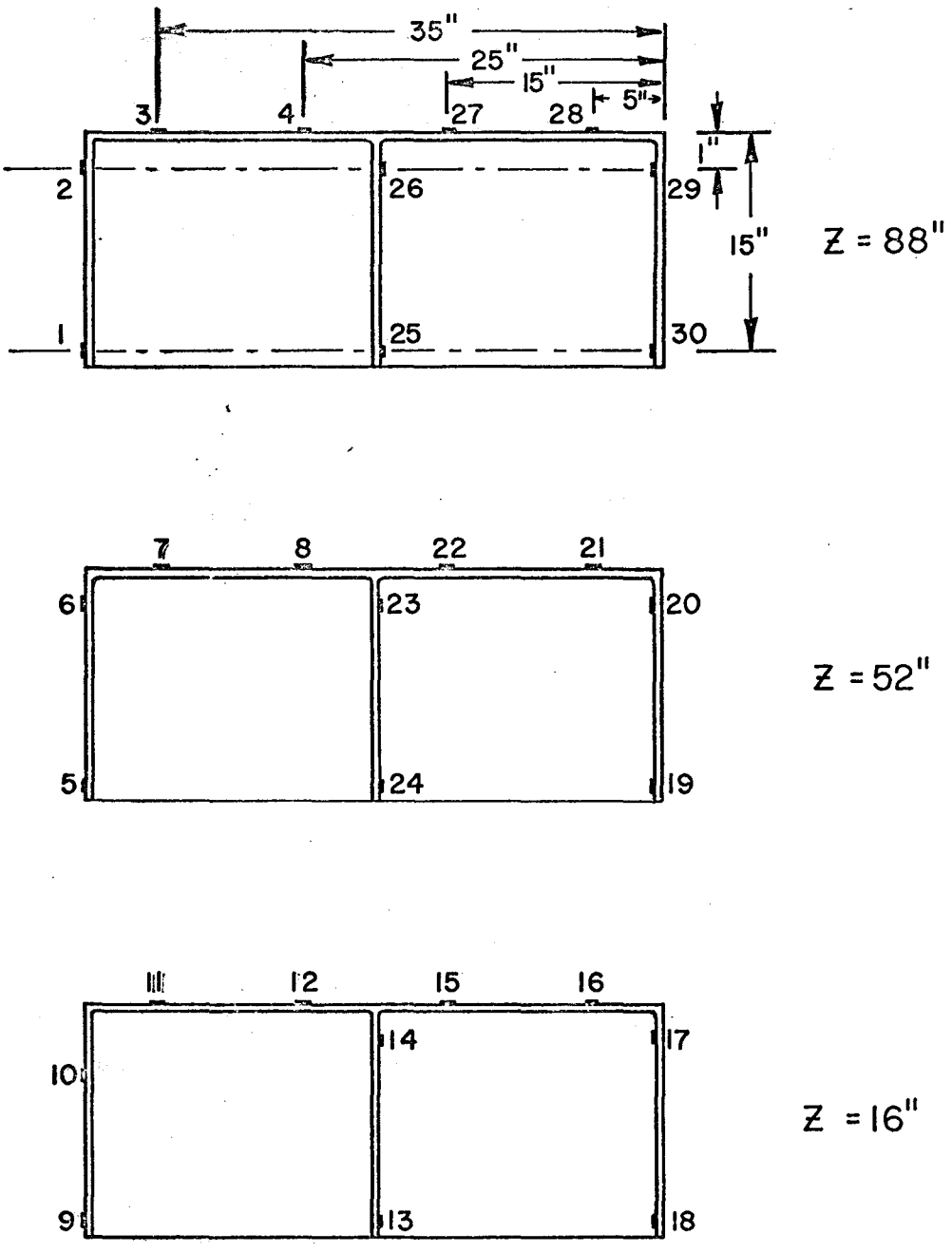

FIGURE 5

STRAIN GAUGE LOCATIONS AND NUMBERING SYSTEM AT LEVELS Z=16"; Z=52"; Z=88";

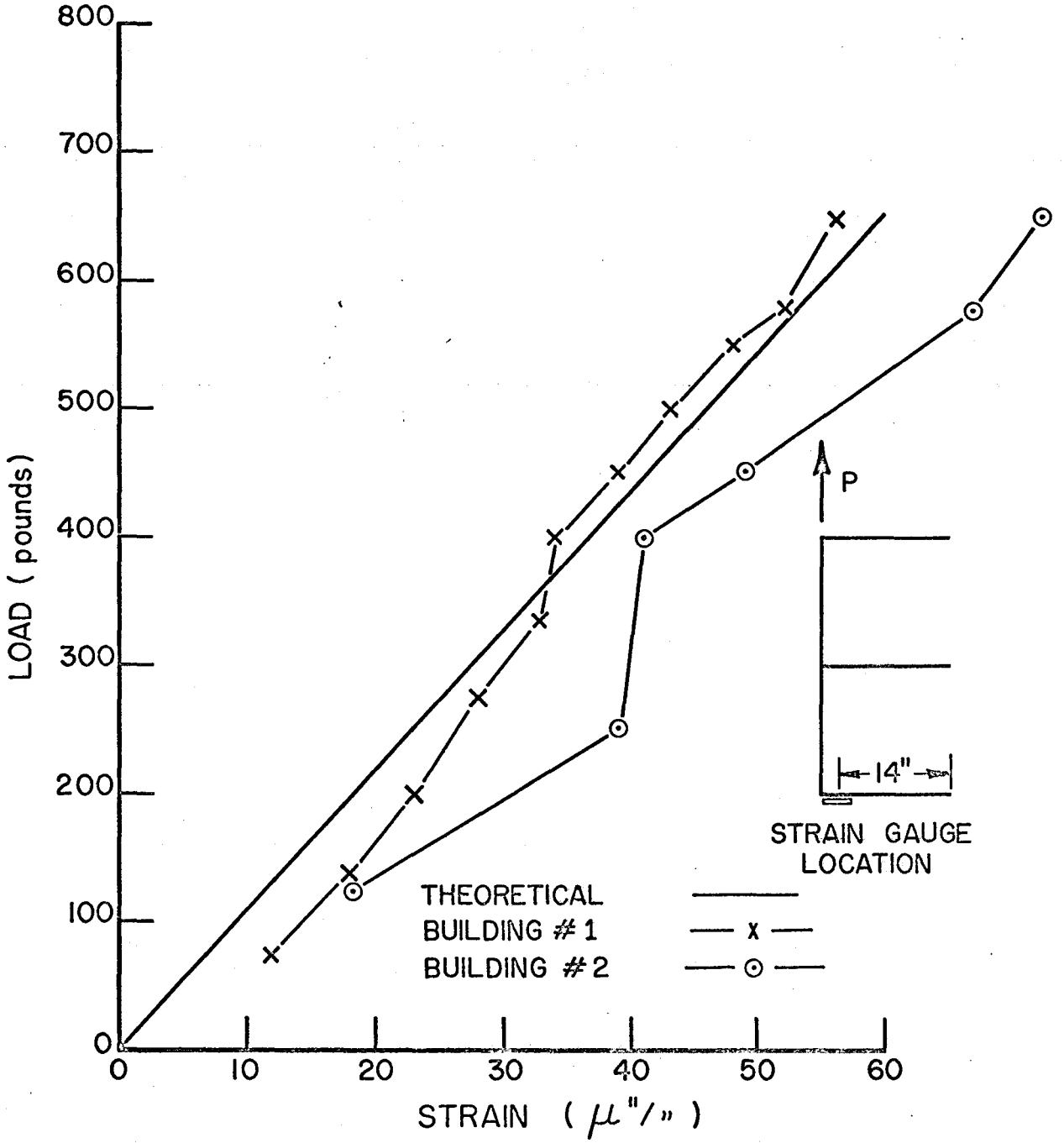

FIGURE 6

LOAD-STRAIN CURVES FOR SECTION $Z = 4"$

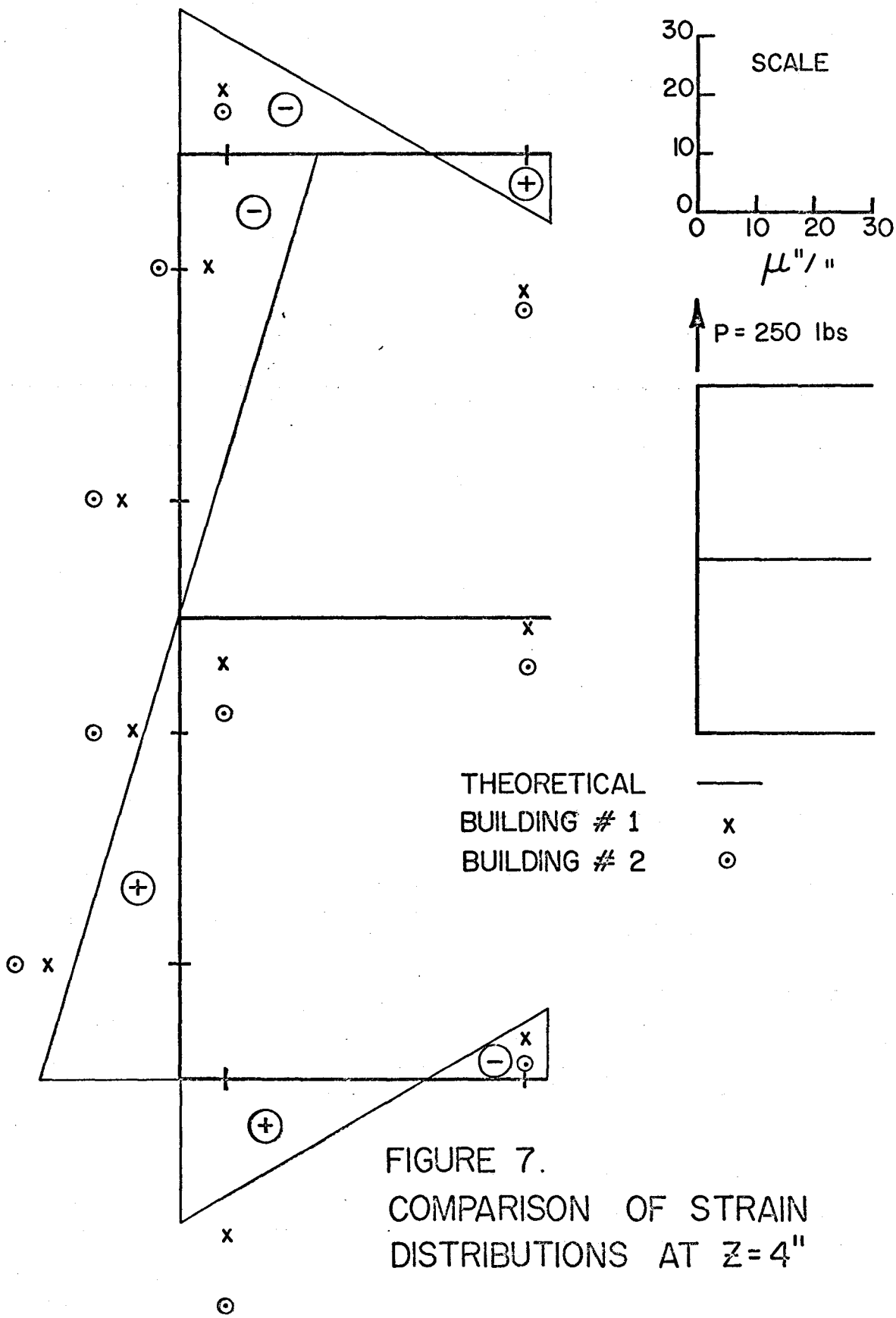

FIGURE 7.
COMPARISON OF STRAIN DISTRIBUTIONS AT Z = 4"

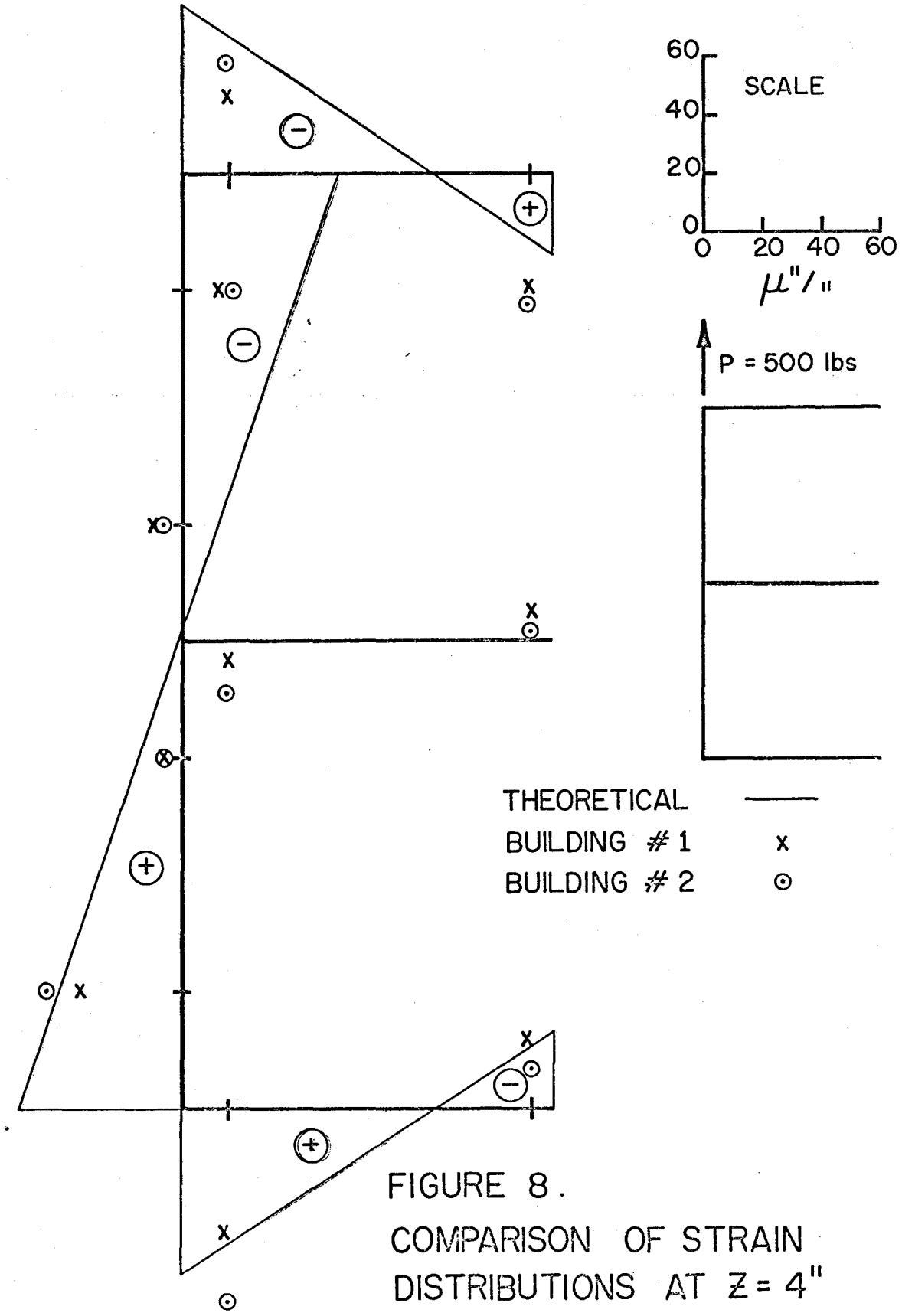

FIGURE 8.
COMPARISON OF STRAIN DISTRIBUTIONS AT Z = 4"

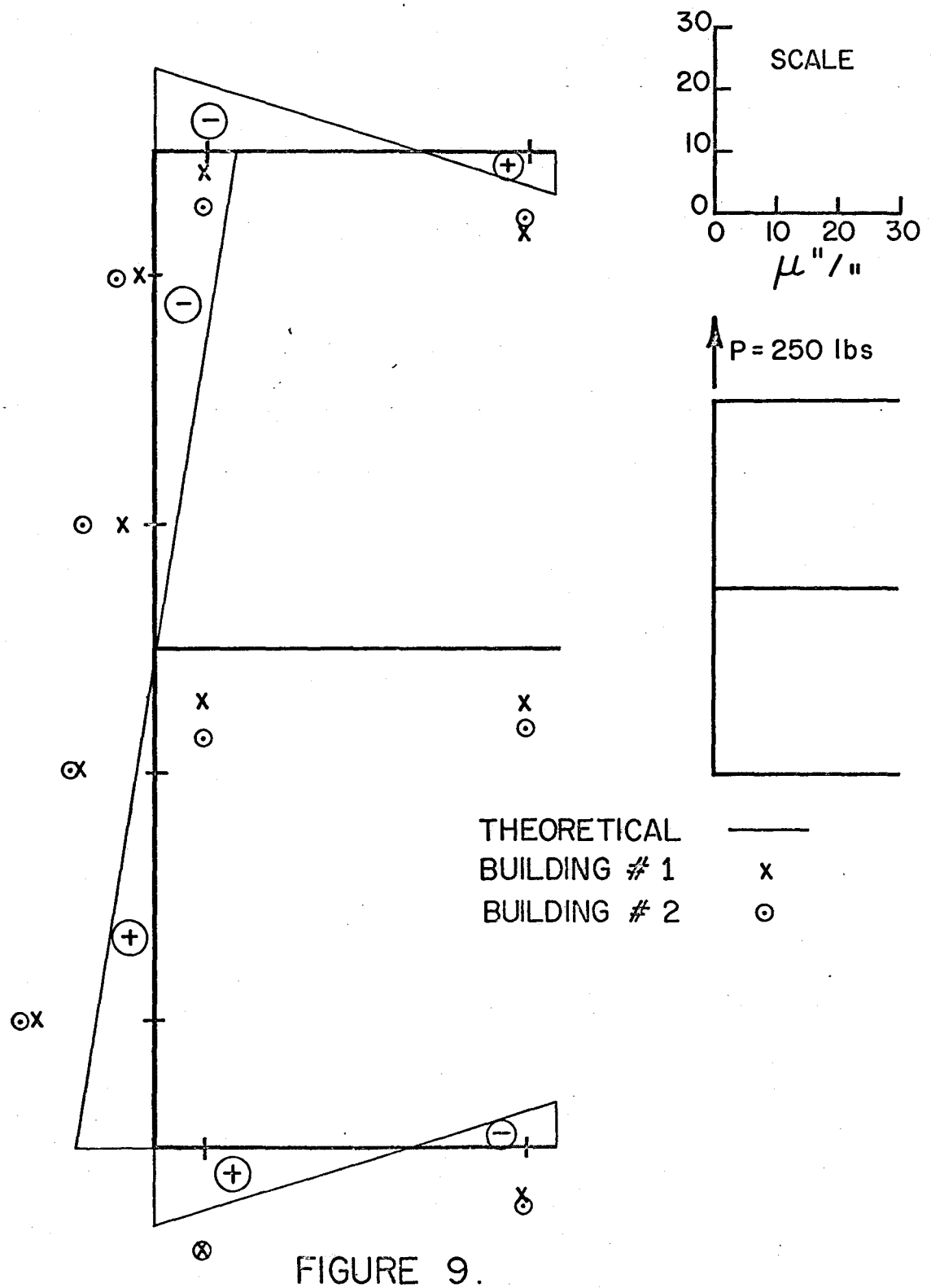

FIGURE 9.
COMPARISON OF STRAIN
DISTRIBUTIONS AT Z = 52"

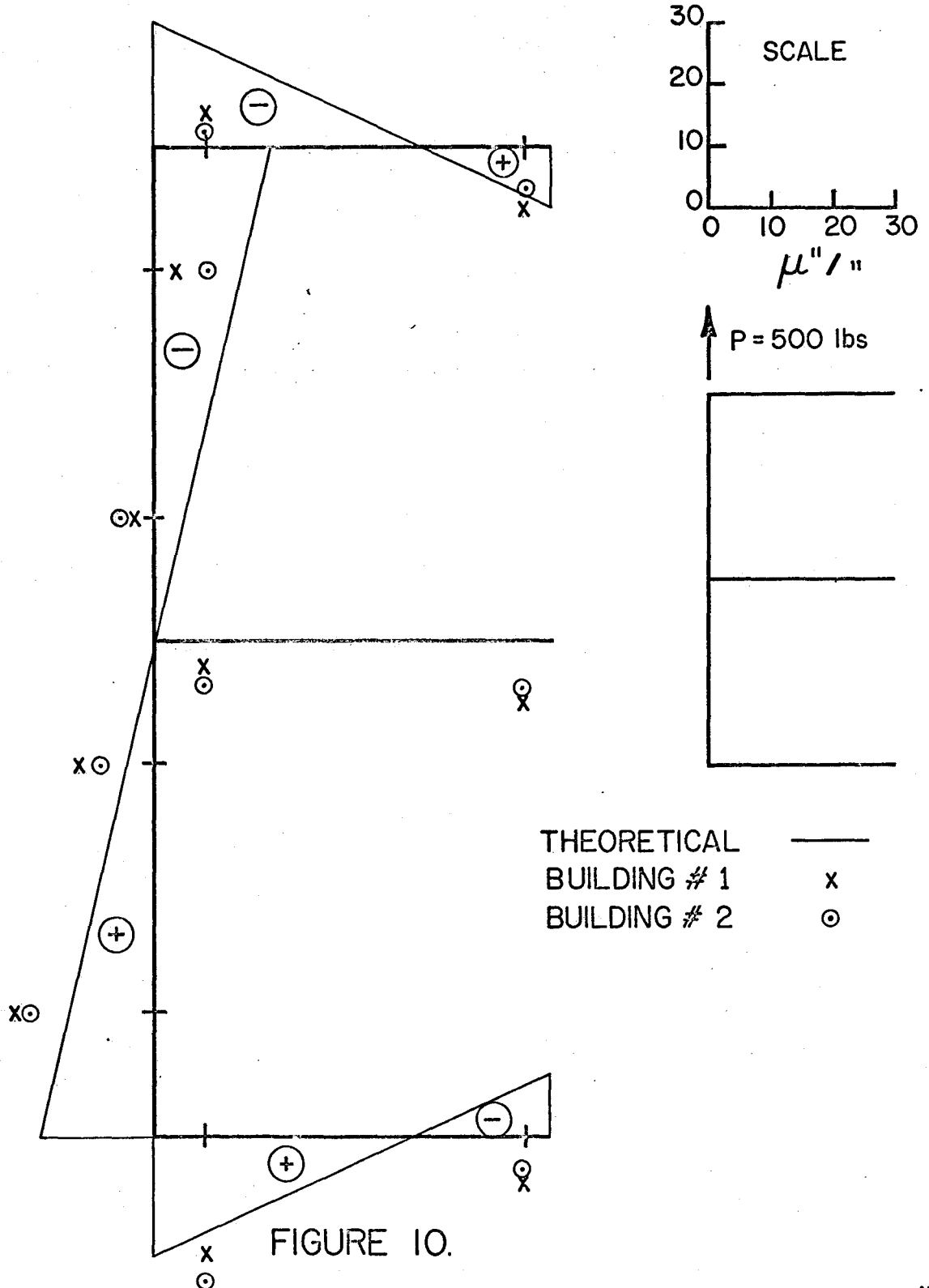

FIGURE 10.

COMPARISON OF STRAIN DISTRIBUTION AT Z=52"

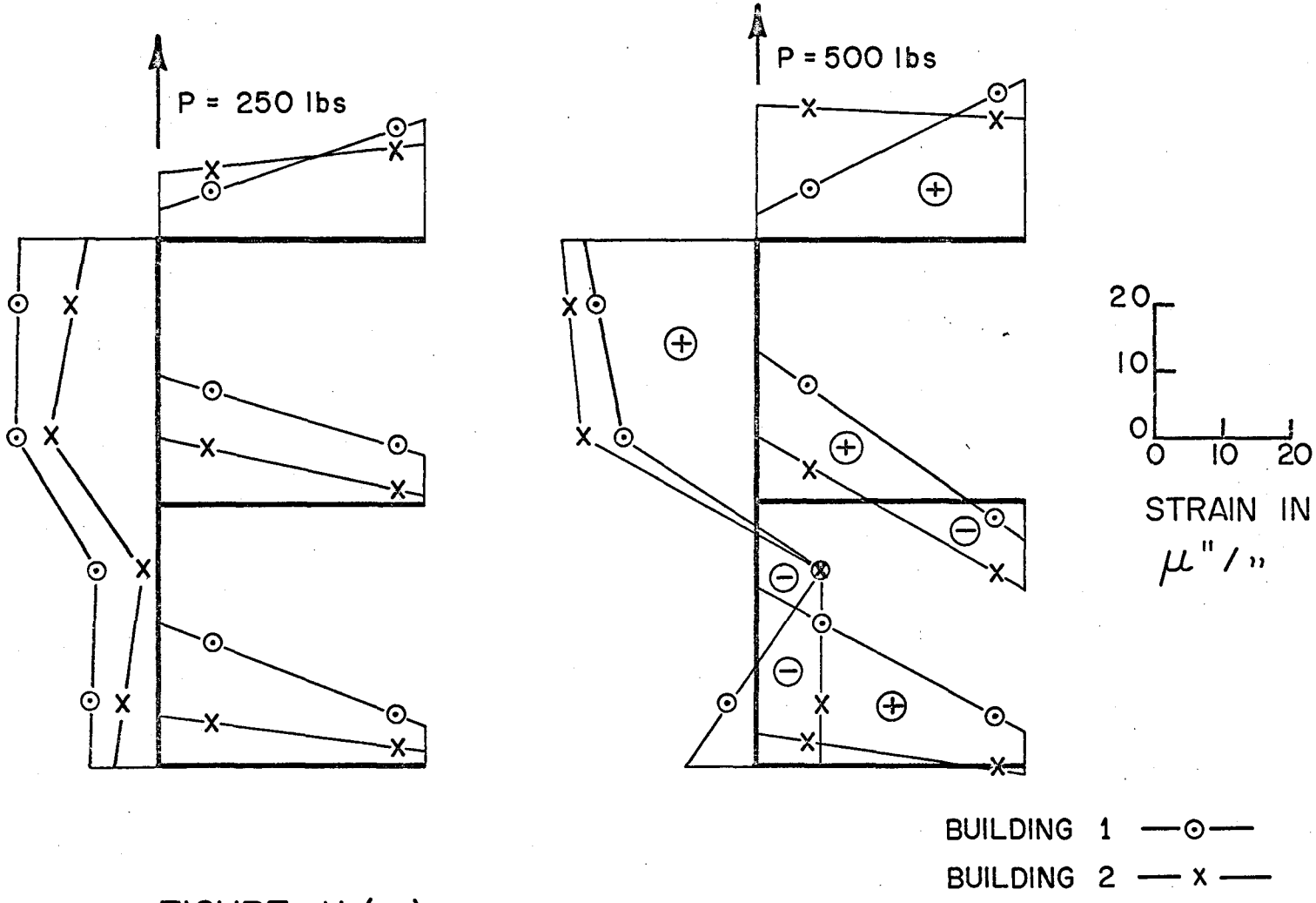

FIGURE 11 (a)

APPARENT TENSION SHIFTS AT LEVEL Z = 4"

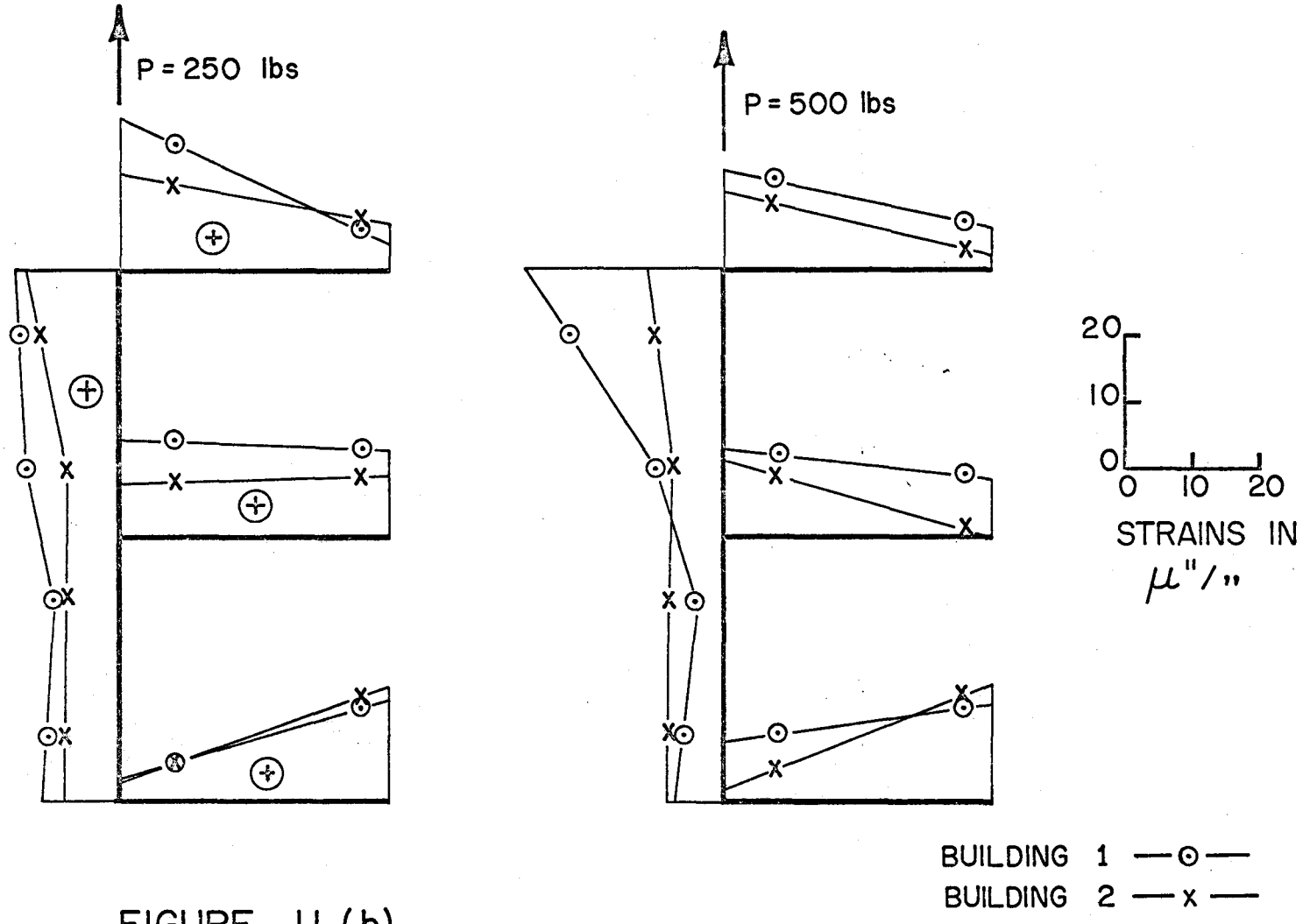

FIGURE 11 (b)

APPARENT TENSION SHIFTS AT LEVEL Z = 52"

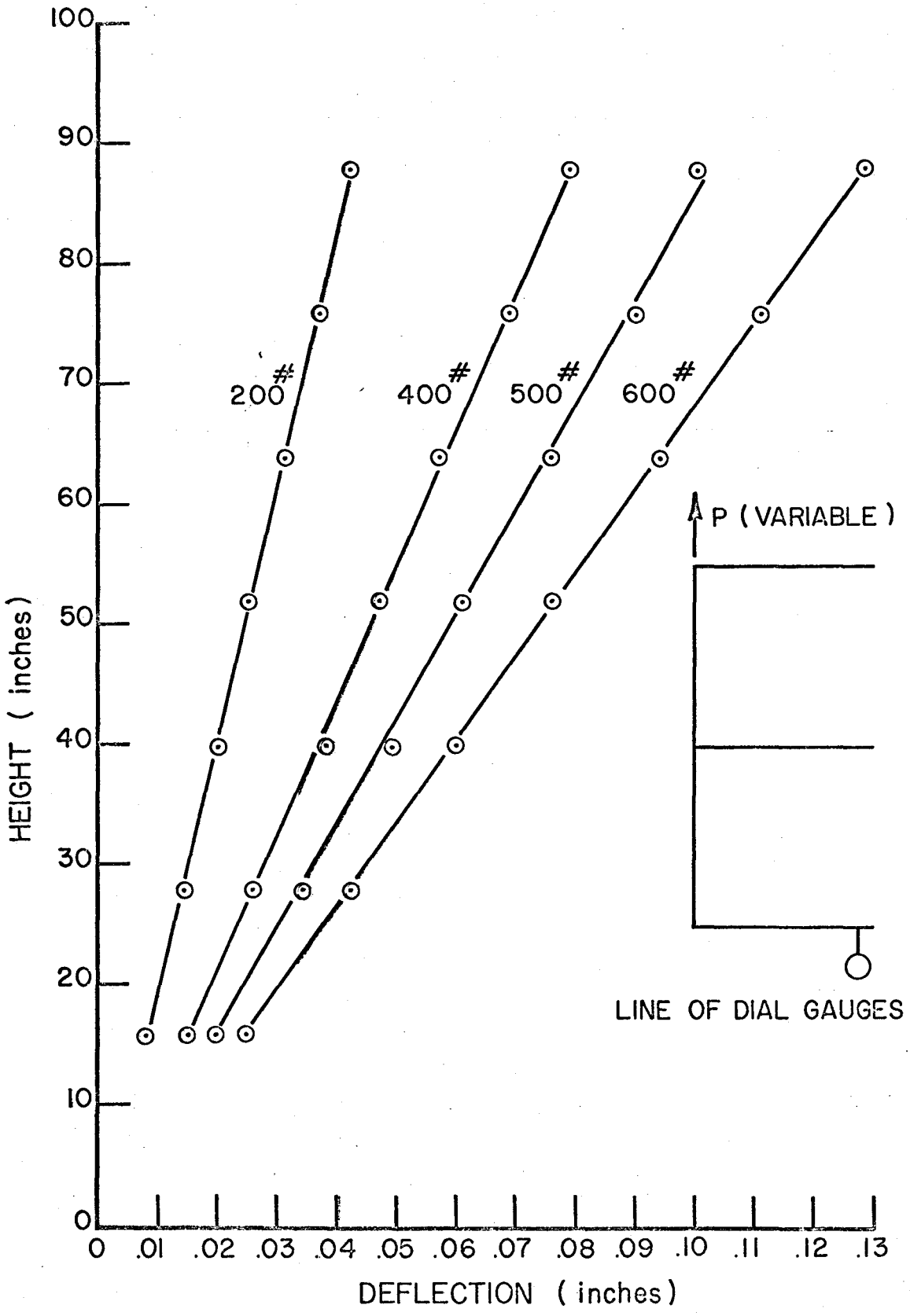

FIGURE 12 .
DEFLECTION PATTERNS ALONG THE HEIGHT OF BUILDING # 1

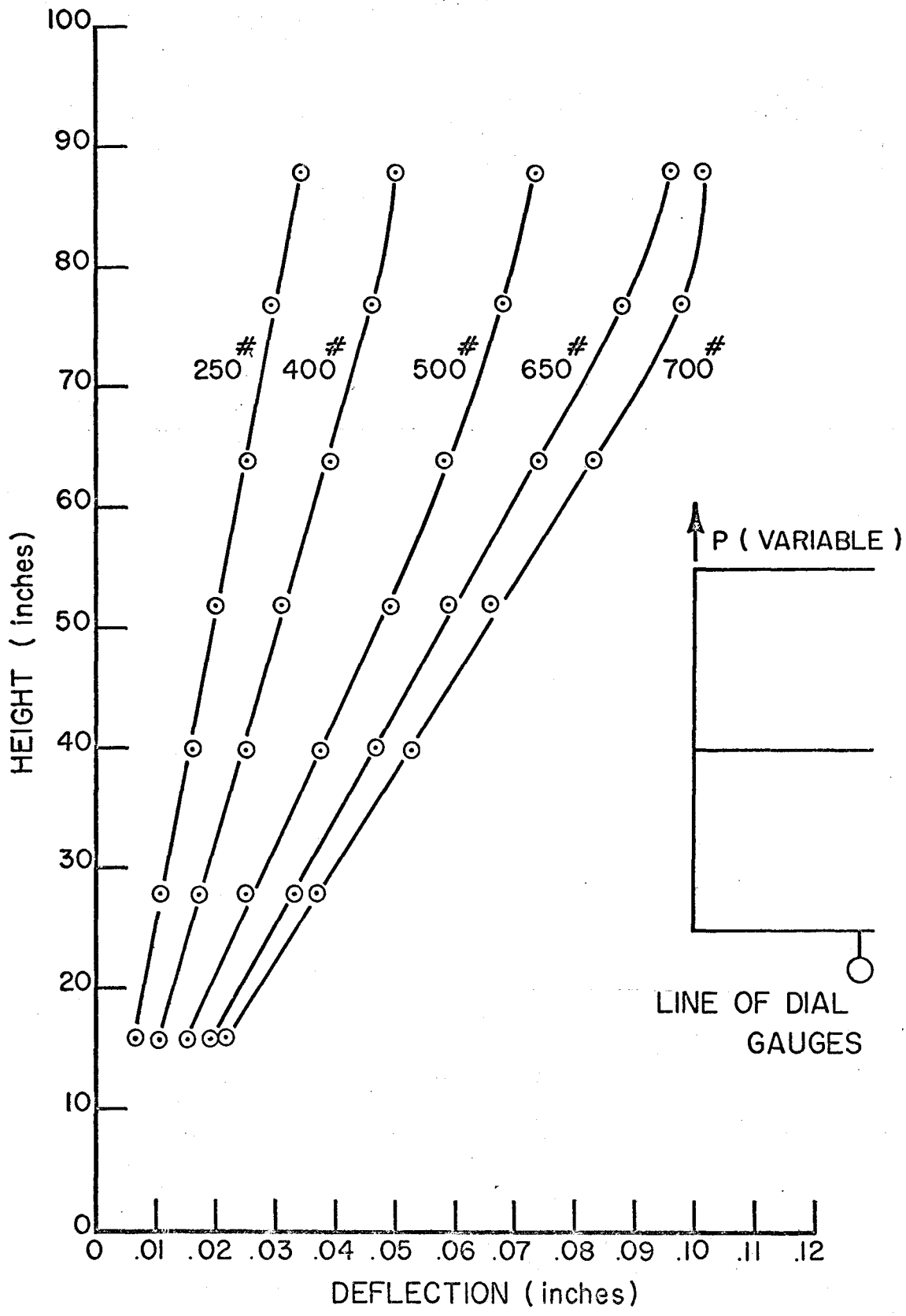

FIGURE 13
DEFLECTION PATTERNS ALONG THE HEIGHT OF BUILDING # 2 .

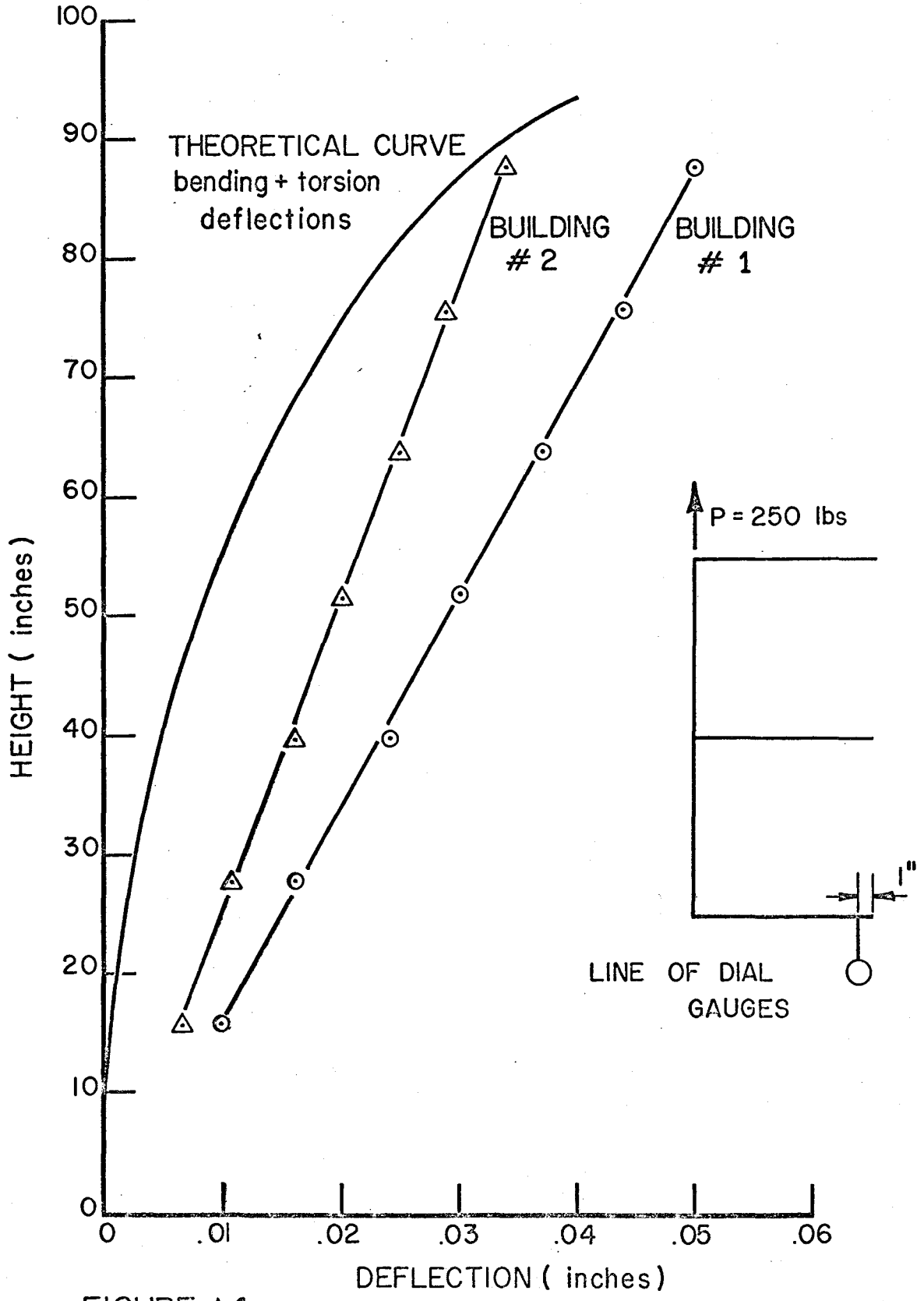

FIGURE 14.
COMPARISON OF THEORETICAL AND EXPERIMENTAL DEFLECTIONS

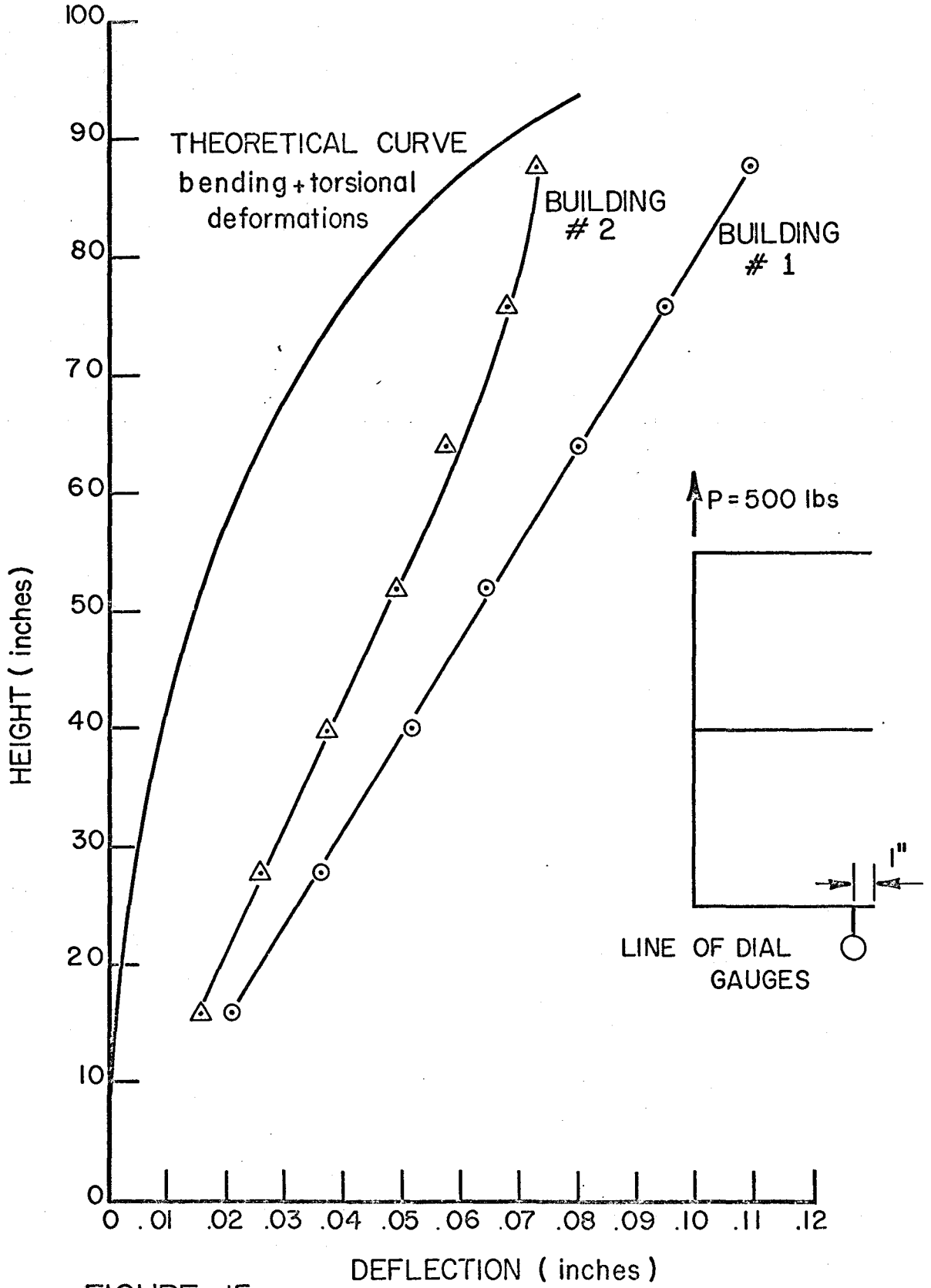

FIGURE 15.
COMPARISON OF THEORETICAL AND
EXPERIMENTAL DEFLECTIONS

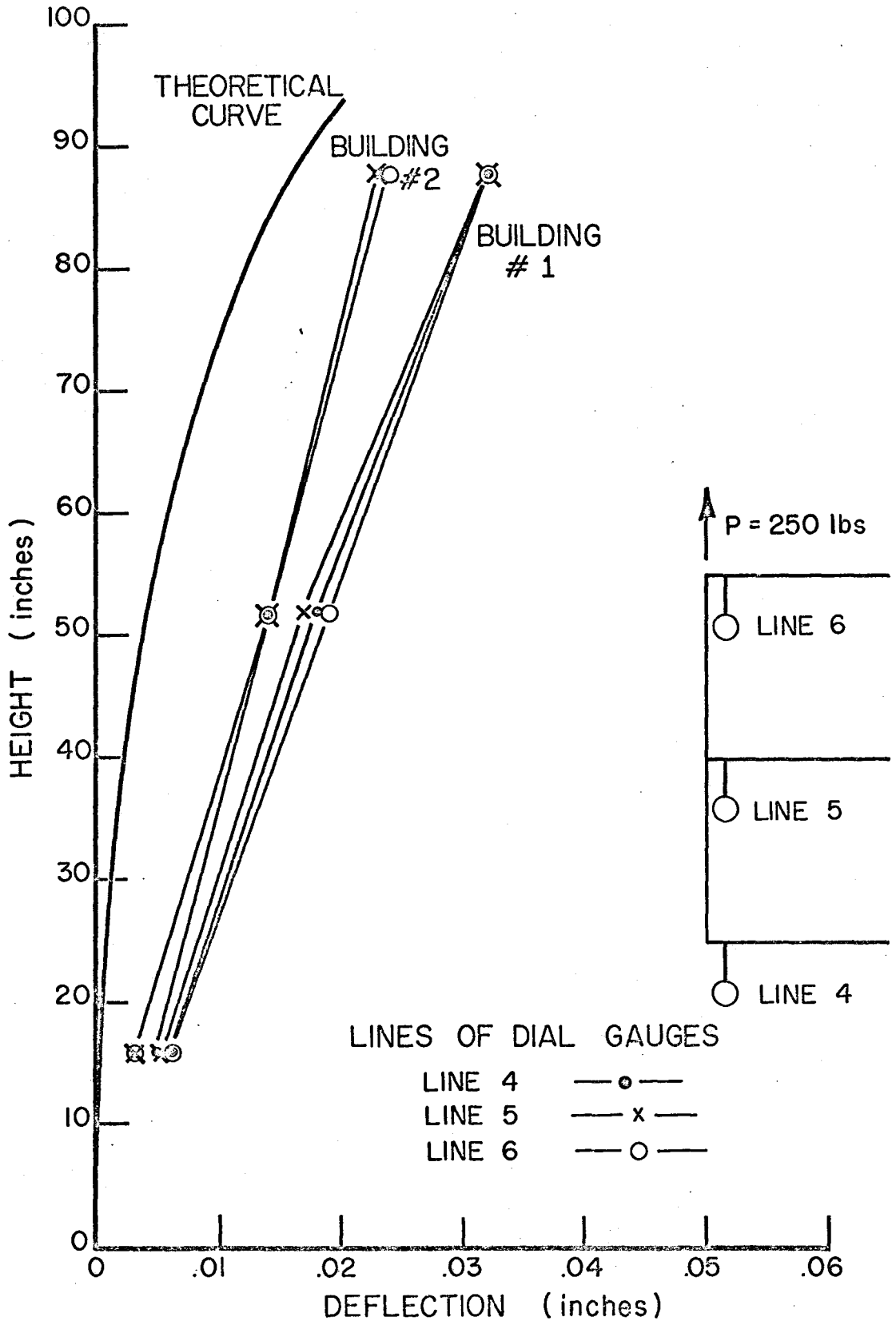

FIGURE 16
COMPARISON OF THE BEHAVIOUR OF THE THREE WALLS.

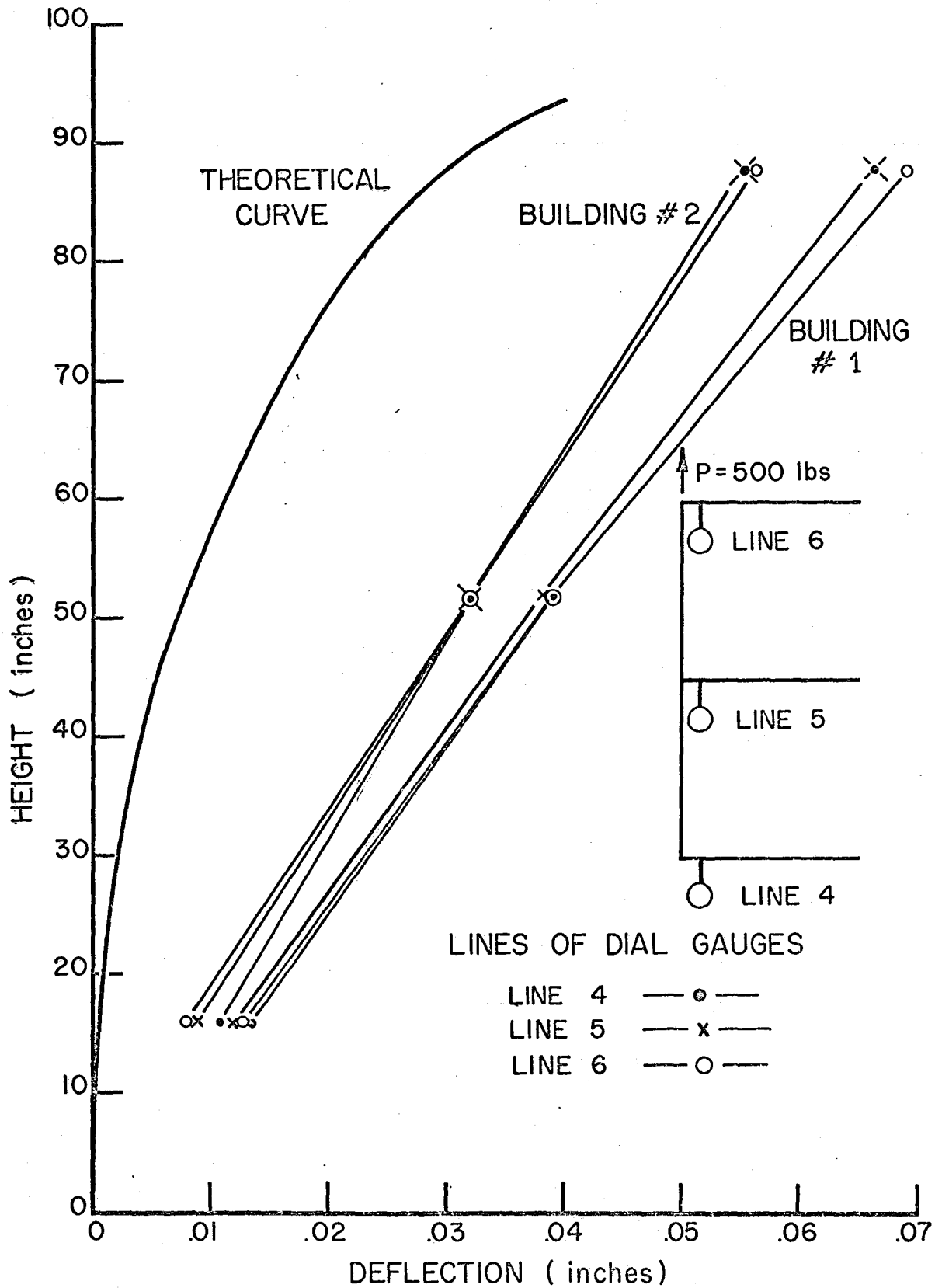

FIGURE 17.
COMPARISON OF THE BEHAVIOUR OF THE INTERIOR POINTS ON THE THREE FLANGES

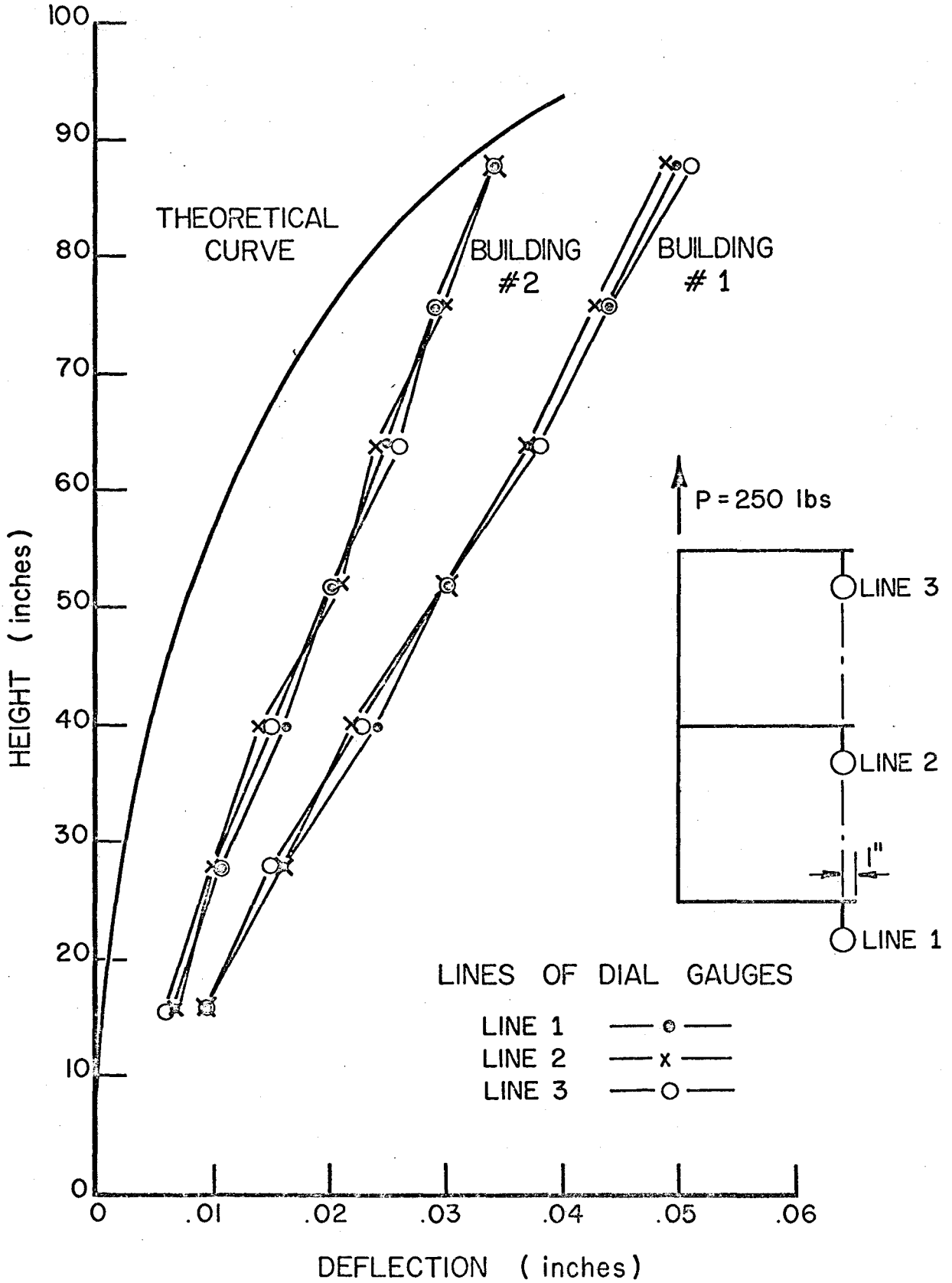

FIGURE 18.
COMPARISON OF THE BEHAVIOUR OF THE THREE WALLS

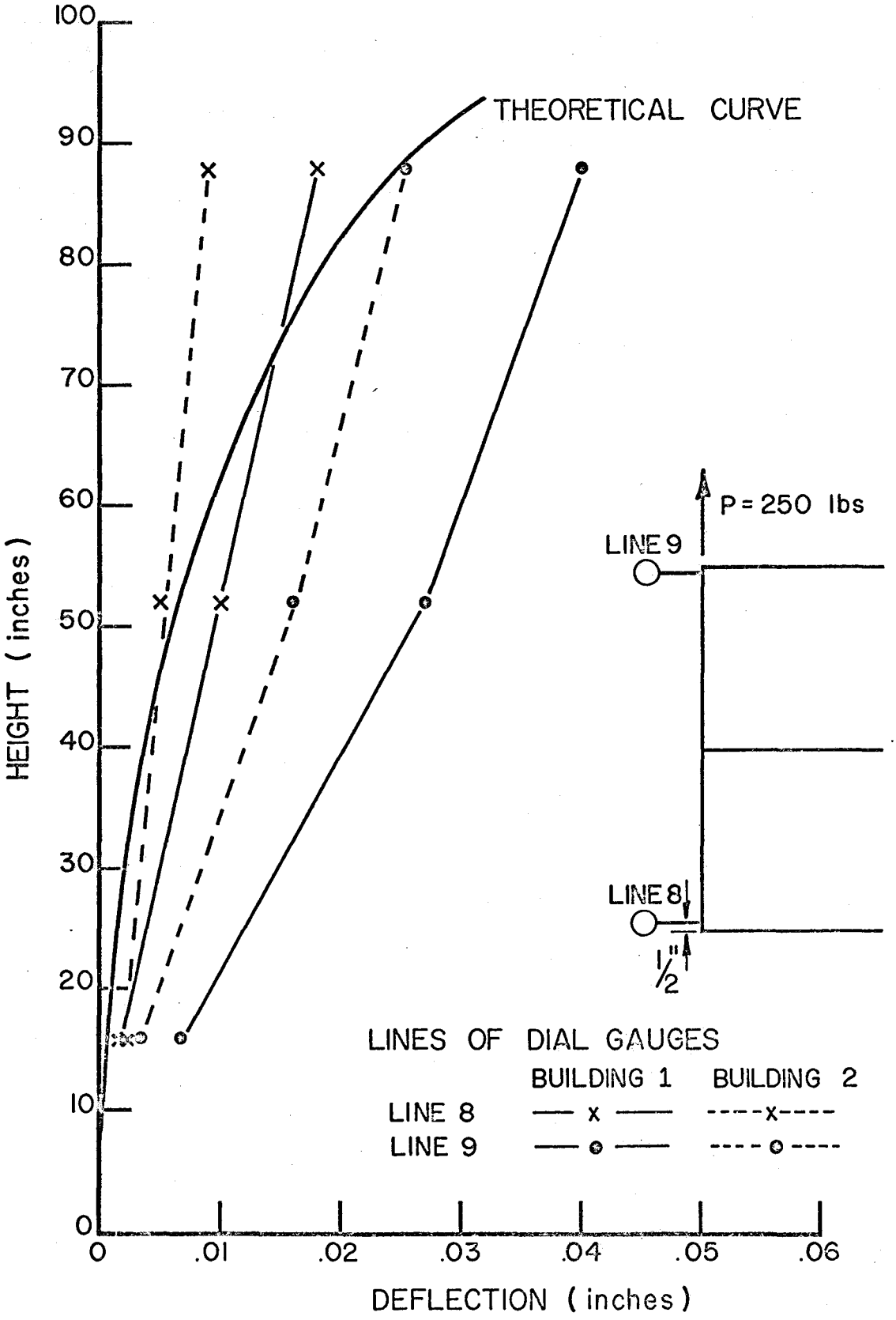

FIGURE 19.
COMPARISON OF DEFLECTIONS AT THE TWO BACK CORNERS.

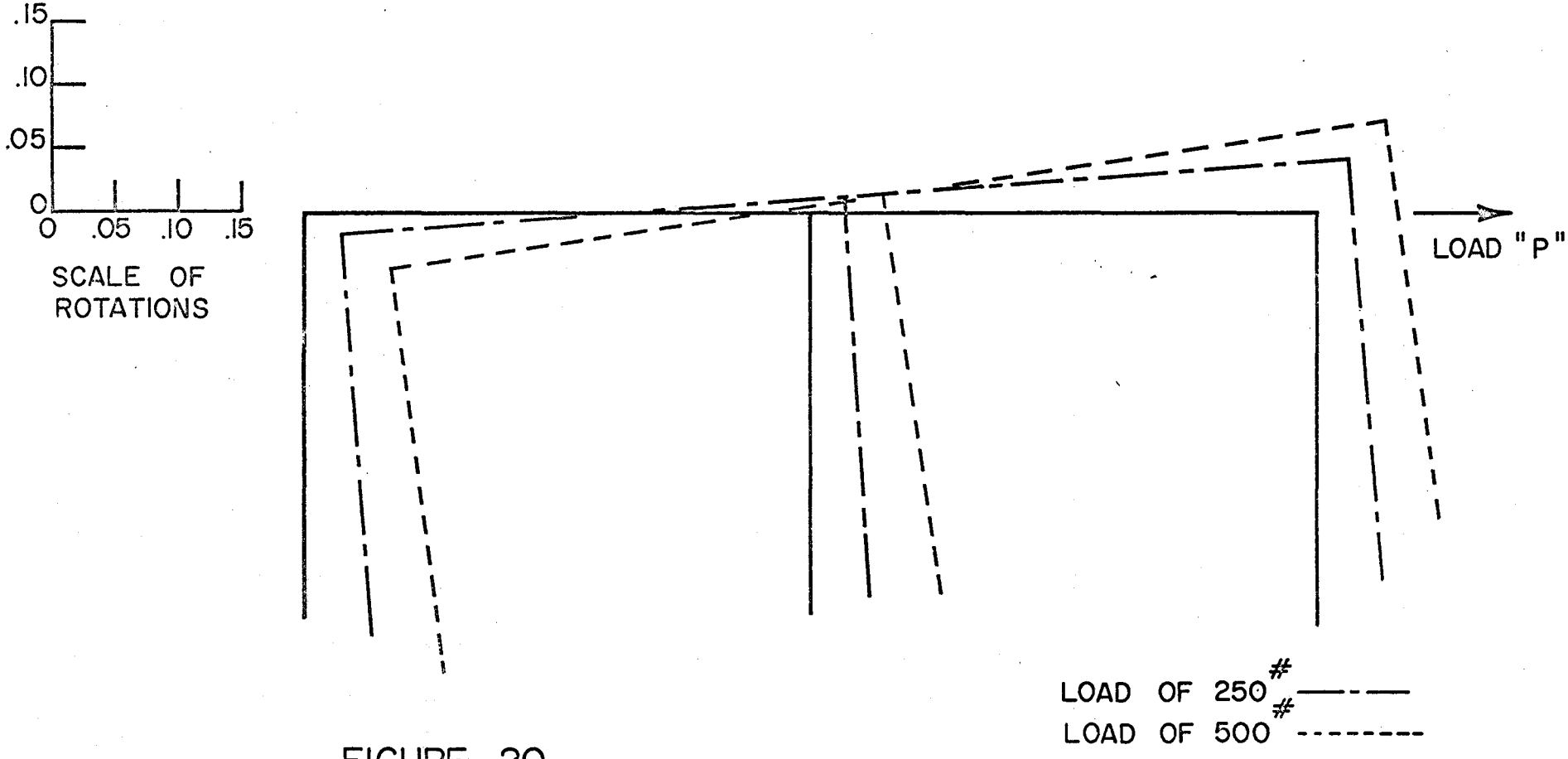

FIGURE 20.
ROTATION OF BUILDING # 1 AT LEVEL Z = 88"

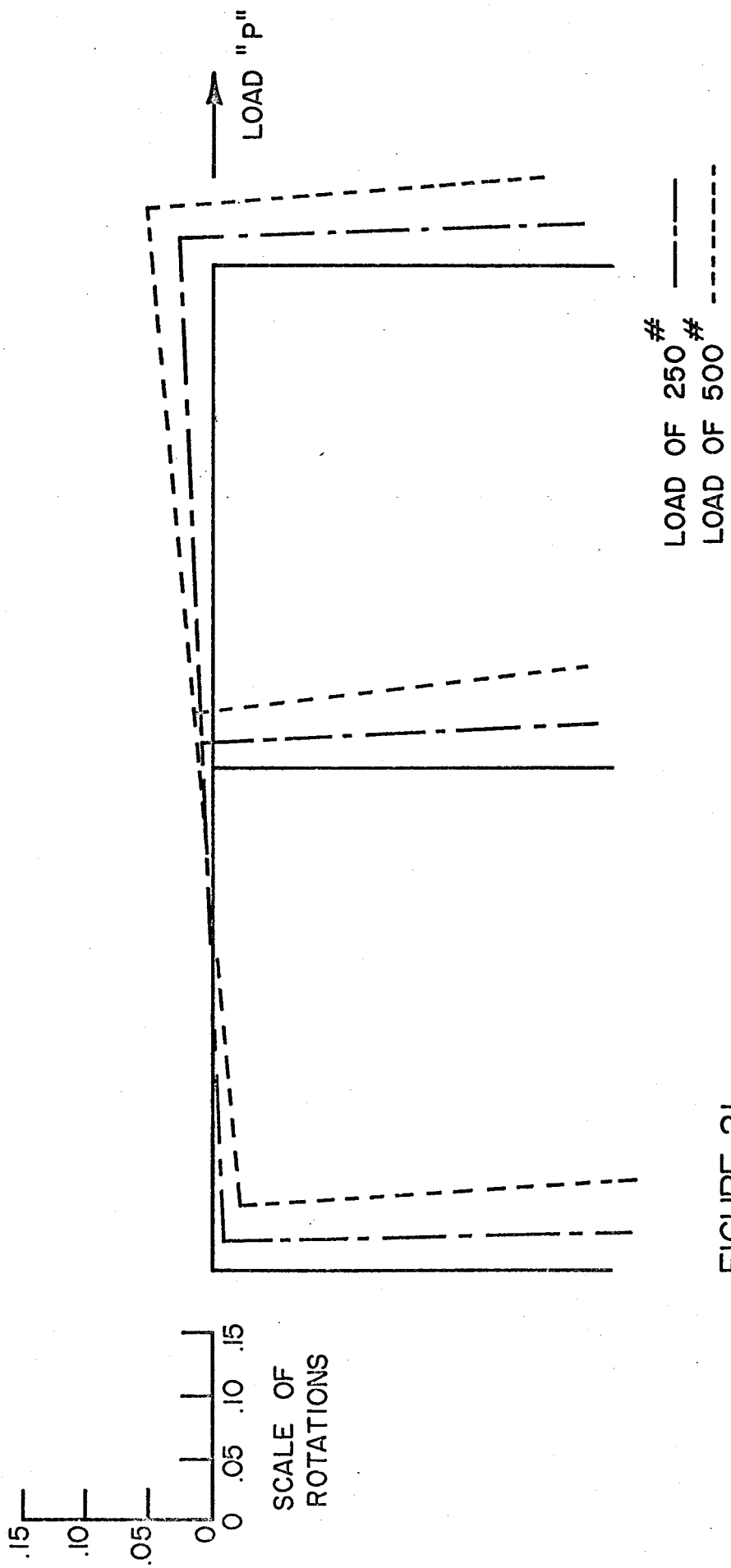

FIGURE 21.
ROTATION OF BUILDING # 2 AT LEVEL Z = 88"

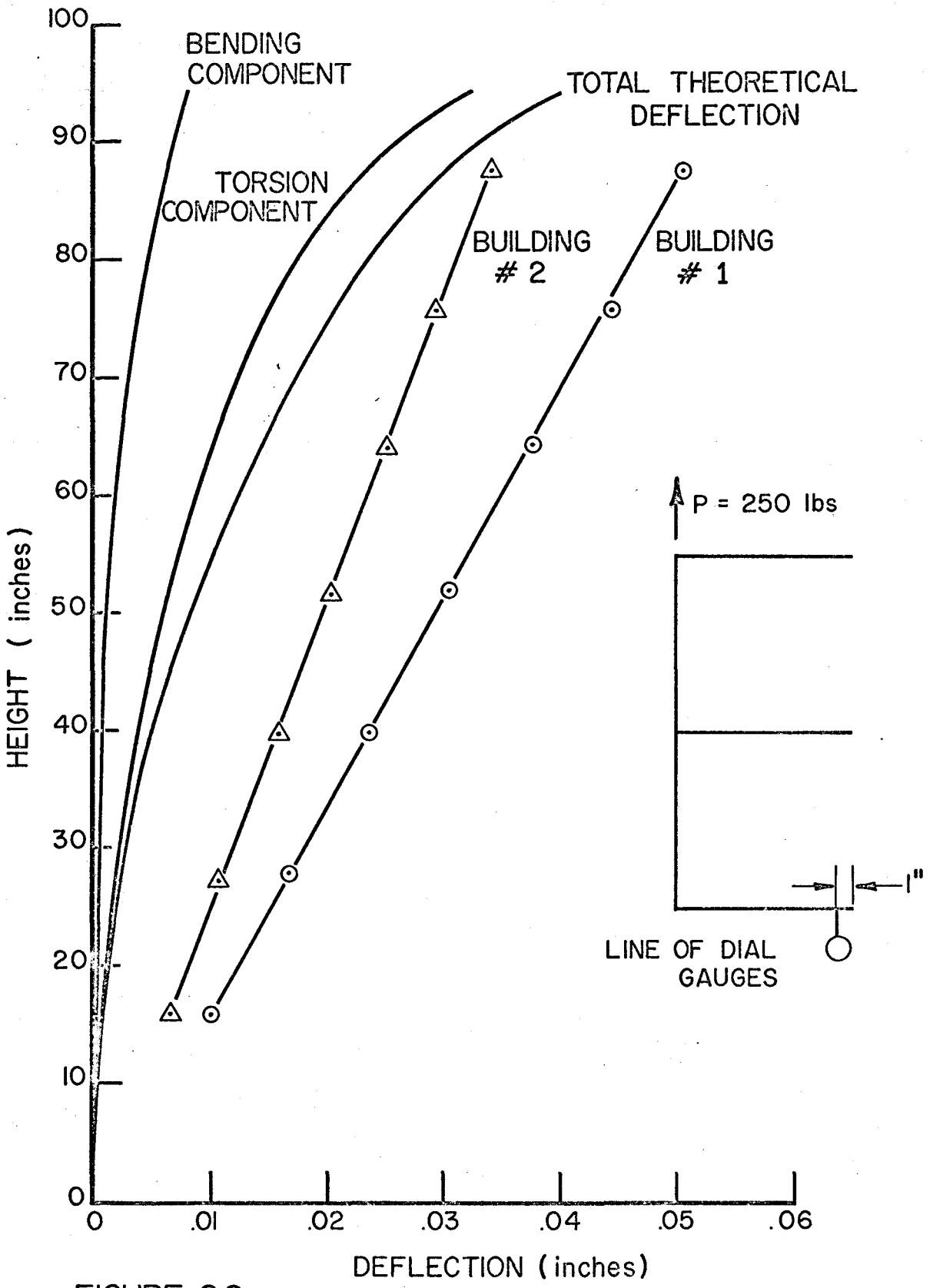

FIGURE 22.
THEORETICAL DEFLECTIONS DUE TO BENDING AND TORSION

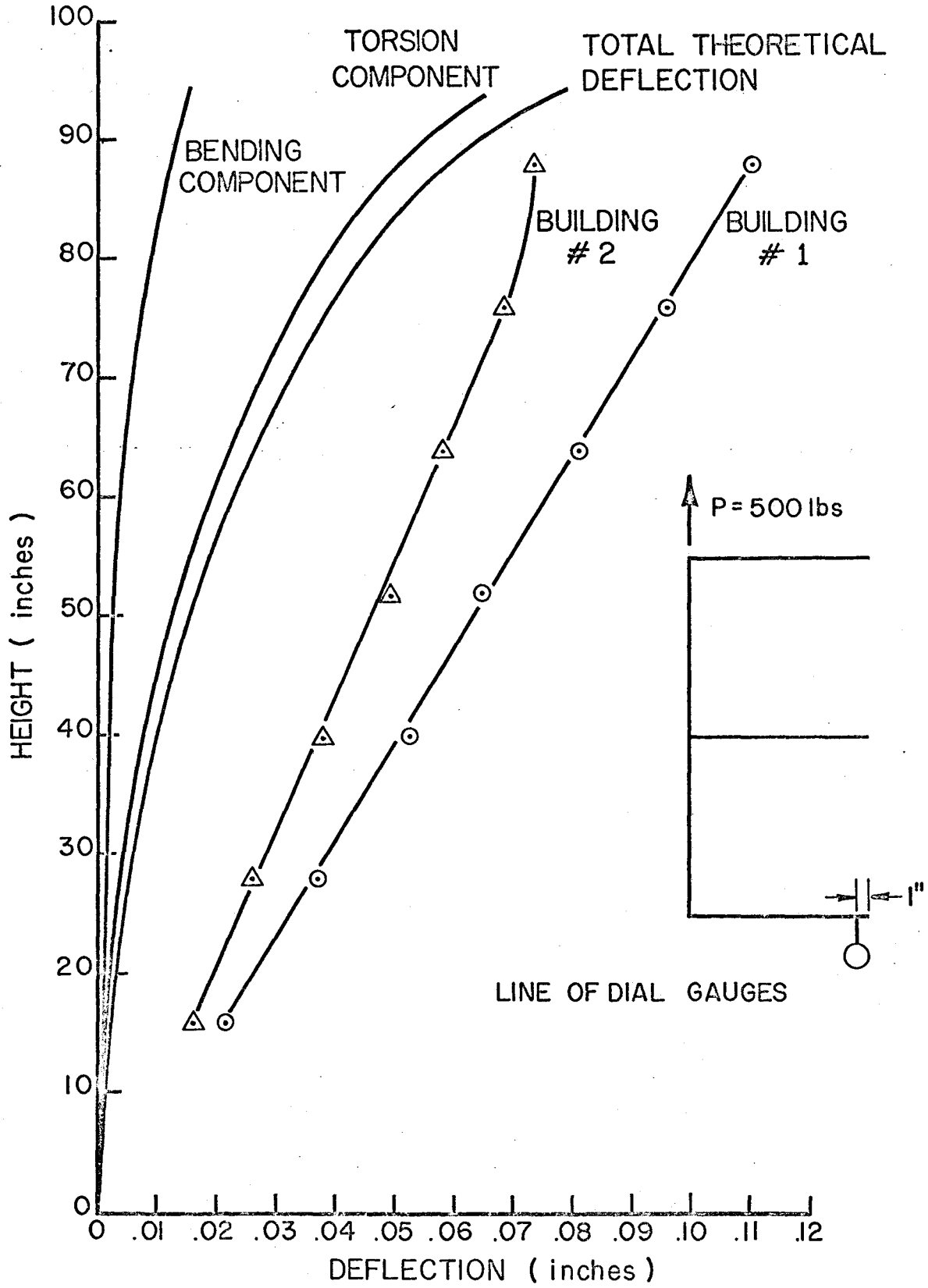

FIGURE 23.

THEORETICAL DEFLECTIONS DUE TO BENDING AND TORSION

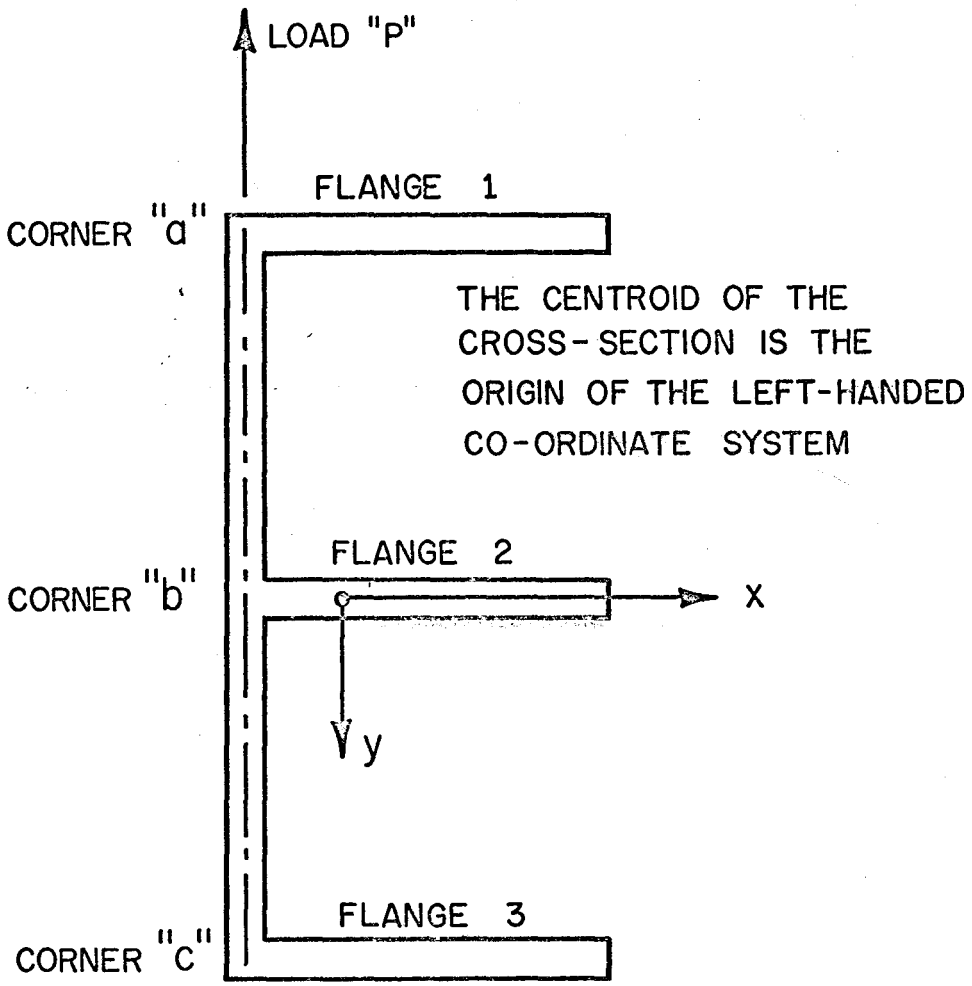

FIGURE 24.
IDENTIFICATION OF THE CORNERS AND FLANGES OF THE BUILDING

PLATE 1 INSTALLATION OF THE LAST LEVEL OF FLOOR SLABS IN BUILDING 1

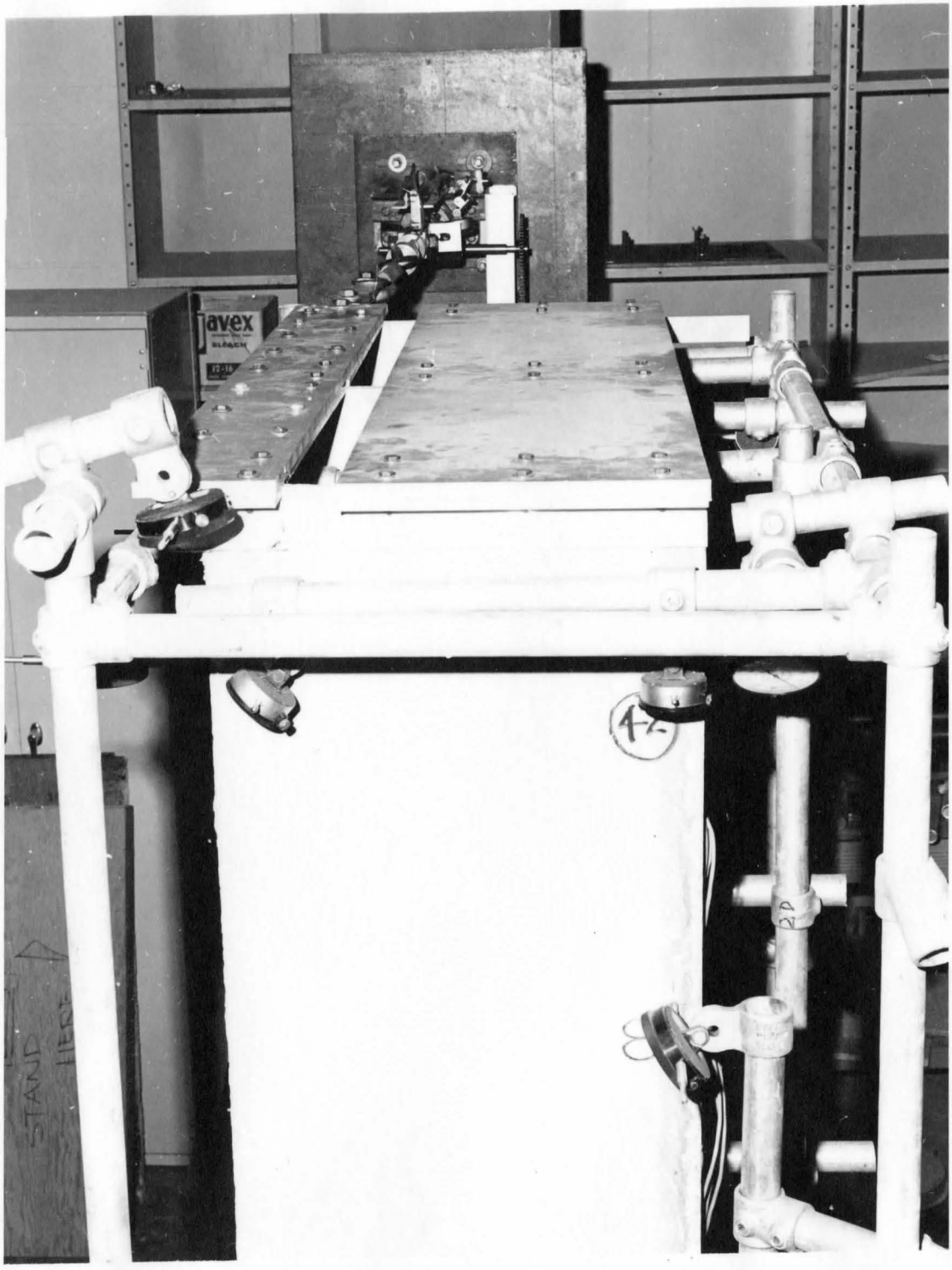

PLATE 2 ALUMINUM CAPPING SYSTEM IN POSITION ON BUILDING 11

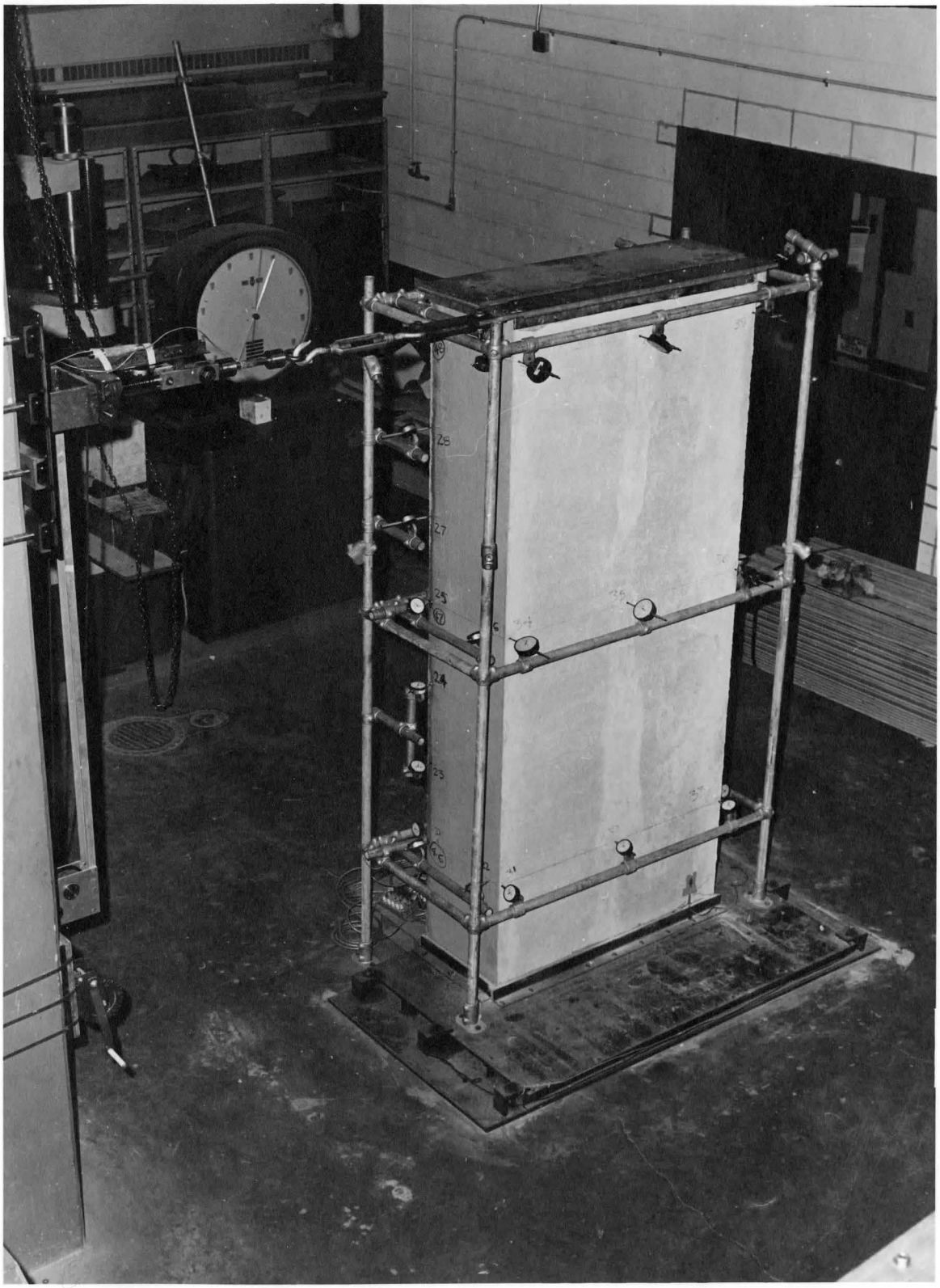

PLATE 3 LOADING APPARATUS IN POSITION FOR THE TESTING OF BUILDING 11

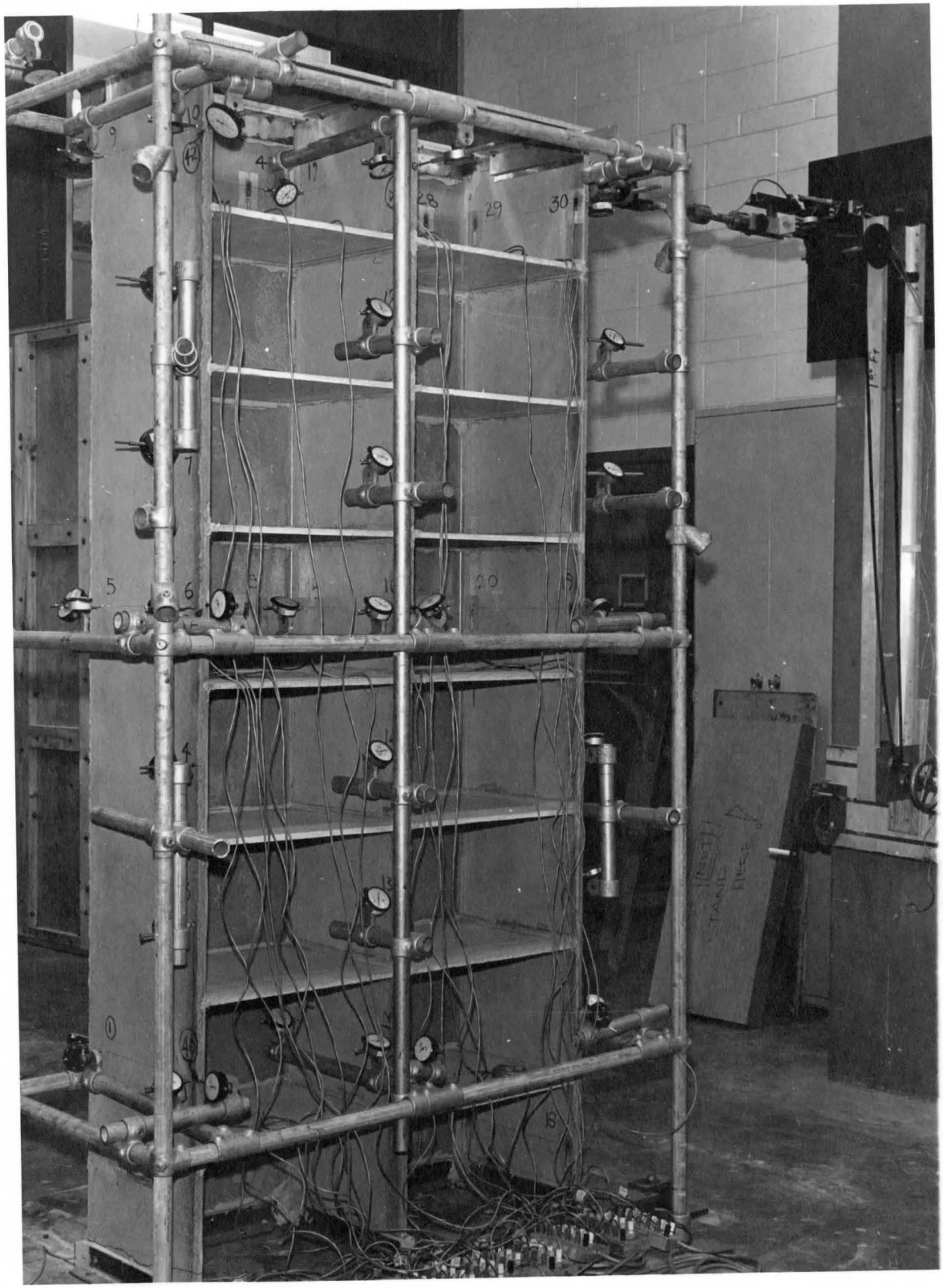

PLATE 4 FULLY INSTRUMENTED BUILDING 11 READY FOR TESTING

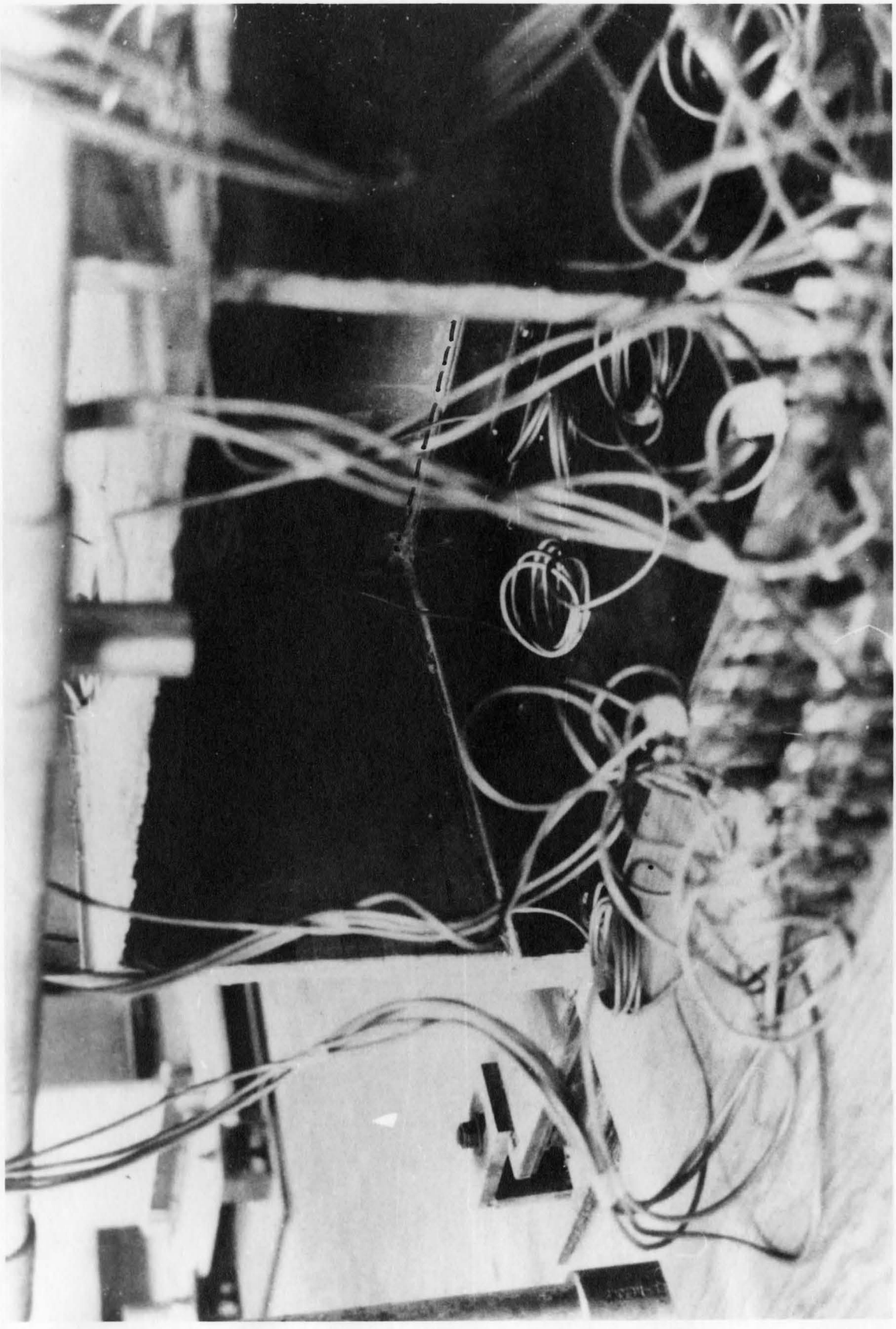

PLATE 5 CRACKING PATTERN IN CORNER C OF BUILDING 1

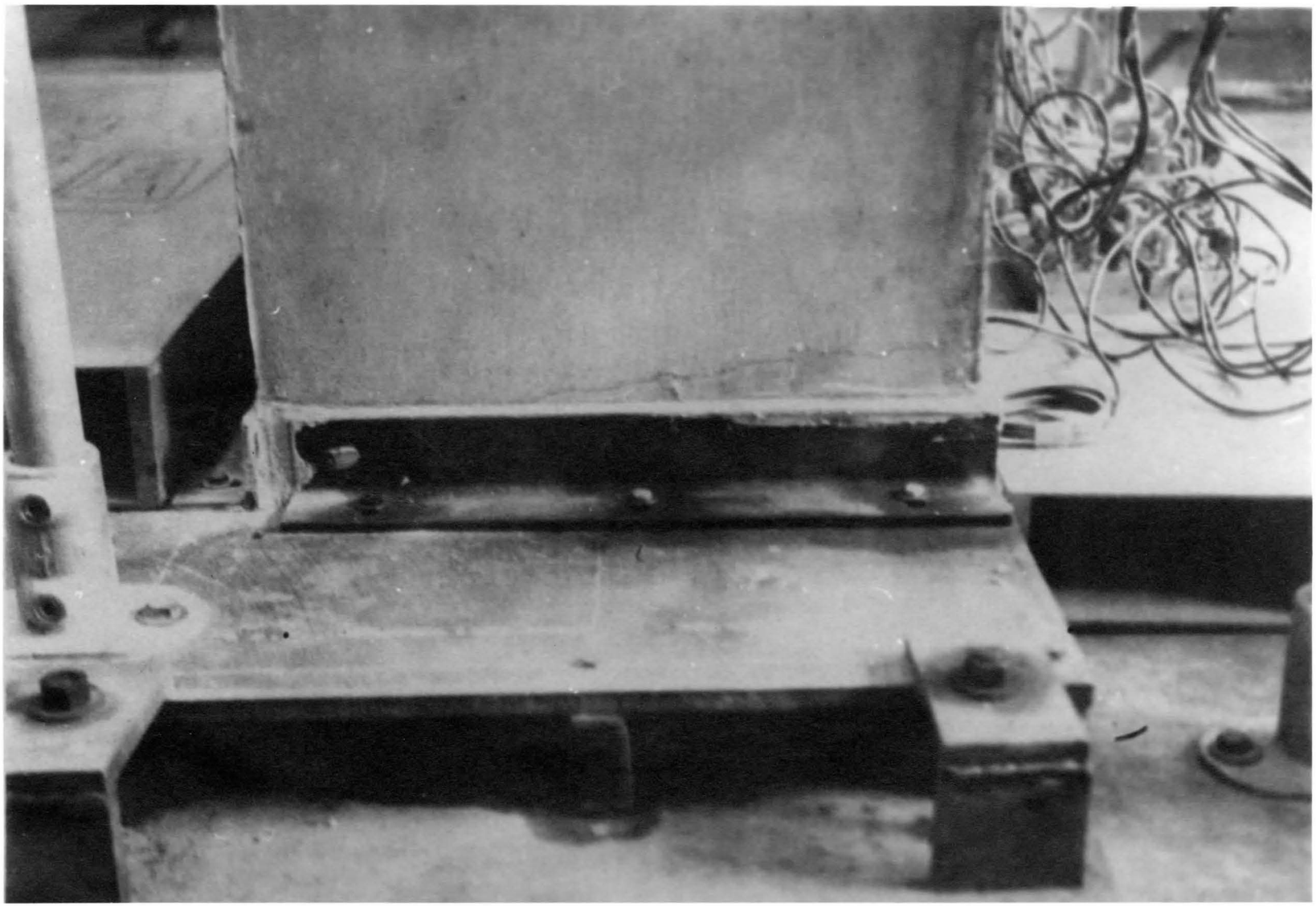

PLATE ¢ CRACKING PATTERN ALONG FLANGE 3 OF BUILDING 1

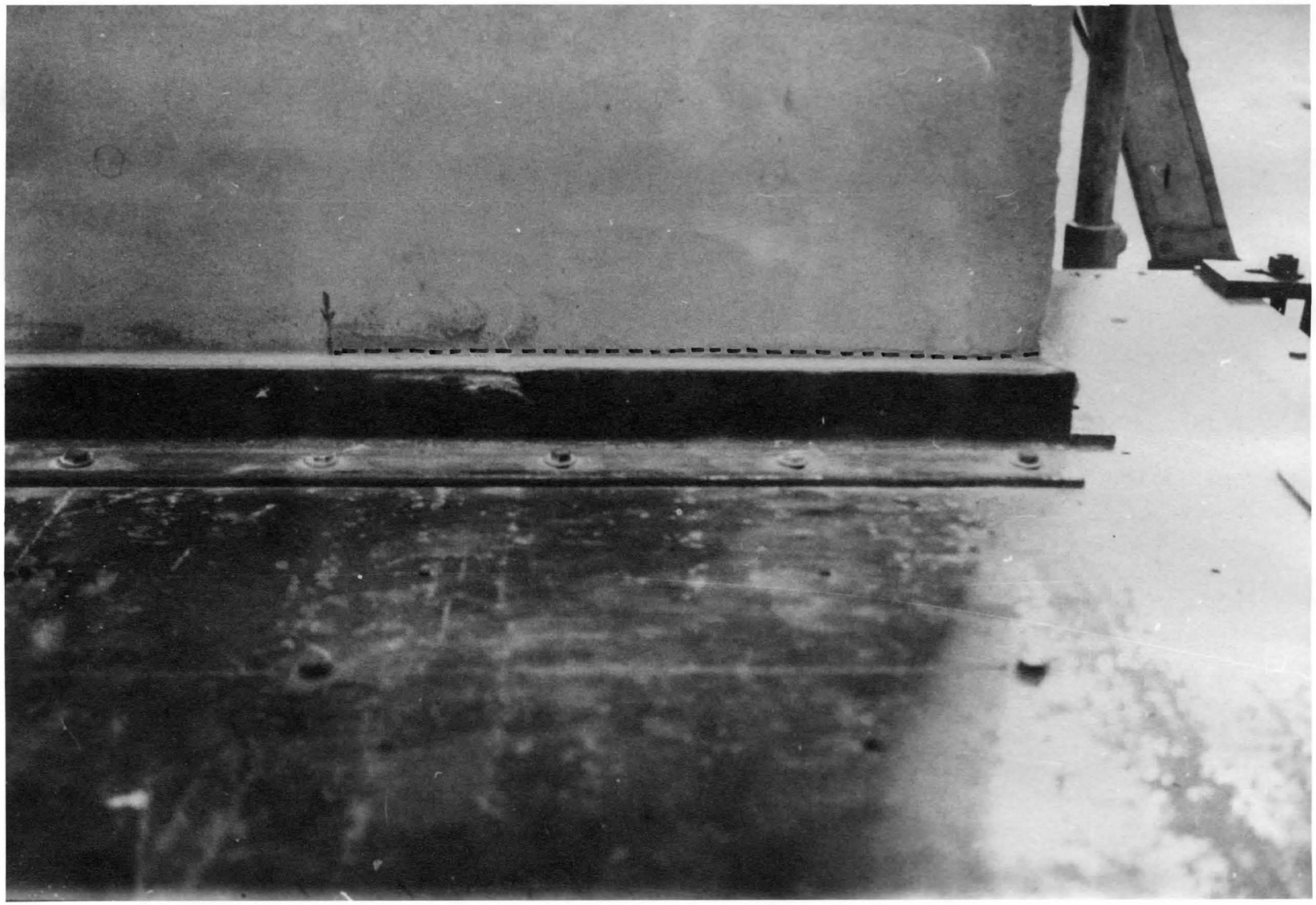

PLATE 7 CRACKING PATTERN ALONG THE BACK WALL OF BUILDING 1

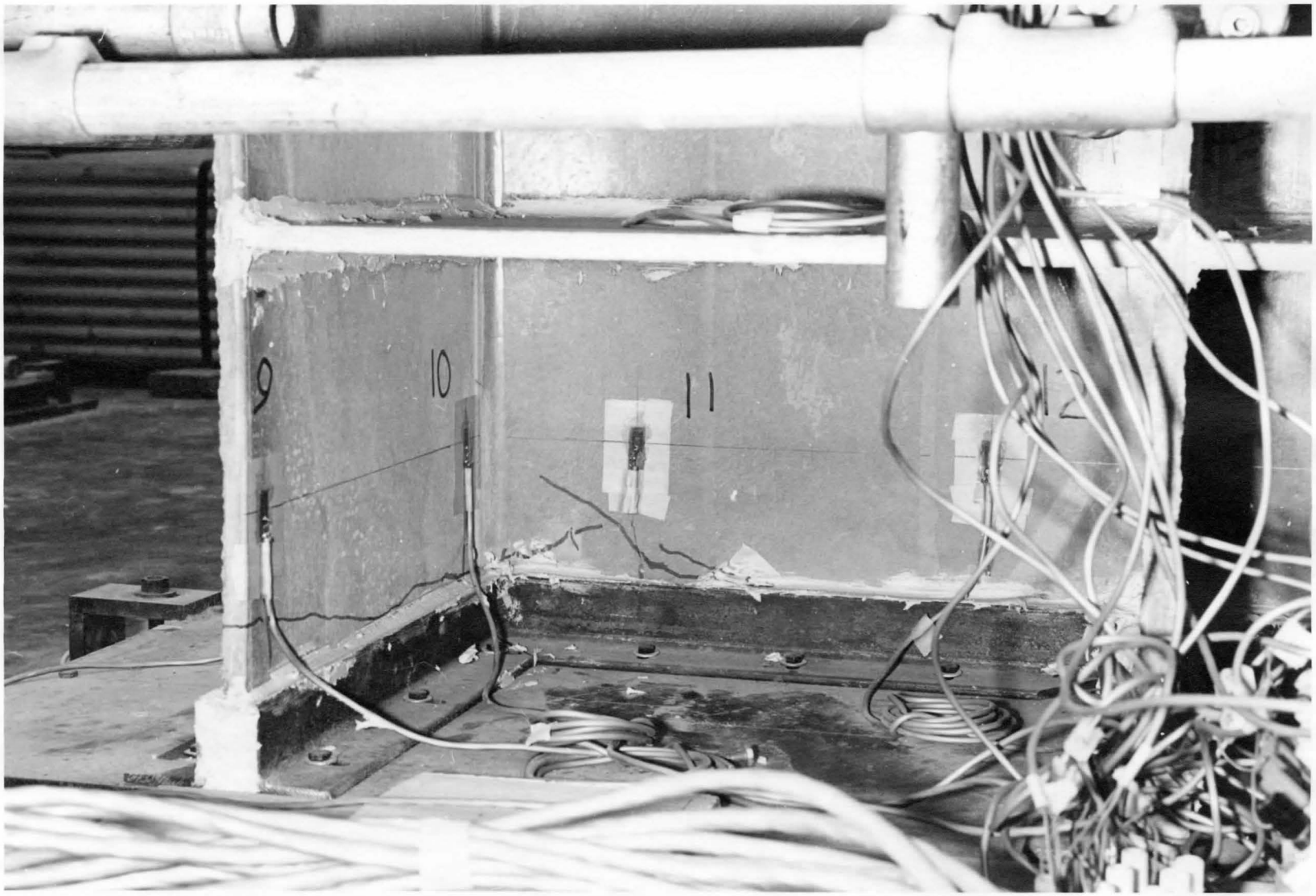

PLATE 8 CRACKING PATTERN ON THE INSIDE OF CORNER C OF BUILDING 11

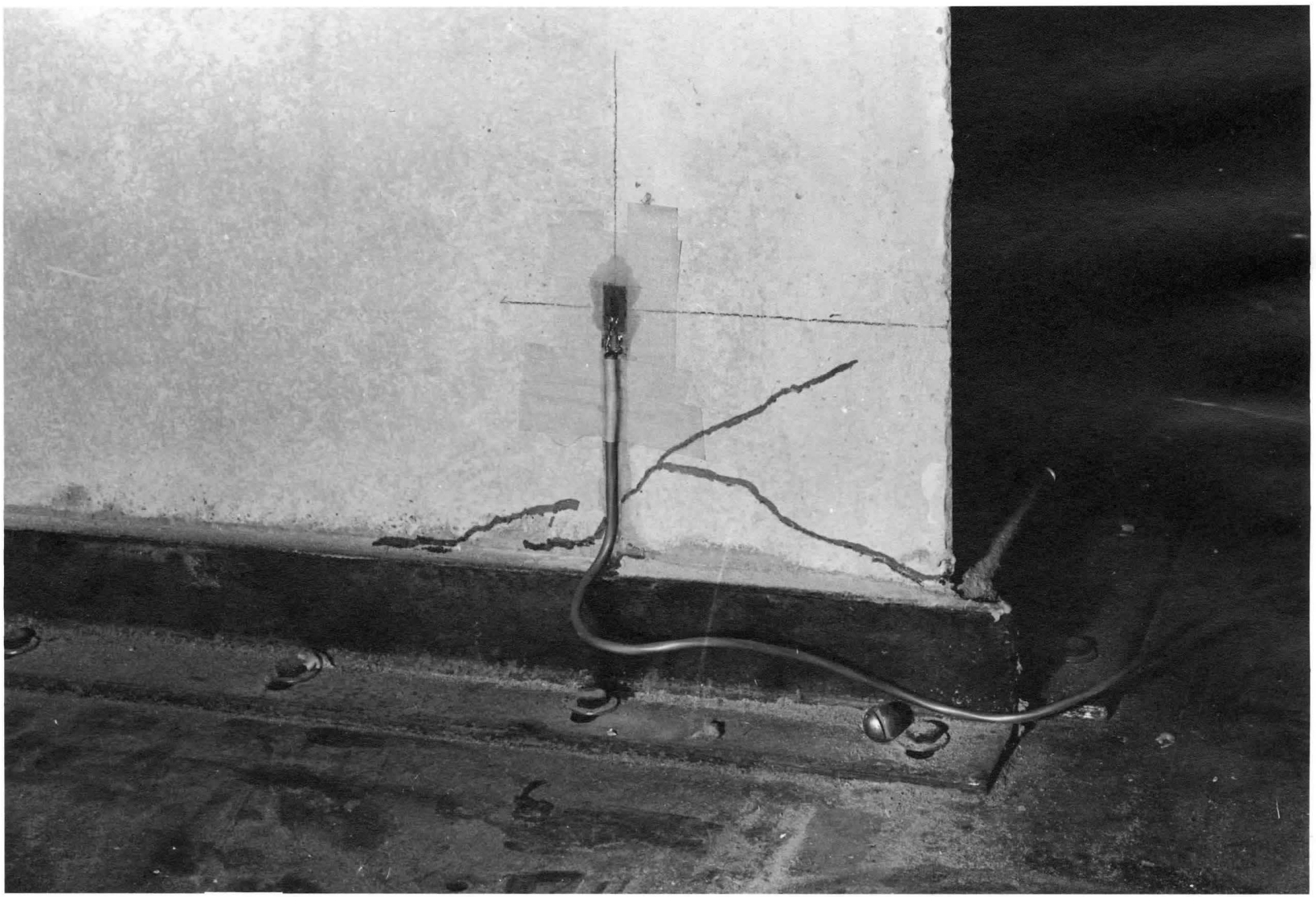

PLATE 9 CRACKING PATTERN ON THE OUTSIDE OF CORNER C OF BUILDING 11

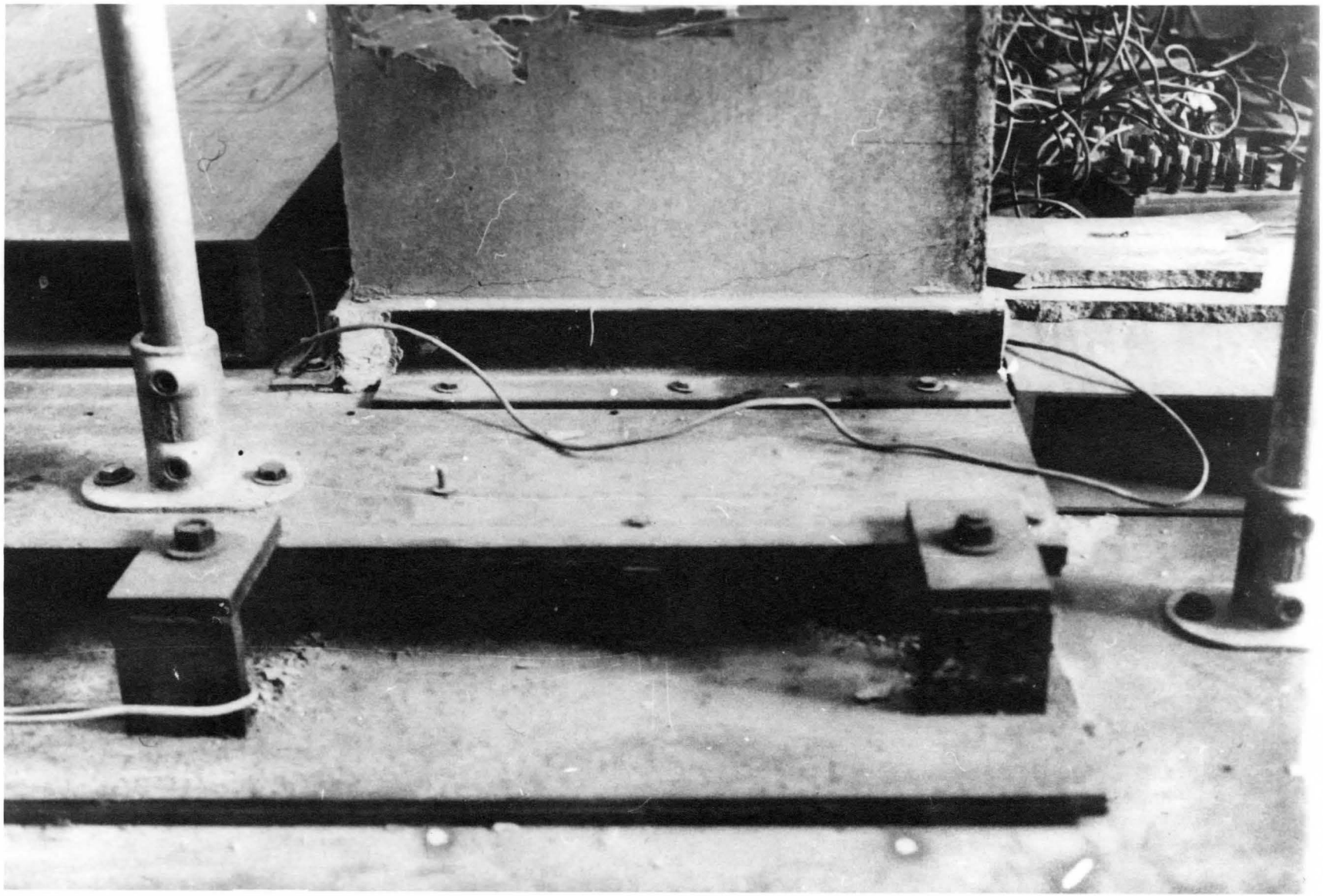

PLATE 10 CRACKING PATTERN ALONG FLANGE 3 OF BUILDING 11

APPENDIX A

GEOMETRIC PROPERTIES OF THE BUILDING CROSS-SECTION

A comprehensive summary of the geometric properties of the cross-section of the basic small-scale shear wall building has been compiled by Afsar (1). In this Appendix, a description of the major geometric properties will be given. All expressions discussed in this Appendix are defined by Vlasov (8).

(1) CO-ORDINATES OF THE SHEAR CENTRE

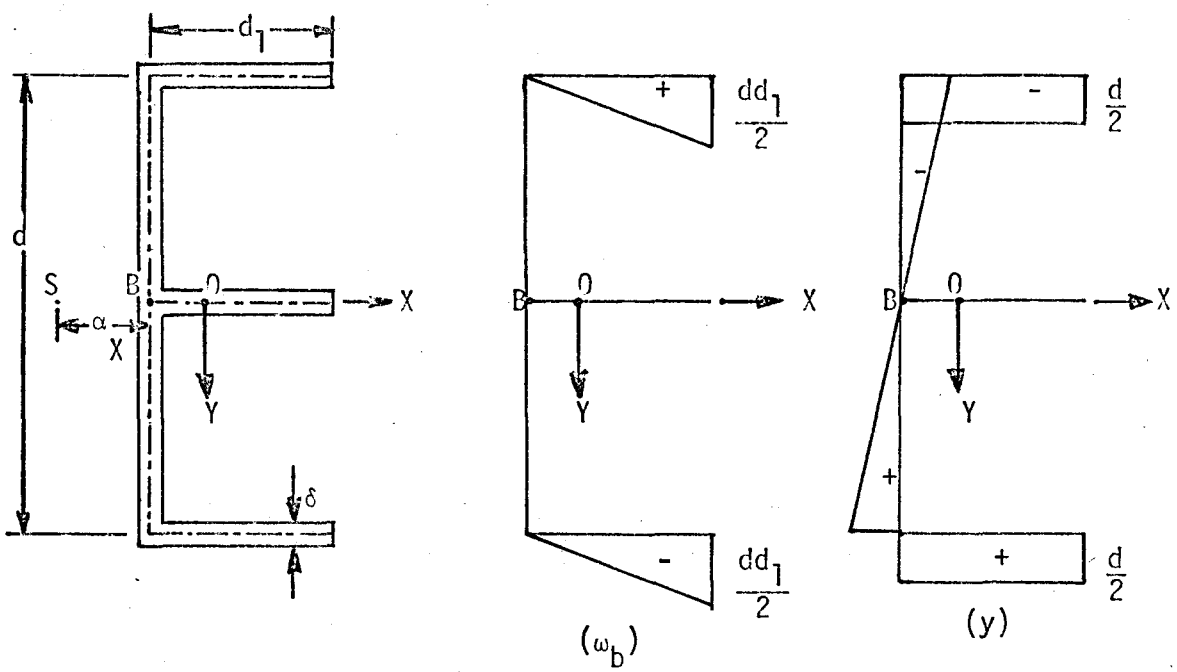

FIGURE 25 CO-ORDINATES OF THE SHEAR CENTRE

The shear centre, S, with co-ordinates a_X, a_Y lies on the axis of symmetry, OX. Point 0 is the centroid of the cross-section and is the origin of the left-handed orthogonal co-ordinate system. The sectorial

zero point at the intersection of the axis of symmetry and the profile line serves as the auxiliary pole, B. The co-ordinates of point B are b_X and b_Y.

The diagrams of the sectorial area ω_b, with respect to the auxiliary pole, B, and the ordinates y are shown in Figure 25.

If α_X represents the distance of the shear centre from the point B, then

$$\alpha_X = a_X - b_X$$

$$= \frac{1}{I_X} \int_A \omega_B \, y \, dA$$

$$= -2 \frac{1}{I_X} \frac{d}{2} \frac{d}{2} \delta \int_0^{d_1} x \, dx$$

$$= - \frac{d_2 \delta d_1^2}{4 I_X}$$

$$\alpha_Y = 0$$

(2) SECTORIAL AREA

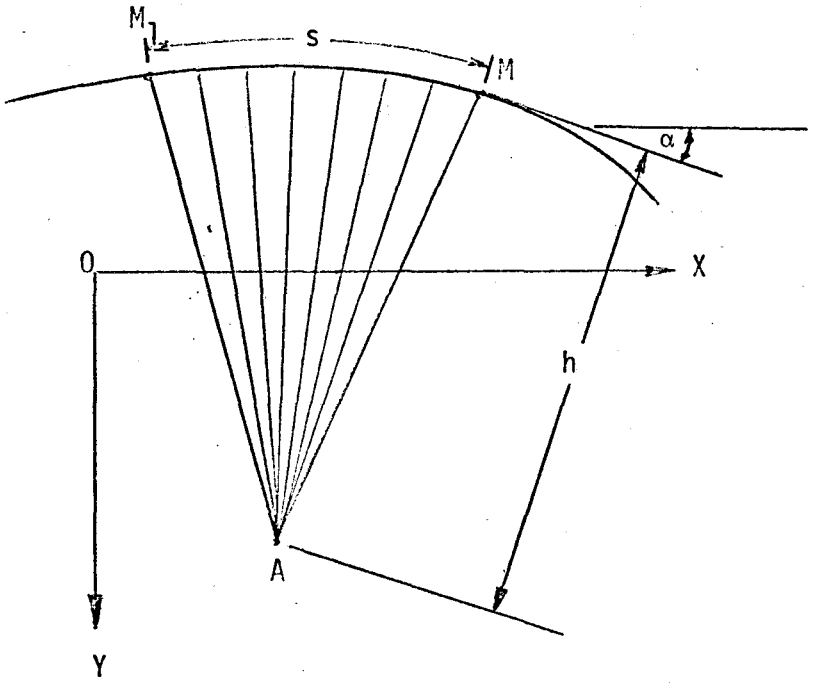

FIGURE 26 SECTORIAL AREA

The sectorial area for any point M on the profile line is twice the area of the sector enclosed between the arc M_1M of the profile line and the two lines AM_1 and AM. These two lines join the ends of the segment with point A. Point A is called the pole of the sectorial areas and point M_1 is the sectorial origin. The line AM connecting the pole A with the movable point M is the mobile radius vector. The sectorial area for the point M is positive if the mobile radius vector, AM, moves clockwise when sweeping out the sector; if observed from the negative Z direction.

(3) PRINCIPAL SECTORIAL AREA (ω)

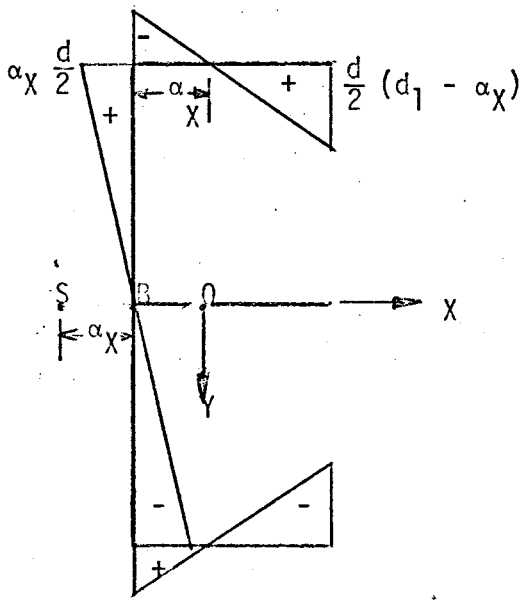

FIGURE 27 PRINCIPAL SECTORIAL AREA

The determination of the principal sectorial area for the cross-section considered is given in detail by Afsar (1). The shear centre, S, is the pole for the principal sectorial areas. Point B, at the point of intersection of the axis of symmetry, OX, and the profile line; serves as the origin of the areas. The diagram of the principal sectorial areas as seen in Figure 27, is skew-symmetric with respect to the OX axis. The sectorial areas for the points on the web below the OX axis will be positive since these areas are swept out in the clockwise sense by the radius vector. The absolute value of the sectorial areas for the flanges of the section decreases as the distance from the web increases. At a point on the flange, at a distance from the centre of the web equal to the distance of the shear centre from the centre of the

web, the principal sectorial area vanishes. Beyond this point the principal sectorial area increases in the negative value for the bottom flange and increases in the positive value for the top flange.

(4) DISPLACEMENT OF THE CROSS-SECTION UNDER FLEXURAL-TORSIONAL LOADING

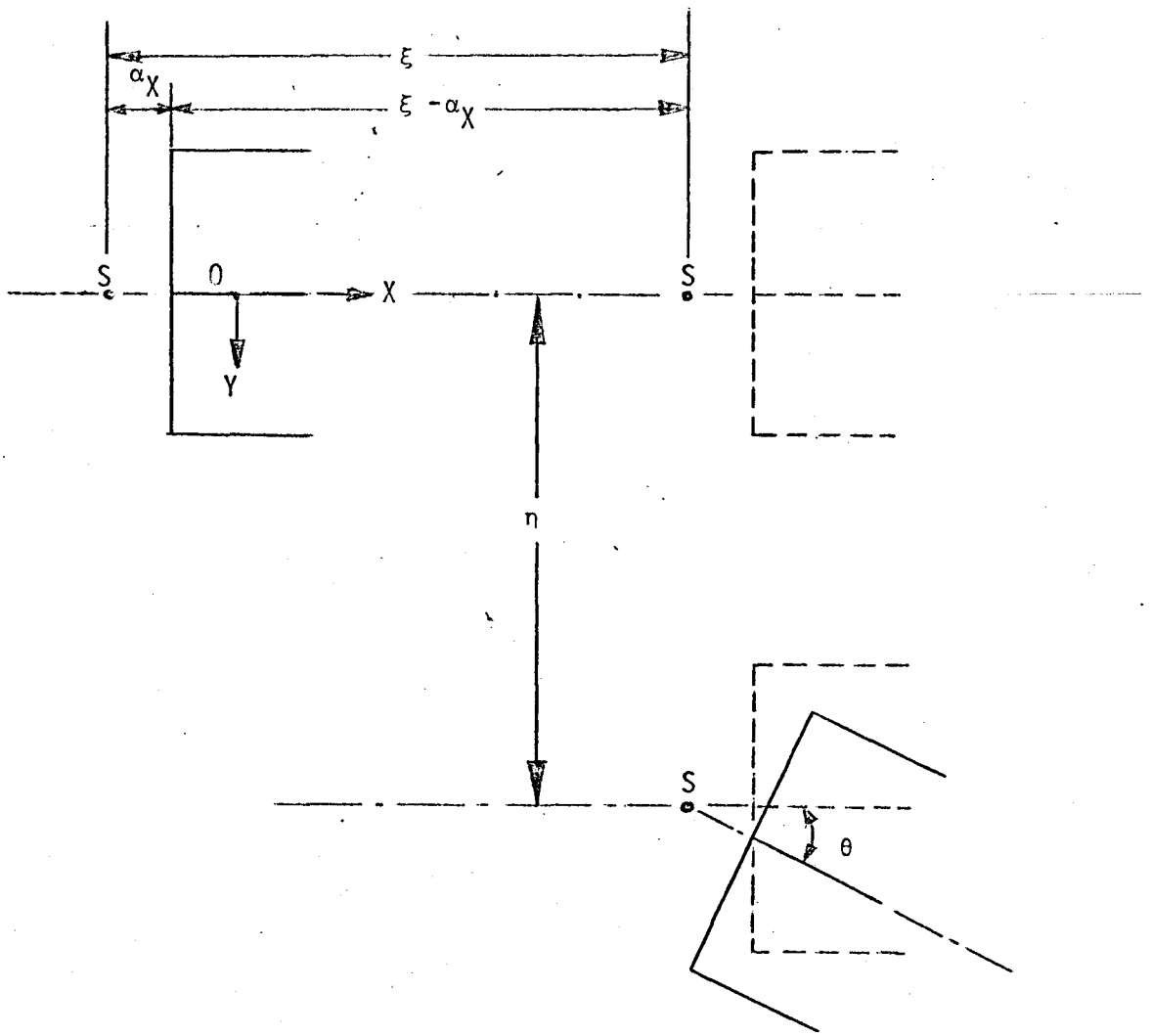

FIGURE 28 DISPLACEMENT OF THE CROSS-SECTION UNDER FLEXURAL-TORSIONAL LOADING

On the basis of Vlasov's first hypothesis, the deformation of a section of a thin-walled beam in its own plane shall consist of a rigid body translation and rotation.

In Figure 28, point O is the centroid of the cross-section and point S, the shear centre, is a distance α_X from the middle of the web on the OX axis.

In this figure, ξ and η are the displacements of the shear centre, S, in the OX and OY directions respectively. The section rotates through an angle θ as a rigid body about the shear centre. If v and w are respectively the displacements of a point on the cross-section in the OX and OY directions then,

$$v(z,y) = \xi(z) - (y - a_Y)\,\theta(z)$$

$$w(z,x) = \eta(z) - (x - a_X)\,\theta(z)$$

APPENDIX B

EXPERIMENTAL DATA

TABLE 6(a)

DEFLECTIONS IN INCHES RECORDED DURING THE SECOND TEST CYCLE OF BUILDING I (LOADING)

Dial Gauge Number	LOADING (pounds) 25	60	100	125	165	190	230	250
1	.0004	.0012	.0020	.0026	.0034	.0041	.0053	.0059
2	.0008	.0021	.0034	.0044	.0057	.0068	.0084	.0095
3	.0015	.0035	.0060	.0075	.0095	.0115	.0145	.0160
4	.002	.006	.009	.011	.015	.017	.021	.024
5	.001	.004	.007	.008	.011	.013	.016	.018
6	.003	.007	.011	.014	.018	.022	.027	.030
7	.003	.008	.013	.017	.023	.027	.033	.037
8	.003	.009	.016	.020	.026	.031	.038	.044
9	.003	.008	.012	.015	.019	.023	.028	.032
10	.004	.011	.019	.023	.030	.036	.044	.050
11	.0002	.0010	.0017	.0023	.0030	.0036	.0047	.0054
12	.0007	.0019	.0033	.0042	.0054	.0065	.0082	.0092
13	.001	.003	.006	.007	.009	.011	.014	.016
14	.002	.005	.008	.010	.014	.016	.020	.022
15	.002	.003	.006	.008	.010	.012	.015	.017
16	.003	.007	.011	.014	.018	.021	.026	.030
17	.003	.009	.014	.017	.023	.027	.033	.037
18	.004	.010	.016	.020	.026	.031	.039	.043
19	.002	.007	.012	.015	.020	.023	.028	.032
20	.004	.011	.018	.023	.030	.036	.045	.049
21	.007	.020	.034	.044	.056	.067	.084	.096
22	.0002	.0011	.0019	.0026	.0035	.0041	.0052	.0058
23	.0001	.0021	.0047	.0066	.0089	.0107	.0134	.0153
24	.0015	.0040	.0075	.0105	.0140	.0160	.0200	.0225
25	.002	.007	.011	.014	.018	.021	.026	.030
26	.001	.004	.007	.009	.011	.031	.016	.018
27	.004	.009	.014	.018	.023	.028	.034	.038
28	.003	.009	.016	.020	.026	.031	.039	.044
29	.005	.012	.019	.024	.031	.036	.045	.051
30	.003	.007	.011	.014	.019	.023	.028	.032
31	.0005	.0015	.0026	.0033	.0042	.0050	.0061	.0067
32	.0001	.0004	.0008	.0010	.0013	.0014	.0016	.0018
33(-)	.0001	.0003	.0006	.0008	.0010	.0012	.0015	.0018
34	.003	.007	.011	.014	.017	.020	.024	.027
35	.001	.002	.003	.004	.005	.005	.006	.006
36(-)	.001	.001	.002	.005	.006	.007	.009	.010
37	.006	.010	.016	.020	.026	.030	.036	.040
38	.001	.004	.007	.009	.011	.012	.014	.015
39(-)	.001	.004	.006	.007	.010	.012	.015	.018

TABLE 6(b)

DEFLECTIONS IN INCHES RECORDED DURING THE SECOND TEST CYCLE OF BUILDING I

(UNLOADING)

Dial Gauge Number	UNLOADING			
	180	125	60	0
1	.0058	.0041	.0029	.0012
2	.0083	.0060	.0038	.0012
3	.0140	.0100	.0065	.0020
4	.021	.015	.009	.003
5	.015	.010	.006	-.001
6	.026	.018	.011	.003
7	.032	.023	.014	.004
8	.037	.026	.016	.004
9	.027	.020	.012	.004
10	.043	.031	.019	.006
11	.0052	.0039	.0025	.0010
12	.0081	.0058	.0037	.0012
13	.014	.010	.006	.002
14	.019	.013	.008	.002
15	.014	.011	.006	.001
16	.025	.018	.011	.003
17	.032	.023	.014	.004
18	.037	.027	.017	.005
19	.028	.021	.013	.004
20	.043	.030	.019	.006
21	.0083	.0059	.0037	.0011
22	.0055	.0040	.0025	.0010
23	.0130	.0096	.0078	.0016
24	.0195	.0140	.0085	.0020
25	.025	.018	.011	.003
26	.016	.011	.007	.001
27	.033	.024	.015	.005
28	.038	.028	.017	.004
29	.048	.031	.020	.006
30	.027	.020	.012	.003
31	.0060	.0043	.0025	.0004
32	.0017	.0011	.0005	-.0002
33(-)	.0016	.0013	.0011	.0007
34	.023	.016	.010	.001
35	.003	.003	.001	-.001
36(-)	.009	.007	.005	.003
37	.035	.025	.015	.002
38	.013	.009	.005	-.001
39(-)	.016	.012	.009	.004

TABLE 7

DEFLECTIONS IN INCHES RECORDED DURING THE FAILURE CYCLE OF BUILDING I

Dial Gauge Number	LOADING (pounds) 75	140	200	250	340	400
1	.0017	.0034	.0050	.0066	.0082	.0097
2	.0030	.0054	.0080	.0104	.0127	.0150
3	.0050	.0095	.0140	.0180	.0220	.0260
4	.008	.014	.020	.026	.032	.038
5	.006	.011	.016	.020	.025	.030
6	.010	.018	.025	.032	.040	.047
7	.011	.022	.031	.040	.048	.057
8	.013	.026	.037	.048	.058	.069
9	.009	.018	.026	.034	.042	.050
10	.015	.030	.042	.055	.067	.079
11	.0016	.0036	.0047	.0063	.0077	.0092
12	.0028	.0056	.0076	.0101	.0124	.0147
13	.005	.009	.013	.017	.021	.025
14	.007	.013	.019	.024	.030	.035
15	.006	.011	.016	.020	.024	.030
16	.004	.017	.025	.033	.040	.047
17	.011	.021	.031	.040	.049	.058
18	.014	.025	.037	.048	.058	.069
19	.010	.018	.027	.035	.043	.051
20	.015	.028	.041	.054	.066	.079
21	.0030	.0054	.0078	.0102	.0125	.0149
22	.0019	.0034	.0049	.0066	.0078	.0095
23	.0050	.0104	.0136	.0175	.0213	.0249
24	.0070	.0135	.0190	.0245	.0300	.0355
25	.009	.018	.025	.032	.039	.047
26	.006	.011	.016	.020	.025	.030
27	.012	.022	.031	.040	.049	.059
28	.014	.027	.037	.048	.058	.070
29	.015	.029	.041	.054	.066	.079
30	.011	.019	.027	.035	.043	.052
31	.0022	.0040	.0055	.0072	.0084	.0095
32	.0007	.0011	.0016	.0019	.0020	.0021
33(-)	.0005	.0012	.0014	.0021	.0028	.0037
34	.009	.015	.021	.027	.033	.038
35	.002	.004	.005	.006	.006	.007
36(-)	.003	.005	.007	.010	.013	.017
37	.013	.024	.033	.042	.049	.057
38	.005	.008	.010	.012	.015	.018
39(-)	.004	.010	.015	.020	.026	.031

TABLE 7 (continued)

Dial Gauge Number	LOADING (pounds) 450	500	550	600	630	660
1	.0113	.0129	.0145	.0161	.0176	.0191
2	.0174	.0198	.0221	.0247	.0270	.0271
3	.0305	.0340	.0380	.0420	.0460	.0470
4	.043	.049	.054	.060	.066	.067
5	.034	.039	.043	.048	.053	.064
6	.054	.061	.068	.076	.083	.084
7	.067	.076	.084	.094	.103	.104
8	.080	.090	.100	.111	.122	.122
9	.058	.066	.074	.082	.090	.106
10	.092	.104	.115	.128	.139	.141
11	.0106	.0122	.0136	.0152	.0166	.0209
12	.0172	.0195	.0217	.0241	.0263	.0279
13	.029	.033	.037	.041	.045	.047
14	.041	.047	.052	.058	.064	.065
15	.034	.038	.043	.048	.053	.063
16	.054	.062	.068	.076	.083	.085
17	.067	.076	.085	.094	.103	.105
18	.080	.091	.101	.112	.122	.124
19	.059	.066	.075	.083	.091	.108
20	.091	.103	.114	.126	.138	.140
21	.0173	.0196	.0220	.0245	.0267	.0279
22	.0111	.0127	.0142	.0157	.0170	.0207
23	.0291	.0333	.0370	.0413	.0413	.0460
24	.0420	.0475	.0530	.0590	.0645	.0655
25	.054	.062	.068	.076	.083	.085
26	.035	.039	.044	.049	.053	.064
27	.068	.077	.085	.095	.103	.104
28	.080	.091	.101	.112	.123	.124
29	.091	.104	.115	.128	.140	.141
30	.061	.169	.077	.087	.095	.109
31	.0107	.0119	.0129	.0140	.0151	.0219
32	.0022	.0022	.0022	.0022	.0022	.0001
33(-)	.0043	.0049	.0057	.0064	.0072	.0076
34	.043	.048	.053	.057	.061	.038
35	.009	.009	.010	.010	.011	.004
36(-)	.020	.024	.027	.031	.034	.029
37	.065	.072	.078	.085	.091	.057
38	.021	.021	.022	.023	.023	.006
39(-)	.037	.044	.051	.057	.064	.055

TABLE 8

DEFLECTIONS IN INCHES RECORDED DURING THE SECOND TEST CYCLE OF BUILDING II

Dial Gauge Number	LOADING (pounds) 60	125	190	250	UNLOADING (pounds) 190	125	60	0
1	.0009	.0019	.0032	.0041	.0029	.0015	.0003	-.0008
2	.0014	.0030	.0050	.0063	.0053	.0036	.0018	.0000
3	.002	.003	.006	.008	.008	.007	.003	.001
4	.0040	.0073	.0120	.0160	.0130	.0090	.0050	.0005
5	.003	.007	.011	.014	.011	.007	.004	.000
6	.005	.010	.016	.021	.017	.012	.007	.001
7	.006	.012	.020	.026	.021	.015	.008	.001
8	.007	.014	.024	.031	.026	.018	.010	.001
9	.006	.012	.019	.025	.020	.014	.002	.001
10	.008	.022	.032	.041	.034	.025	.016	.006
11	.001	.002	.003	.004	.004	.003	.002	.001
12	.002	.003	.005	.007	.006	.004	.003	.001
13	.003	.005	.009	.011	.010	.007	.004	.001
14	.0035	.0071	.0119	.0160	.0134	.0096	.0054	.0009
15	.003	.007	.012	.015	.013	.010	.006	.001
16	.005	.010	.017	.021	.018	.013	.007	.001
17	.006	.012	.020	.026	.022	.015	.009	.001
18	.008	.015	.024	.038	.026	.018	.010	.002
19	.006	.012	.020	.026	.022	.015	.009	.002
20	.009	.017	.028	.037	.030	.021	.012	.002
21	.001	.003	.005	.007	.006	.004	.003	.001
22	.001	.001	.003	.004	.004	.003	.002	.001
23	.0020	.0048	.0083	.0108	.0095	.0066	.0036	.0006
24	.004	.008	.013	.017	.014	.010	.006	.001
25	.005	.010	.016	.021	.018	.012	.007	.001
26	.003	.008	.013	.014	.012	.008	.004	.000
27	.006	.013	.020	.027	.022	.016	.009	.002
28	.005	.015	.024	.032	.026	.018	.010	.002
29	.009	.017	.028	.035	.030	.021	.012	.002
30	.006	.011	.019	.025	.021	.014	.008	.001
31	.0010	.0020	.0033	.0044	.0043	.0034	.0023	.0011
32	.0003	.0007	.0010	.0013	.0013	.0009	.0006	.0003
33(-)	.0005	.0010	.0017	.0023	.0019	.0013	.0009	.0004
34	.004	.007	.012	.016	.013	.009	.005	.000
35	.001	.002	.003	.004	.004	.003	.001	.000
36(-)	.001	.003	.005	.007	.006	.004	.003	.001
37	.007	.013	.020	.026	.022	.016	.008	.000
38	.002	.004	.006	.007	.006	.004	.002	-.001
39(-)	.002	.004	.007	.009	.008	.005	.003	.001
40	.0011	.0019	.0030	.0040	.0035	.0028	.0021	.0013
41	.0015	.0030	.0051	.0067	.0056	.0041	.0027	.0013
42	.0036	.0069	.0115	.0138	.0127	.0092	.0060	.0021
43	.0013	.0015	.0017	.0024	.0024	.0022	.0018	.0014
44	.0010	.0020	.0030	.0040	.0035	.0025	.0015	.0000
45	.002	.003	.005	.006	.005	.004	.002	-.001
46	.0012	.0020	.0031	.0032	.0025	.0014	.0010	.0000
47	.003	.006	.010	.013	.011	.007	.003	-.001
48	.007	.012	.019	.025	.021	.015	.007	.000

TABLE 9

DEFLECTIONS IN INCHES RECORDED DURING THE FAILURE CYCLE OF BUILDING II

Dial Gauge Number	LOADING (pounds) 125	250	390	465	565	650	685	720
1	.0019	.0047	.0076	.0097	.0122	.0138	.0148	.0161
2	.0028	.0064	.0102	.0133	.0173	.0190	.0214	.0216
3	.0045	.0105	.0172	.0225	.0294	.0330	.0369	.0373
4	.0080	.0160	.0250	.0325	.0420	.0470	.0525	.0525
5	.007	.014	.022	.028	.036	.041	.046	.053
6	.009	.020	.031	.045	.053	.059	.066	.067
7	.012	.025	.039	.051	.066	.074	.083	.083
8	.014	.029	.046	.059	.077	.088	.098	.098
9	.011	.023	.037	.048	.063	.072	.080	.095
10	.016	.034	.050	.063	.084	.096	.112	.113
11	.001	.003	.005	.008	.010	.011	.013	.016
12	.003	.007	.010	.013	.017	.019	.021	.022
13	.004	.010	.016	.021	.028	.031	.035	.035
14	.0066	.0148	.0232	.0306	.0299	.0347	.0399	.0405
15	.007	.014	.023	.028	.037	.042	.046	.053
16	.010	.021	.031	.041	.053	.060	.066	.067
17	.011	.024	.038	.050	.064	.073	.081	.082
18	.014	.030	.046	.059	.077	.087	.097	.097
19	.010	.023	.037	.048	.062	.070	.078	.090
20	.015	.034	.053	.069	.089	.100	.113	.113
21	.002	.006	.009	.013	.017	.019	.021	.021
22	.001	.003	.005	.007	.010	.012	.013	.016
23	.0045	.0104	.0168	.0225	.0295	.0330	.0359	.0358
24	.007	.015	.024	.033	.042	.047	.053	.052
25	.010	.020	.032	.041	.054	.059	.066	.067
26	.006	.014	.022	.029	.033	.040	.046	.053
27	.012	.026	.040	.052	.067	.0075	.085	.085
28	.013	.029	.046	.060	.078	.088	.098	.098
29	.016	.034	.052	.068	.088	.100	.111	.112
30	.011	.024	.037	.048	.064	.073	.081	.092
31	.0008	.0032	.0055	.0074	.0095	.0104	.0111	.1006
32	.0003	.0010	.0015	.0018	.0019	.0020	.0020	.0043
33(-)	.0007	.0019	.0035	.0049	.0069	.0080	.0092	.0026
34	.008	.016	.024	.030	.036	.040	.042	.038
35	.002	.004	.005	.005	.006	.007	.006	.011
36(-)	.002	.005	.009	.013	.018	.021	.025	.009
37	.012	.025	.038	.047	.057	.062	.067	.061
38	.005	.008	.010	.012	.014	.015	.014	.022
39(-)	.004	.009	.015	.019	.026	.030	.037	.012
40	.0011	.0027	.0048	.0067	.0091	.0108	.0122	.0193
41	.0022	.0054	.0096	.0139	.0193	.0228	.0268	.0099
42	.0055	.0123	.0207	.0271	.0360	.0416	.0483	.0228
43	.0003	.0008	.0008	.0009	.0009	.0012	.0008	.0038
44	.0015	.0035	.0045	.0055	.0065	.0065	.0060	.0115
45	.004	.007	.008	.009	.009	.006	.004	.012
46	.0016	.0034	.0051	.0067	.0087	.0101	.0107	.0097
47	.006	.013	.020	.026	.032	.035	.037	.032
48	.012	.024	.034	.042	.052	.057	.062	.053

TABLE 10

STRAINS IN μ"/" RECORDED DURING THE SECOND TEST CYCLE OF BUILDING I

Strain Gauge Number	LOADING (pounds)							UNLOADING (pounds)				
	25	60	100	125	165	190	230	250	180	125	60	0
1	2	3	5	6	7	7	9	11	11	12	12	13
2	3	3	4	6	7	7	8	9	10	10	11	11
3	1	2	3	4	4	7	6	8	10	10	10	9
4	4	4	5	6	6	8	7	8	10	11	11	13
5	3	4	5	6	7	6	8	8	10	10	13	13
6	3	3	8	7	10	11	13	17	14	13	12	8
7	6	8	10	12	14	12	15	19	18	16	15	13
8	2	5	6	6	7	8	9	12	11	12	12	12
9	2	0	-1	-1	-4	-5	-6	-7	-1	4	9	13
10	6	9	14	15	18	20	23	27	25	20	16	14
11	5	8	10	13	16	18	19	23	20	18	15	10
12	3	3	4	4	5	6	6	8	8	12	11	9
13	1	2	0	2	1	1	-1	1	2	5	6	8
14	3	4	5	6	6	7	7	8	8	9	10	10
15	2	4	3	7	5	7	6	10	9	9	10	10
16	0	0	-6	-6	-4	-4	-4	-5	-1	0	5	7
17	0	-2	-4	-5	-7	-9	-11	-11	-6	-2	3	8
18	3	7	10	12	15	18	21	24	22	19	15	11
19	3	6	5	6	7	9	12	13	13	11	10	12
20	3	2	1	3	1	2	3	3	4	6	9	10
21	-2	1	1	1	1	-1	1	2	3	6	7	9
22	2	3	3	3	4	5	5	5	6	7	8	10
23	3	3	4	5	5	5	6	8	8	10	10	11
24	3	4	4	6	6	5	5	9	8	11	12	13
25	2	4	5	5	6	8	8	9	10	10	11	10
26	1	3	4	4	5	5	6	8	8	8	9	10
27	1	2	3	4	4	5	6	8	9	9	9	8
28	2	3	4	5	4	6	6	8	8	9	10	10
29	2	2	4	4	4	5	5	7	6	7	8	8
30	1	3	5	5	6	7	7	9	9	9	9	9

TABLE 11

STRAINS IN μ"/" RECORDED DURING THE FAILURE CYCLE OF BUILDING I

Strain Gauge Number	LOADING)pounds)											
	75	140	200	250	340	400	450	500	550	600	630	660
1	8	7	8	8	9	9	11	11	13	12	12	14
2	8	10	9	9	10	10	12	12	12	11	13	15
3	7	11	6	8	12	9	11	11	13	12	12	9
4	7	5	8	9	9	10	10	10	10	9	11	11
5	4	6	5	4	4	6	8	8	5	4	7	10
6	7	12	12	15	16	21	21	20	25	28	28	13
7	7	10	11	14	15	20	20	22	23	26	26	17
8	7	7	7	9	10	12	10	12	13	13	14	12
9	0	-4	-7	-10	-14	-17	-20	-24	-28	-31	-35	57
10	12	18	23	28	31	34	39	43	48	52	56	-2
11	8	14	17	22	24	28	29	34	36	39	42	14
12	6	5	6	6	6	6	6	6	6	6	7	57
13	1	-1	-4	-4	-5	-7	-9	-9	-10	-14	-15	-13
14	5	5	6	6	5	6	5	6	5	5	5	20
15	5	3	7	6	6	8	8	8	9	9	10	14
16	2	-1	-3	-6	-10	-11	-15	-14	-18	-17	-20	-9
17	2	-2	-6	-10	-15	-19	-23	-25	-29	-33	-37	-22
18	2	17	21	25	29	32	37	41	43	48	51	34
19	5	5	7	7	9	9	9	10	12	12	11	7
20	3	1	0	-1	-2	-3	-4	-5	-6	-7	-7	2
21	4	1	1	0	-2	-2	-3	-4	-5	-7	-6	4
22	4	5	5	4	4	3	2	3	2	2	1	7
23	5	4	5	4	4	5	5	4	5	3	4	6
24	6	5	7	6	6	6	10	9	8	8	9	15
25	4	6	6	7	5	5	6	8	7	6	8	10
26	5	4	5	5	5	6	6	6	6	6	6	6
27	5	4	6	6	7	7	7	7	8	8	7	9
28	3	4	4	4	4	4	4	3	3	3	5	6
29	4	4	4	4	4	4	4	3	4	2	3	6
30	2	2	3	4	3	4	5	6	6	6	6	6

TABLE 12

STRAINS IN μ"/" RECORDED DURING THE SECOND TEST CYCLE OF BUILDING II

Strain Gauge Number	LOADING (pounds)				UNLOADING (pounds)			
	60	125	190	250	190	125	60	0
1	0	-6	-6	-1	2	6	9	0
2	-4	-8	-10	-6	-7	1	2	-5
3	-5	-11	-11	-7	-5	-1	0	-7
4	-13	-51	-26	-14	-9	-40	-5	-48
5	-5	-8	-6	-3	-7	4	5	-4
6	1	0	-3	3	-2	4	6	-5
7	-2	-4	-1	3	-1	4	7	-2
8	-5	-8	-8	-7	-9	-5	0	-7
9	-12	-19	-26	-26	-22	-12	-3	-6
10	4	4	10	18	11	12	10	-5
11	0	-2	0	7	2	5	8	-2
12	-2	-9	-10	-3	-8	-2	2	-5
13	-5	-12	-13	-12	-11	-3	3	3
14	-6	-10	-13	-8	-10	-3	2	-5
15	6	-3	-5	1	0	6	10	0
16	-4	-11	-16	-14	-13	-4	3	-4
17	-5	-14	-25	-20	-22	-10	4	-4
18	1	1	4	10	5	10	10	-2
19	-5	-8	-11	-6	-7	-2	3	-5
20	-6	-7	-8	-7	-7	-5	-2	-5
21	-2	-10	-14	-10	-10	-6	0	-6
22	-6	-9	-11	-9	-9	-2	3	-5
23	-7	-11	-11	-5	-10	-4	1	-7
24	-3	-7	-7	-7	-5	0	5	-4
25	-4	-8	-9	-7	-7	-1	4	-4
26	-3	-8	-8	-6	-7	-1	4	-4
27	-4	-8	-8	-7	-6	-1	4	-3
28	-4	-9	-9	-6	-7	1	4	-4
29	-7	-11	-12	-10	-10	-5	1	-7
30	1	-2	-3	-1	-7	0	3	-4

TABLE 13

STRAINS IN μ"/" RECORDED DURING THE FAILURE CYCLE OF BUILDING II

Strain Gauge Number	LOADING (pounds)							
	125	250	390	465	565	650	685	720
1	4	16	5	5	9	5	19	12
2	6	17	6	6	12	8	24	16
3	6	16	7	5	15	12	26	18
4	3	16	5	4	9	8	23	17
5	3	9	2	2	6	1	18	12
6	12	17	13	15	25	22	38	24
7	9	21	17	16	20	19	38	26
8	3	13	7	7	9	7	24	29
9	-2	-2	-20	-20	-12	-17	-5	25
10	18	39	41	49	67	72	98	224
11	15	29	26	32	47	43	73	6
12	8	15	4	6	6	2	15	41
13	2	9	6	3	-2	10	7	7
14	9	17	10	3	9	5	18	16
15	5	15	6	3	8	6	20	14
16	1	3	-10	-20	-16	-21	-8	-6
17	-5	-7	-22	-35	-37	-48	-36	-30
18	11	27	21	29	44	42	63	46
19	4	12	4	3	7	5	20	14
20	4	10	2	3	5	7	18	16
21	1	6	3	2	9	10	11	6
22	3	11	4	0	5	2	18	12
23	5	14	5	3	7	5	21	14
24	5	13	6	3	8	5	20	15
25	4	14	4	2	8	6	18	13
26	4	14	5	4	10	7	22	13
27	5	14	6	4	10	4	22	15
28	6	14	4	2	7	5	18	13
29	4	13	3	1	6	4	17	13
30	1	16	9	2	6	7	24	20

BIBLIOGRAPHY

1. AFSAR, M.

"Lateral Loading of Shear Wall Models", Thesis submitted to Department of Civil Engineering and Engineering Mechanics in partial fulfilment of the requirements for the degree of Master of Engineering, McMaster University, August 1967.

2. QURESHI, A.A.

"Behaviour of Shear Wall Models With Circular Wall Openings", Thesis submitted to the Department of Civil Engineering and Engineering Mechanics in partial fulfilment of the requirements for the degree of Master of Engineering, McMaster University, February 1968.

3. COULL, A. and SMITH, S.B.

"Analysis of Shear Wall Structures", A review of previous research, Symposium on Tall Buildings, University of Southampton, April 1966, Pergamon Press, London.

4. BECK, H.

"Contribution to the Analysis of Shear Walls", Journal of the American Concrete Institute, 33, 1962.

5. ERIKSSON, O.E.

"Analysis of Wind Bracing Walls in Multistorey Housing", Ingenioren International Edition 5, 115, 1961.

6. ROSMAN, R.

"Approximate Analysis of Shear Walls Subject to Lateral Loads", Journal of the American Concrete Institute, 35, 1964.

7. McLEOD, I.A.

"Lateral Stiffness of Shear Walls with Openings", Symposium on Tall Buildings, University of Southampton, April 1966, Pergamon Press, London.

8. VLASOV, V.Z.

"Thin-Walled Elastic Beams", Isreal programme for scientific translations, Jerusalem, Isreal, 1961.

9. BENJAMIN, J.R.; WILLIAMS, H.A.

"Reinforced Concrete Shear Wall Assemblies", Journal of Structural Division, Proceedings of ASCE, Vol. 86, No. ST8, August 1960, pp. 1 - 32.

10. TARANATH, B.S.; MORICE, P.B.

"Torsion-Bending in Slab Structures", Symposium on Tall Buildings, April 1966, Pergamon Press, pp. 483 - 491.

11. TEZCAN, S.S.

"Analysis and Design of Shear Wall Structures", Symposium on Tall Buildings, April 1966, Pergamon Press, pp. 307 - 316.

12. KHAN, F.R. and SBAROUNIS, J.A.

"Interaction of Shear Walls and Frames", Journal of the Structural Division, ASCE, Vol. 90, No. ST3, pp. 285 - 335, June 1964.

13. CLOUGH, R.W.

"The Finite Element Method in Plane Stress Analysis", American Society of Civil Engineers, pp. 345 - 378, 2nd Conference on Electronic Computation, Pittsburgh, P.A. September 8, 1960.

14. TEZCAN, S.S.

"Application of Matrix Algebra to the Problems of Plane Stress, Plane Strain, Bending of Plates and Cylindrical Shells", Proceedings of the 3rd International Conference on the Application of Mathematics in Engineering, Weirnar, Germany, June 1965.

15. JENKINS, W.M.;HARRISON

"Analysis of Tall Buildings with Shear Walls under Bending and Torsion", Symposium on Tall Buildings, April 1966, Pergamon Press, pp. 251 - 282.

16. BARNARD, P.R. and SCHWAIGHOFER, J.

"The Interaction of Shear Walls Connected Solely Through Slabs", Symposium on Tall Buildings, April 1966, Pergamon Press, pp. 19 - 35.

17. COULL, A.

"Tests on a Model Shear Wall Structure", Civil Engineering and Public Works Rev. Vol. 61, No. 721, August 1966, pp. 1129 - 1133.

18. CHITTY, L.

"On the Cantilever Composed of a Number of Parallel Beams Interconnected by Cross-Bars", Phil. Mag., Series 7, Vol. 38, 1947, p. 685.